Deltares

3D effects for a coarse sand barrier

3D effects for a coarse sand barrier

Author(s)
Esther Rosenbrand
Vera van Beek
Geeralt van den Ham

3D effects for a coarse sand barrier

Client	Waterschap Rivierenland
Contact	
Reference	Referenties
Keywords	Keywords

Document control	
Version	1.0
Date	03-02-2021
Project nr.	11200952-060
Document ID	11200952-060-GEO-0002
Pages	118
Status	final

Author(s)		
	Esther Rosenbrand	
	Vera van Beek	
	Geeralt van den Ham	

Doc. version	Author	Reviewer	Approver	Publish
1.0	Vera van Beek  Esther Rosenbrand  Geeralt van den Ham 	Adam Bezuijen 	Goaitske de Vries 	

Summary

The coarse sand barrier (CSB) is an innovative method to reinforce existing dikes against the process of backward erosion piping (BEP). The CSB consists of a trench filled with coarse sand in the path of the pipe, below the blanket layer, which prevents the pipe from progressing upstream due to the higher resistance of the barrier against BEP. The top of the CSB can be level with the top of the aquifer, or the CSB can protrude into the cover layer. In practice the second option is most likely to be applied.
Experiments in the laboratory at different scales where the top of the CSB is level with the top of the aquifer show that when a pipe encounters the CSB, it progresses parallel to the barrier in the aquifer sand. This parallel progression of the pipe along the barrier will continue as long as the resistance to pipe formation parallel to the barrier is smaller than the resistance to breach through the barrier. Continued erosion results in an effectively 2D flow field in the barrier. Ideally, in a homogeneous situation, this also occurs in the field (Fig 1., l.h.s.). However, in the field the progression of the pipe parallel to the barrier may be limited, for instance by the presence of heterogeneity, in the path of the pipe (Fig 1. r.h.s.). This could result in a strong concentration of flow at the edge of the pipe along the barrier increasing the load on the barrier grains. The 3D factor is defined as the ratio of the gradient that occurs due to the concentration of flow in a 3D situation over the gradient that would occur in a 2D situation.

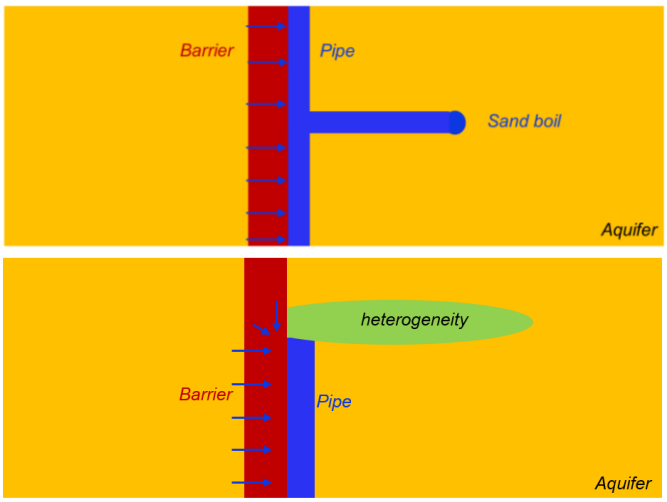

Figure 1 *Plan view of the top of the aquifer with a CSB for a situation where the top of the CSB is level with the top of the aquifer, left hand side ideal homogeneous situation, right hand side situation with heterogeneity (not to scale)*

When the barrier protrudes above the sand layer into the blanket layer, a slope will form in the barrier material, reaching from the pipe towards the upstream edge of the barrier. In the case of a heterogeneity in the background sand, such as a clay lens, the pipe in front of the barrier stops progressing. As with the previous case there is concentration of flow from the side in the barrier, but now this causes the slope to extend to the side, resulting in an elongated amphitheatre shape in the barrier. The slope to the side will flatten to some extent, the equilibrium slope angle to the side will depend on the configuration. This situation could not be observed in experiments due to the limited width, however, it appears probable that this will result in an equilibrium situation, whereby the exact slope that forms from the end of the pipe in front of the barrier to the side parallel to the barrier edge, is dependent on the configuration and the critical gradient for a particular location. The 3D effect for such a situation will be less due to the formation of this slope, but it will still be present due to the inflow from the side. It is even possible that horizontal pipes form at the top of the barrier.

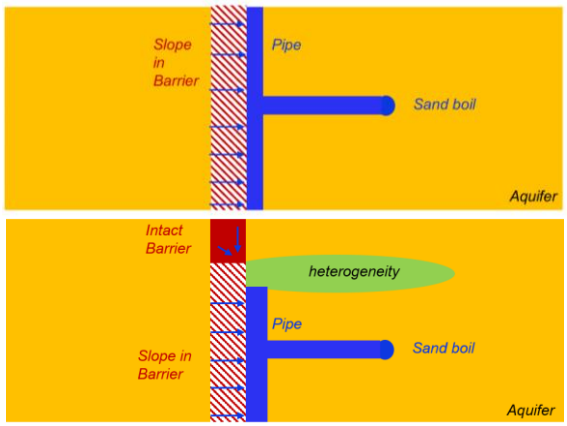

Figure 2 *Plan view of the top of the aquifer with a CSB for a situation where the CSB protrudes into the cover layer, left hand side ideal homogeneous situation, right hand side situation with heterogeneity (not to scale)*

The design approach for a CSB is based on numerical modelling in 2D finite element groundwater flow models in order to compute the local gradient inside the barrier $i_{barrier}$ (Fig. 2). This local gradient is compared to the maximum local gradient inside the barrier that the barrier can retain $i_{c,\ barrier}$. The value of $i_{c,barrier}$ is specific to the CSB material and dependent on the relative density of the barrier and can be determined based on laboratory experiments. However, the local gradient in the barrier will be underestimated in 2D models if the pipe is stopped at some distance along the barrier.

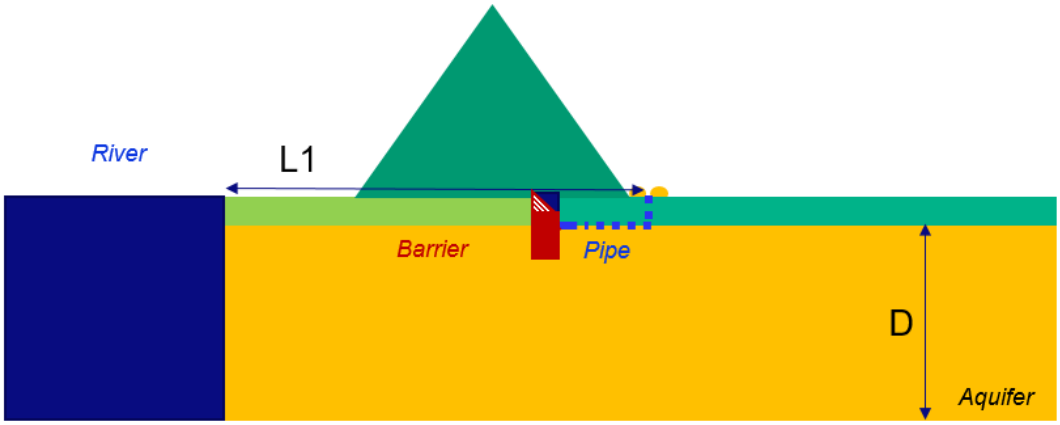

Figure 3 *2D Model in cross section used for design of CSB. The pipe runs from the sand boil to the barrier (dotted blue line) and subsequently progresses parallel to the barrier interface (solid blue line). Dashed triangle indicates situation with a CSB protruding into the cover layer, blue is eroded barrier*

This report addresses the 3D effect for the CSB based on finite element 3D computations. The 3D effect is defined as the ratio of the gradient inside the barrier in a situation where the pipe has only developed a limited distance parallel to the barrier along the width of the model, $i_{barrier,3D}$ to the gradient in the situation where the pipe has progressed along the entire width of the barrier $i_{barrier,\ 2D}$.

In the report, first a sensitivity analysis was performed to assess which factors affect the 3D effect. Subsequently the effect of the shape of the barrier, whether this protrudes into the cover layer or not, was investigated. Finally, the situation for the pilot application at Gameren was modelled.

In this report, for the purpose of studying the 3D factor in the sensitivity analysis, the slope is replaced by a pipe without head loss that has partly penetrated the barrier. This assumption is allowed, since the flow towards the barrier largely controls the 3D effect, for which the precise

geometry is not relevant. An exception to this, is the presence of a slope towards the sides (amphitheatre), which softens the 3D effect at the edges.

Results
Parameters which affect the 3D effect strongly are listed below:

- The leakage length on the polder side of the levee, a long leakage length causes stronger concentration of flow to the pipe and a higher 3D effect.
- The shape of the situation, aquifer depth *D*, aquifer width (model width) *W*, length of the floodplain and base of the embankment *L1*.
  - A smaller *D* gives a higher 3D effect.
  - A larger *W* increases the 3D effect, up to a certain limit which is situation specific.
  - A larger *L1* increases the effect of the two components above.
- The extent that the pipe progresses along the barrier width, the further the pipe progresses, the smaller the 3D effect.
- The anisotropy (ratio of horizontal to vertical hydraulic conductivity $A = k_h/k_v$) of the aquifer, a higher *A* increases the 3D effect.
- The hydraulic conductivity contrast between the CSB and the aquifer. A higher contrast increases the 3D effect.

The complexity resides in the fact that the relative effect of these parameters differs depending on the value of the other parameters. This means that no generic 3D factor exists that can be applied to all situations. A 3D factor should therefore be derived in 3D models that represent the design situations. This was done for the field situation in Gameren using a model without a protruding barrier. The numerical complexity of modelling a protruding barrier is such that it prohibits modelling the entire field situation, and the important geohydrological factors such as leakage length, multiple layers, and sufficient width of the model to the required extent. Analysis of the gradients in the protruding barrier for a simplified situation suggests that the 3D effect will be comparable for a protruding barrier, allowing for this form of analysis. Hereby it is important to note that the formation of a slope inside the barrier to the side will reduce the 3D effect as opposed to the modelled 3D effect. To account for the effect of the slope to the side starting at the pipe extent, the 3D effect is best evaluated at some distance from the furthest extent of the pipe as detailed below.
The situation specific model has two strong remaining uncertainties, namely:

1. The lateral extent of the pipe parallel to the barrier, which will not be known in advance
2. The modelled effect of 3D concentration of flow is strongest at the very furthest extent of the parallel pipe. However, as noted above, for a protruding barrier the peak modelled gradients are unlikely to occur due to the formation of a slope to the side.

The first uncertainty can be addressed by considering the degree of heterogeneity along the barrier width. Geological insight into the subsurface, and site investigation can be used to assess the likely spacing between heterogeneities, and the nature of the heterogeneity and the extent to which it is likely that the pipe will stop progressing. In case of a protruding barrier, the pipe may stop, but the slope will still form sideward in the barrier, which is homogeneous. It is expected that the slope will flatten and reach until the top of the protrusion, from where horizontal pipes may start to form. These pipes will reduce the 3D factor.
The second uncertainty is more difficult to assess and is based on an analysis of the effect of different options for modelling the ends of the pipe in the barrier.
For the situation at Gameren, a qualitative assessment of the local geology, the type of heterogeneity that might occur and the spacing among heterogeneities, in combination with qualitative evaluation of the effect of different parameters, was used to map out the likely 3D effects shown in Table 1. The most likely values range from ca. 3 to 6, however, the scenario of a 2D situation is not entirely ruled out. It is also noted that the higher the 3D effect becomes,

the higher the loading from the side on the pipe is. That makes it more likely that the slope to the side in the protruding barrier will level off further, reducing the 3D effect. However, there is a limit to this, as the toe of that slope remains at the end of the pipe parallel to the barrier. Finally, it is important to note that in situations with a high 3D effect, the critical head drop will be lower which results in a lower flow rate in the pipe downstream of the barrier, resulting in a shallower pipe and more resistance. That additional resistance could be accounted for in the design calculations for specific cross sections, as it will also depend on the length of the pipe downstream of the barrier.

Table 1 Estimated 3D factors for different lateral pipe extents (full-space) and a perpendicular pipe. The green larger values are considered more likely to occur, the red smaller values less likely

		Estimated 3D factors for Gameren all with correction for perpendicular pipe				
	Increase to 5 m parallel pipe **Upper limit effect of a shorter lateral pipe**	**Increase to 5 m parallel pipe weakest effect** **Lower limit effect of a shorter lateral pipe**	**Basis model, 10 m parallel pipe,**	**Increase to 50 m parallel pipe** **Upper limit effect of a longer lateral pipe,**	**Increase to 50 m parallel pipe** **Lower limit effect of a longer lateral pipe**	**2D situation**
At 0% of distance from centre axis	4.2	3.1	2.4	0.9	1.7	1
At 20% of distance from centre axis	4.8	3.5	2.7	1.1	1.9	1
At 40% of distance from centre axis	5.1	3.7	2.8	1.1	2.0	1
At 60% of distance from centre axis	5.5	4.0	3.1	1.2	2.1	1
At 80% of distance from centre axis	6.1	4.4	3.4	1.3	2.4	1
At 90% of distance from centre axis	9.0	6.5	5.0	2.0	3.5	1
At 95% of distance from centre axis	11.0	7.9	6.1	2.4	4.3	1
At 99% of distance from centre axis	14.6	10.5	8.1	3.2	5.7	1

Contents

1 Introduction

For reasons of simplicity, the design method for a CSB consists of 2D flow calculations. However, in reality the flow towards the barrier, the pipe and the exit is three-dimensional. For regular piping calculations without barrier the flow is also 3D, and although it is not yet common to take this into account, there are several reasons to consider this effect in the design of the CSB:

- It is known that 3D flow can have a large influence on the critical head
- The 3D effect may be different (more severe) for a coarse sand barrier, due to its draining effect
- The 3D effect for a CSB is largely related to the flow towards the barrier, which can be predicted with the current state of knowledge.

It is therefore considered appropriate to account for this effect using a 3D-factor, F_{3D}, defined as the ratio of the barrier gradient in 3D and the barrier gradient in 2D (details on how these barrier gradients are defined are explained in the text). The 3D factor is a convenient way of dealing with the 3D effects, since it will allow for a design in 2D.

Since many parameters may play a role in the determination of the 3D factor, a three-phased approach was pursued. The different phases allow for determination of the effect of parameters separately and allows for a gradual development of the 3D factor for Gameren in an efficient manner. The sensitivity of parameters is important in relation to the uncertainty by which these parameters can be determined for the situation of Gameren.

Phase 1 consists of a sensitivity study with a simplified geometry. The simplified geometry allows for a quick assessment of influential parameters, like permeability contrasts, aquifer and barrier depths and lateral development of the pipe along the barrier. In the second phase, more detail related to the protrusion is added to the 3D calculation, such as the size and shape of the amphitheatre. Modelling the protrusion also allowed for assessment of gradients perpendicular to the barrier (slope erosion) and vertically (heave). In the third phase, the 3D factor for the situation of Gameren is determined, using the scenarios that can be expected locally and the insights on relevant parameters as assessed in phase 1 and 2.

In the following chapters (2, 3 and 4) phases 1, 2 and 3 are summarized, followed by a conclusion on the 3D factor for Gameren en recommendations for other situations in Chapter 4.

2 Phase 1: Sensitivity analysis with simplified geometry

In this phase a simplified geometry is used to assess the effect of parameters on the 3D factor. The simplification involves mainly the shape of the barrier, which is modelled as a rectangular box without protrusion. The pipe is modelled in and downstream of the barrier. Despite of the simplifications, it is expected that the gradients in the barrier provide a decent estimate of the effect of parameters on the 3D factors.

2.1 Geometry and parameters

This phase consists of computations in two types of models in phase 1a, a model with a cover layer is used, as is illustrated in Figure 2.1, showing a top view and side view of the aquifer and the barrier. In phase 1b, the model is similar, but the cover layer is not modelled, allowing for more flexibility in mesh generation.

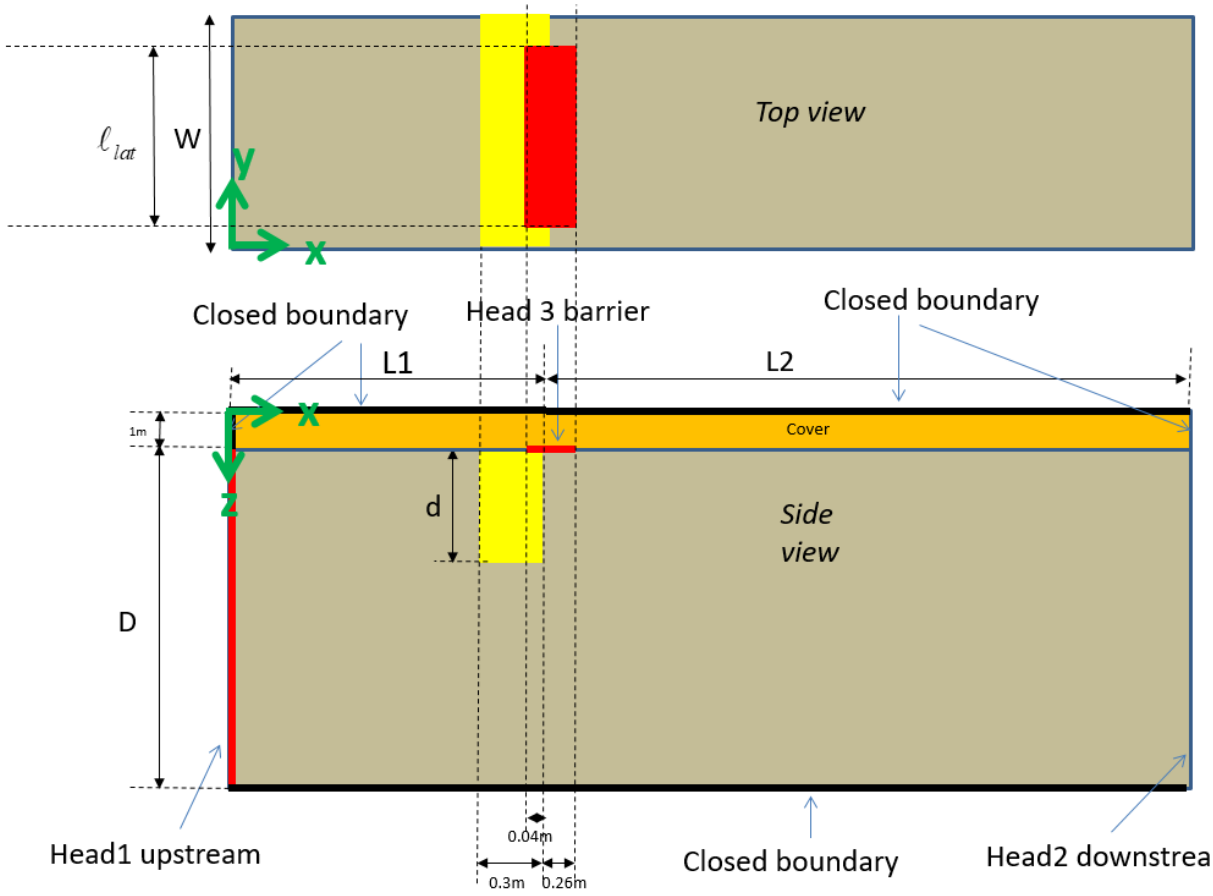

Figure 2.1 Simplified geometry with CSB (yellow) and eroded zone (red)

The parameter variations that are studied are the aquifer depth (D), aquifer width (W), the depth of the barrier (d), the hydraulic conductivity contrast of barrier and aquifer, the length to the upstream (L1) and to the downstream boundary (L2), and the pipe extent lateral to the barrier (l_{lat}) details are provided in Table 2.1.

Note that since the top boundary of the aquifer downstream of the pipe is closed, varying the distance to the downstream outflow boundary approximates the effect of seepage through the polder, i.e. this can be considered as equivalent to varying the leakage length.

Table 2.1 Parameter variation in phase 1, the bold parameters are varied, non-bold are fixed, values that were used in the basis calculation phase 1a are in Italics. In phase 1b, both hydraulic conductivity contrasts 4 and 12 are used for all computations

Parameter	Symbol	Values
Thickness aquifer	D [m]	8, 20, *40*
Width aquifer	W [m]	*100*, 200, 300
Length CSB to downstream boundary	L2 [m]	50, *130*, 200
Length CSB to upstream boundary	L1 [m]	*20*, 50 100
Thickness CSB	w [m]	0.30
Depth CSB	d [m]	1, *2*
Lateral pipe development	ℓ_{lat} [m]	1, 5, *50*
Pipe zone in CSB	[m]	0.04
Pipe zone downstream of CSB	[m]	0.26
Hydraulic conductivity contrast CSB/aquifer	k_{CSB}/k_s [-]	*4*, 12

Since the protrusion is not modelled in this simplified geometry, the horizontal gradient is used for the calculation of the 3D factor. It is expected that the parameter sensitivity on the 3D factor will be similar for the situation with and without protrusion. It must be realized that some parameters affect both the gradient in 2D and in 3D. Therefore, for each of the variations, a 2D variety with the pipe developed across the full width of the aquifer is conducted.

Computations are done for incompressible water and soil properties.

2.2 Mesh and software

Computations are performed using the finite element groundwater flow model DgFlow, version 1.4 (phase 1b) and 1.5 (phase 1a). Pre-processing of the data is done using GiD version 13 (phase 1a) and version 14 (phase 1b). Results are post processed using python (phase 1a) or using Paraview and Matlab (phase 1b).

In phase 1 an unstructured mesh is used in order to allow for the required refinement at the barrier. In phase 1a, the mesh is refined to approximately 0.05 m elements inside the CSB, and the basis mesh elements are in the order of 5 m. In phase 1b a mesh analysis was conducted, as reported in Appendix A. This mesh analysis considered the effects of a finer mesh (with 0.04 m elements inside the barrier) and a coarser mesh (0.06 m elements inside the barrier. For groundwater flow models this is still very fine, however, it must be realised that the refinement is needed as this affects the number of nodes upstream of the pipe that are used to compute the criterion and thereby the extent to which concentration of flow to the pipe can be resolved. With a finer mesh, a higher gradient will be computed. The mesh analysis shows however that the effect is relatively small, in the order of 5%. Considering other uncertainties, a coarser mesh is therefore considered adequate.

For the analysis of results, results are compared between results with the same mesh refinement in phase 1b (as comparing results between a model and a finer and a coarser mesh can lead to under or over-estimation of the effects of a parameter).

2.3 Overview of computations

The tables below show an overview of the computations in phase 1a and in phase 1b. Note that for each model, an equal model only with a fully developed pipe is computed ($l_{lat} = W$) in order to compute the 3D effect due to a partially developed pipe ($l_{lat} < W$).

Table 2.2 Models used in phase 1a, only one mesh type is used

Model name	L1, m	L_lat, m	W, m	D, m	L2, m	Contrast, -	d, m
2Aa	20	50	100	40	130	4	2
3Aa	20	5	100	40	130	4	2
4Aa	20	1	100	40	130	4	2
2Ba	20	50	100	40	130	4	1
2BaS	20	50	100	20	130	4	2
2Ab	20	50	100	40	130	8	2

Table 2.3 Models used in phase 1b, all models have barrier depth (d) 2 m for contrast 12. Spacing in tables indicates models indicates which models are to be compared amongst each other

Variation	L1, m	L_lat, m	W, m	D, m	L2, m	Contrast, -	Mesh
Aquifer depth 40 m, pipe 50 m	20	50	100	40	130	12	fine
Aquifer depth 8 m, pipe 50 m	20	50	100	8	130	12	fine
Pipe length 50 m	20	50	100	8	130	12	fine
Pipe length 5 m	20	5	100	8	130	12	fine
Mesh fine	20	50	100	40	130	12	fine
Mesh coarse	20	50	100	40	130	12	coarse
L2: 130 m	20	50	100	40	130	12	fine
L2: 50 m	20	50	100	40	50	12	fine
L2: 200 m	20	50	100	40	200	12	fine
L1 20 m; W 100 m	20	50	100	40	130	12	coarse
L1 50 m; W 100 m	50	50	100	40	130	12	coarse
L1 100 m; W 100 m	100	50	100	40	130	12	coarse

Variation	L1, m	L_lat, m	W, m	D, m	L2, m	Contrast, -	Mesh
L1 20 m; W 200 m	20	50	200	40	130	12	coarse
L1 50 m; W 200 m	50	50	200	40	130	12	coarse
L1 100 m; W 200 m	100	50	200	40	130	12	coarse
L1 50 m; W 300 m	50	50	300	40	130	12	coarse
L1 100 m; W 300 m	100	50	300	40	130	12	coarse
W 100 m; L1 20 m	20	50	100	40	130	12	coarse
W 200 m; L1 20 m	20	50	200	40	130	12	coarse
W 100 m; L1 50 m	50	50	100	40	130	12	coarse
W 200 m; L1 50 m	50	50	200	40	130	12	coarse
W 300 m; L1 50 m	50	50	300	40	130	12	coarse
W 100 m; L1 100 m	100	50	100	40	130	12	coarse
W 200 m; L1 100 m	100	50	200	40	130	12	coarse
W 300 m; L1 100 m	100	50	300	40	130	12	coarse
No perpendicular pipe	20	50	100	40	130	12	Fine
Perpendicular pipe (width 0.4 m and length 50 m).	20	50	100	40	130	12	Fine
Isotropic	20	50	100	40	130	12	Fine
Anisotropy ratio 15	20	50	100	40	130	12	Fine

2.4 Results

Figure 2.2 gives an example of the horizontal gradient upstream of the eroded zone along the entire width of the aquifer. When the eroded zone is present along the entire width of the aquifer, a 2D situation is obtained, with the horizontal gradient equal along the entire length. For a partial developed pipe, the gradients are highest at the corners of the eroded zone. This is expected, since the corners are singular points, where the flow theoretically will go to infinity. The peak in the gradient is limited by the size of the mesh: a decrease of mesh size will lead to further increase of the peak. This behaviour is often encountered in piping analysis (Van Beek et al., 2014). Due to this singularity, it is unlikely that the peak gradient represents a reliable value. The lowest value is not reliable either: due to the concentration of flow near the corners of the eroded zone gradients are truly higher than those in the middle, although this effect is softened by the resistance in the pipe that is not modelled and will increase towards the corners, thus reducing the gradients.
The 3D horizontal gradient is therefore determined at 90, 95 and 99% of the distance from the centre axis, as illustrated in Figure 2.3. The gradient for the 2D situation is determined by averaging the horizontal gradient along the width of the aquifer.

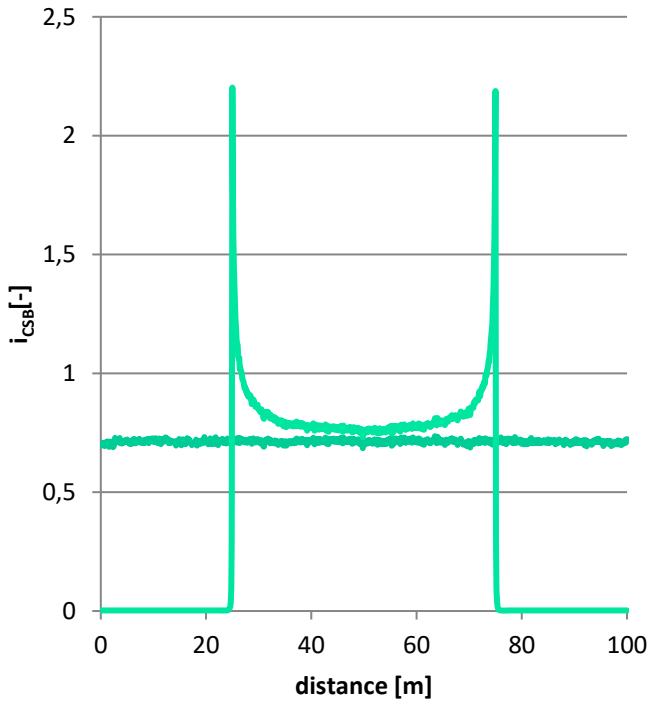

Figure 2.2 Illustration of horizontal gradients along the width of the aquifer with fully developed pipe (blue) and with partially developed pipe (green)

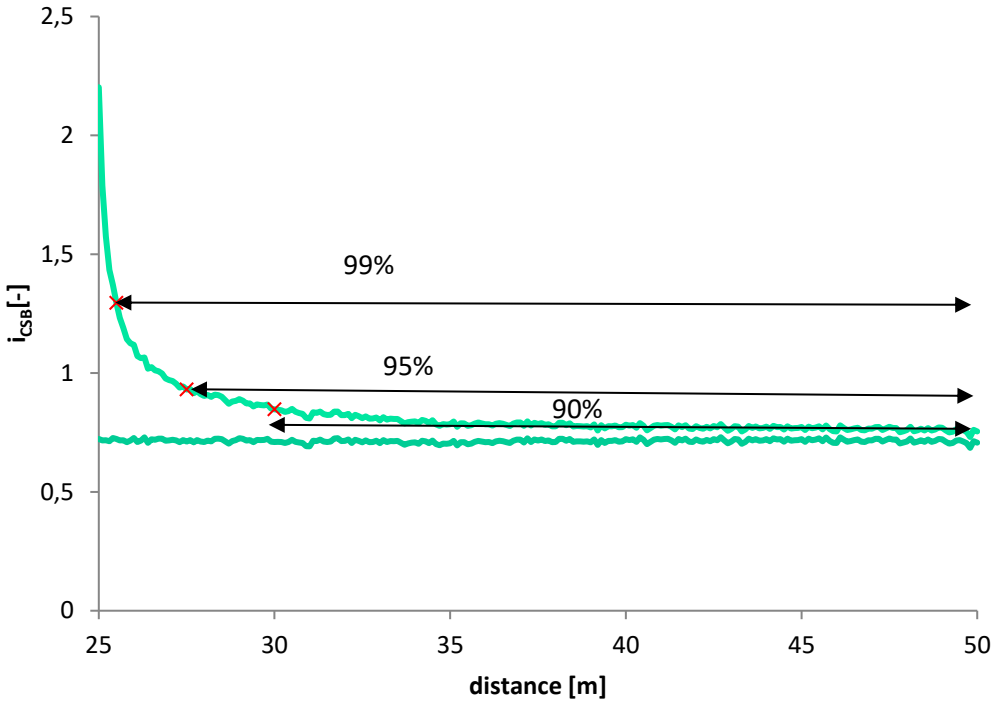

Figure 2.3 Illustration of determination of 90, 95 and 99% gradients

2.4.1 Overview of all results

The tables below present the results for all computations, these are discussed in further detail in the next sections.

Table 2.4 Results for phase 1a, only one mesh type is used

Model name	2D gradient	Gradient at 99% of distance from centre axis	Gradient at 95% of distance from centre axis	Gradient at 90% of distance from centre axis	3D effect for 99% of distance from centre axis	3D effect for 95% of distance from centre axis	3D effect for 90% of distance from centre axis
2Aa	0.71	1.30	0.93	0.85	1.8	1.3	1.2
3Aa	0.71	2.34	1.76	1.53	3.3	2.5	2.1
4Aa	0.71	3.13	2.93	2.72	4.4	4.1	3.8
2Ba	0.69	1.24	0.87	0.80	1.8	1.3	1.2
2BaS	0.63	1.16	0.81	0.74	1.8	1.3	1.2
2Ab	0.48	1.00	0.65	0.58	2.1	1.4	1.2

Table 2.5 Results for phase 1b with contrast 12, all models have barrier depth (d) 2 m. Spacing in tables indicates models indicates which models are to be compared amongst each other

Variation	2D gradient	Gradient at 99% of distance from centre	Gradient at 95% of distance from centre	Gradient at 90% of distance from centre	3D effect for 99% of distance from centre	3D effect for 95% of distance from centre	3D effect for 90% of distance from centre
Aquifer depth 40 m, pipe 5 m	0.37	0.40	1.07	0.64	2.9	1.7	1.4
Aquifer depth 8 m, pipe 50 m	0.20	0.72	0.44	0.36	3.6	2.2	1.8
Pipe length 50 m	0.20	0.72	0.44	0.36	3.6	2.2	1.8
Pipe length 8 m	0.20	1.50	1.24	1.05	7.4	6.1	5.2
Mesh fine	0.37	0.40	1.07	0.64	2.9	1.7	1.4
Mesh coarse	0.36	0.95	0.59	0.49	2.7	1.6	1.4
L2: 130 m	0.37	0.40	1.07	0.64	2.9	1.7	1.4
L2: 50 m	0.33	0.91	0.55	0.45	2.8	1.7	1.4
L2: 200 m	0.39	1.11	0.67	0.55	2.9	1.7	1.4
L1 20 m; W 100 m	0.36	0.95	0.59	0.49	2.7	1.6	1.4
L1 50 m; W 100 m	0.22	0.65	0.40	0.34	3.0	1.8	1.5
L1 100 m; W 100 m	0.14	0.43	0.27	0.22	3.2	2.0	1.6

Variation	2D gradient	Gradient at 99% of distance from centre	Gradient at 95% of distance from centre	Gradient at 90% of distance from centre	3D effect for 99% of distance from centre	3D effect for 95% of distance from centre	3D effect for 90% of distance from centre
L1 20 m; W 200 m	0.35	0.97	0.61	0.50	2.8	1.7	1.4
L1 50 m; W 200 m	0.22	0.72	0.44	0.37	3.3	2.0	1.7
L1 100 m; W 200 m	0.13	0.51	0.31	0.26	3.8	2.4	1.9
L1 50 m; W 300 m	0.22	0.73	0.45	0.37	3.4	2.1	1.7
L1 100 m; W 300 m	0.13	0.53	0.32	0.27	4.0	2.4	2.0
W 100 m; L1 20 m	0.36	0.95	0.59	0.49	2.7	1.6	1.4
W 200 m; L1 20 m	0.35	0.97	0.61	0.50	2.8	1.7	1.4
W 100 m; L1 50 m	0.22	0.65	0.40	0.34	3.0	1.8	1.5
W 200 m; L1 50 m	0.22	0.72	0.44	0.37	3.3	2.0	1.7
W 300 m; L1 50 m	0.22	0.73	0.45	0.37	3.4	2.1	1.7
W 100 m; L1 100 m	0.14	0.43	0.27	0.22	3.2	2.0	1.6
W 200 m; L1 100 m	0.13	0.51	0.31	0.26	3.8	2.4	1.9
W 300 m; L1 100 m	0.13	0.53	0.32	0.27	4.0	2.4	2.0
No perpendicular pipe	0.37	1.07	0.64	0.53	1.07	1.7	1.4
Perpendicular pipe (width 0.4 m and length 50 m).	0.37	1.01	0.61	0.50	2.7	1.6	1.3
Isotropic	0.37	1.07	0.64	0.53	2.9	1.7	1.4
Anisotropy ratio 15	0.22	0.80	0.47	0.36	3.7	2.1	1.7

Table 2.6 Results for phase 1b with contrast 4, all models have barrier depth (d) 2 m. Spacing in tables indicates models indicates which models are to be compared amongst each other

Variation	2D gradient	Gradient at 99% of distance from centre axis	Gradient at 95% of distance from centre axis	Gradient at 90% of distance from centre axis	3D effect for 99% of distance from centre axis	3D effect for 95% of distance from centre axis	3D effect for 90% of distance from centre axis
Aquifer depth 40 m, pipe 5 m	0.73	1.57	1.09	0.96	2.2	1.5	1.3
Aquifer depth 8 m, pipe 50 m	0.43	1.12	0.79	0.69	2.6	1.8	1.6
Pipe length 50 m	0.43	1.12	0.79	0.69	2.6	1.8	1.6
Pipe length 8 m	0.43	2.16	1.83	1.59	5.0	4.3	3.7
Mesh fine	0.73	1.57	1.09	0.96	2.2	1.5	1.3
Mesh coarse	*0.70*	1.42	1.00	0.90	2.0	1.4	1.3
L2: 130 m	0.73	1.57	1.09	0.96	2.2	1.5	1.3
L2: 200 m	*0.64*	1.34	0.93	0.82	2.1	1.5	1.3
L2: 200 m	*0.76*	1.64	1.13	0.99	2.2	1.5	1.3
L1 20 m; W 100 m	*0.70*	1.42	1.00	0.90	2.0	1.4	1.3
L1 50 m; W 100 m	0.45	1.01	0.71	0.64	2.2	1.6	1.4
L1 100 m; W 100 m	0.28	0.68	0.48	0.43	2.4	1.7	1.5
L1 20 m; W 200 m	*0.70*	1.44	1.04	0.92	2.1	1.5	1.3
L1 50 m; W 200 m	0.44	1.09	0.77	0.68	2.4	1.7	1.5
L1 100 m; W 200 m	0.28	0.78	0.55	0.49	2.8	2.0	1.8
L1 50 m; W 300 m	0.44	1.10	0.78	0.69	2.5	1.8	1.6
L1 100 m; W 300 m	0.28	0.80	0.57	0.51	2.9	2.0	1.8
W 100 m; L1 20 m	*0.70*	1.42	1.00	0.90	2.0	1.4	1.3

Variation	2D gradient	Gradient at 99% of distance from centre axis	Gradient at 95% of distance from centre axis	Gradient at 90% of distance from centre axis	3D effect for 99% of distance from centre axis	3D effect for 95% of distance from centre axis	3D effect for 90% of distance from centre axis
W 200 m; L1 20 m	*0.70*	1.44	1.04	0.92	2.1	1.5	1.3
W 100 m; L1 50 m	0.45	1.01	0.71	0.64	2.2	1.6	1.4
W 200 m; L1 50 m	0.44	1.09	0.77	0.68	2.4	1.7	1.5
W 300 m; L1 50 m	0.44	1.10	0.78	0.69	2.5	1.8	1.6
W 100 m; L1 100 m	0.28	0.68	0.48	0.43	2.4	1.7	1.5
W 200 m; L1 100 m	0.28	0.78	0.55	0.49	2.8	2.0	1.8
W 300 m; L1 100 m	0.28	0.80	0.57	0.51	2.9	2.0	1.8
No perpendicular pipe	0.73	1.57	1.09	0.96	2.2	1.5	1.3
Perpendicular pipe (width 0.4 m and length 50 m).	0.73	1.48	1.02	0.90	2.03	1.40	1.23
Isotropic	0.73	1.57	1.09	0.96	2.2	1.5	1.3
Anisotropy ratio 15	0.52	1.35	0.92	0.78	2.6	1.8	1.5

2.4.2 2D calculations

2D calculations are required to serve as a reference for the 3D calculations. Since the aquifer depth, distance to the upstream and downstream boundaries, and permeability contrasts are variables for the determination of the 3D factor, these parameters are varied in their 2D equivalents as well.

The 2D gradients increase for:

- Increasing aquifer depth
- Increasing leakage length
- Shorter floodplain length, (i.e. distance to upstream boundary)
- Decreasing hydraulic conductivity contrast between the barrier and the aquifer.

The aquifer width and the depth of the barrier (difference between 1 and 2 m deep barrier in phase 1a) do not have a significant effect on the 2D gradient.

As sensitivity of results of 2D gradients are analyses specifically for the pilot location in the design report, these results are not analysed in detail here.

2.4.3 Effect of lateral pipe development on the 3D factor

The figure below presents the effect of lateral development of the pipe on the 3D factors for the three percentages based on the results in phase 1a and phase 1b. As expected, the 3D factor decreases with increasing lateral pipe development, because this creates a larger outflow area in the barrier.

The phase 1b results show higher 3D factors, which is are due to the smaller aquifer depth, as discussed later in this Chapter. In those models the minimum pipe extent is 5 m. The models from phase 1a show that the 3D factor becomes significantly higher for a shorter pipe of only 1 m.

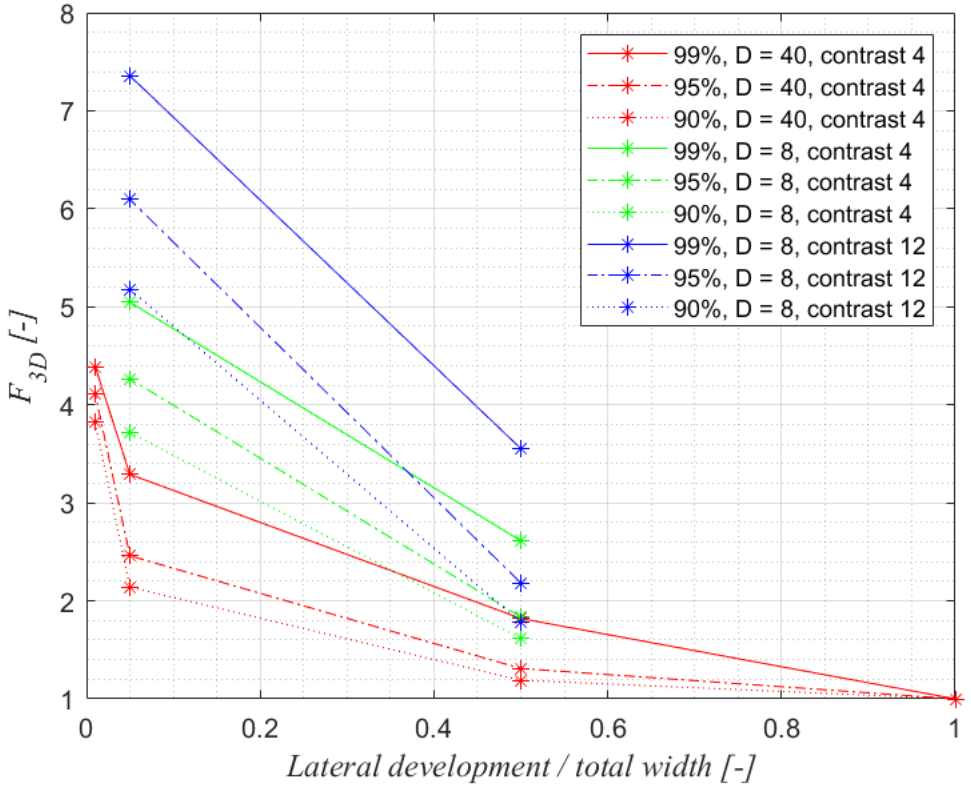

Figure 2.4 Effect of normalized lateral pipe development on the 3D factor

The factors are a lot lower for longer lateral pipes, even though the peak gradients are not that much lower for larger lateral pipes in comparison with shorter ones as shown below.

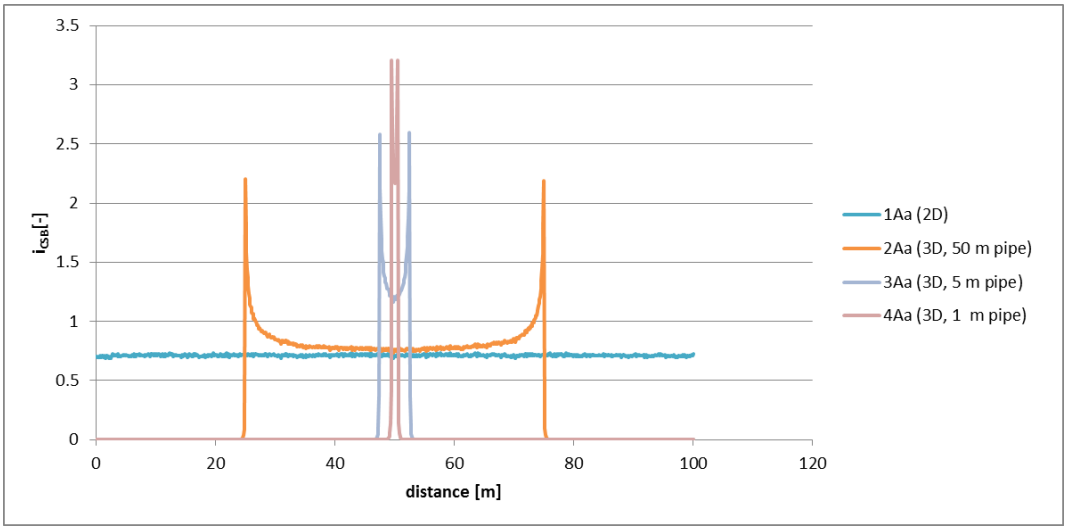

Figure 2.5 Effect of distance from centre axis on the modelled head profile in models from phase 1

The considerably lower factors for longer lateral pipes are due to a larger outflow area in the barrier. For a field situation, additional factors may contribute to a lower 3D effect with longer lateral pipes, as there will be head loss in the pipe. A lower 3D effect at the end of the pipe makes it less likely that the pipe breaks through exactly at the end of a pipe, also from a statistical perspective (a longer pipe means more chance of a weaker spot somewhere else along its length).

For the phase 1a results with the lateral pipe lengths of 1 and 5 m, it was necessary to interpolate between the numerical results, and the 95 and 99% are very close to the first node, which therefore may be unreliable. Probably these underestimate the gradients as the convergence of flow is less well resolved in coarser models.

2.4.4 Effect of barrier depth on the 3D factor

The effect of barrier depth on the 3D factor was studied by changing the barrier depth from 2 m to 1 m in phase 1a, for a fully developed pipe and a lateral pipe of 50 m. The effect is presented in Table 2.7. There is no significant effect of barrier depth on the 3D factor.

Table 2.7 Effect of barrier depth for a partially developed pipe with length of 50 m

%	F_{3D} [-] CSB depth 2 m	F_{3D} [-] CSB depth 1 m
99%	1.8	1.8
95%	1.3	1.3
90%	1.2	1.2

2.4.5 Effect of aquifer depth on the 3D factor

The effect of aquifer depth on the 3D factor was studied by changing the aquifer depth from 40 m to 20 m for a fully developed pipe and a lateral pipe of 50 m in phase 1a. The effect is presented in Table 2.8. In contrary to what would be expected, the effect of aquifer depth on the 3D factor is small. Possibly this is related to the relatively small length upstream of the barrier in relation to the depth of the aquifer or to the relatively small permeability contrast.

Table 2.8 Effect of aquifer depth for a partially developed pipe with length of 50 m

%	F_{3D} [-] aquifer depth of 40 m	F_{3D} [-] aquifer depth of 20 m
99%	1.8	1.8
95%	1.3	1.3
90%	1.2	1.2

Therefore, the effect was also studied by changing the aquifer depth from 40 m to 8 m in phase 1b, for contrasts of 4 and 12. The effect is presented in Table 2.9 and Table 2.10. The 3D effect is somewhat larger in the shallower 8 m models than in the deeper 40 m models, and the difference is larger for the higher contrast. The maximum difference is in the order of 20-30%. Thus, aquifer depth does have an effect on the 3D effect and the effect is stronger with a larger contrast.

Table 2.9 Effect of aquifer depth for a partially developed pipe with length of 50 m for models with λ 130 m, depth 40 m, aquifer width 100 m, barrier depth 2 m and contrast 4

%	F_{3D} [-] aquifer depth of 40 m	F_{3D} [-] aquifer depth of 8 m
99%	2.2	2.6
95%	1.5	1.8
90%	1.3	1.6

Table 2.10 Effect of aquifer depth for a partially developed pipe with length of 50 m for models with λ 130 m, depth 40 m, aquifer width 100 m, barrier depth 2 m and contrast 12

%	F_{3D} [-] aquifer depth of 40 m	F_{3D} [-] aquifer depth of 8 m
99%	2.9	3.6
95%	1.7	2.2
90%	1.4	1.8

The reason for the effect of depth is possibly related to the shape of the model. Both the relation of the floodplain length relative to the aquifer depth, and the relation of the aquifer depth to the leakage length affect the convergence of flow to the pipe. The figures of the head distribution and contour lines shown below indicate that the head beyond the barrier is lower for the shallower model.

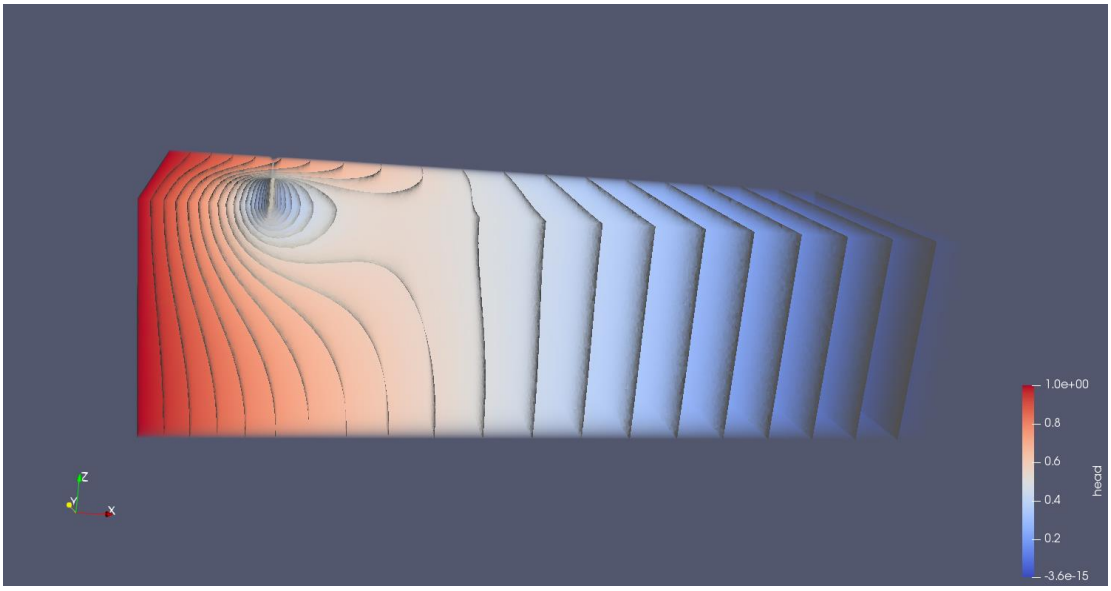

Figure 2.6 Contours of head (spaced 0.5 m) for model 40 m deep, L1 = 20 m, L2 = 130 m, W = 100 m, l_{lat} = 50 m, contrast 12

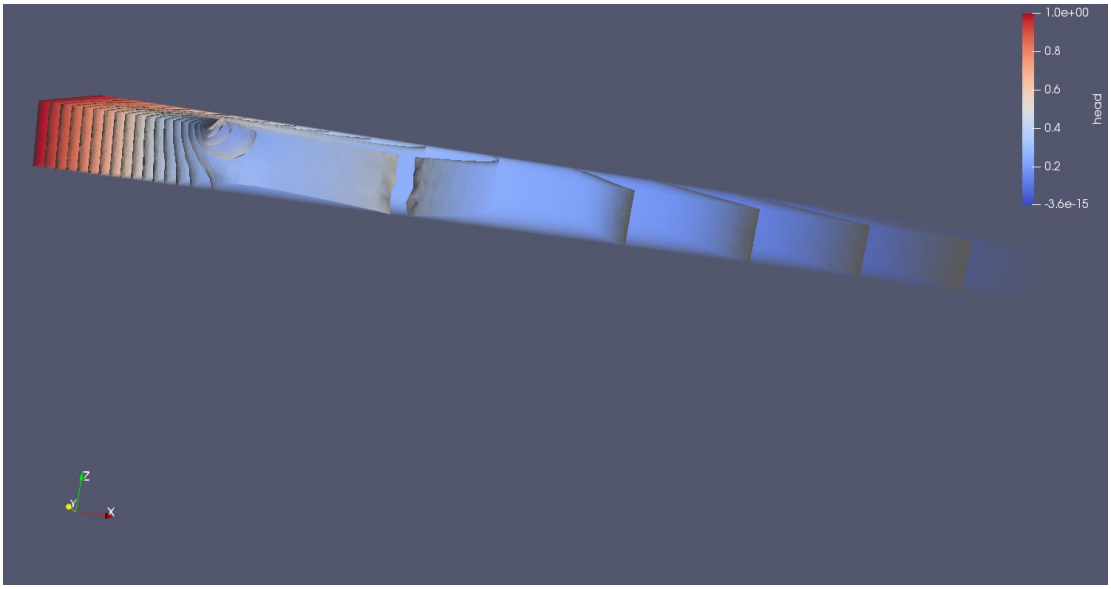

Figure 2.7 Contours of head (spaced 0.5 m) for model 8 m deep, L1 = 20 m, L2 = 130 m, W = 100 m, l_{lat} = 50 m, contrast 12

2.4.6 Effect of hydraulic conductivity contrast on the 3D factor

The effect of hydraulic conductivity contrast on the 3D factor was studied by changing the contrast from 4 to 8, for a fully developed pipe and a lateral pipe of 50 m in phase 1a. The effect is presented in Table 2.11 . The effect is considerably larger than the effect of barrier depth and aquifer depth in the phase 1a models.

Table 2.11 Effect of hydraulic conductivity contrast for partially developed pipe with lateral length of 50 m for λ 130 m, depth 40 m, aquifer width100 m, barrier depth 2 m

%	F_{3D} [-] contrast of 4	F_{3D} [-] contrast of 8
99%	1.8	2.1
95%	1.3	1.4
90%	1.2	1.2

The effect was also analysed for a contrast of 4 and a contrast of 12 for all variations of phase 1b. The result is shown in Table 2.12 for a 40 m deep model and in Table 2.13 for an 8 m deep model. The effect of contrast 4 as opposed to 12 is slightly larger in the 8 m deep model than in the 40 m deep model. The maximum effect of contrast is in the order of 40%. The effect of contrast in combination with aquifer width (W), leakage length (L2) and floodplain length (L1) is shown in the sections that relate to those effects.

Table 2.12 Effect of hydraulic conductivity contrast for partially developed pipe with lateral length of 50 m for models with λ 130 m, depth 40 m, aquifer width 100 m, barrier depth 2 m

%	F_{3D} [-] contrast of 4	F_{3D} [-] contrast of 12
99%	2.2	2.9
95%	1.5	1.7
90%	1.3	1.4

Table 2.13 Effect of hydraulic conductivity contrast for partially developed pipe with lateral length of 50 m for models with λ 130 m, aquifer depth 8 m, aquifer width 100 m, barrier depth 2 m.

%	F_{3D} [-] contrast of 4	F_{3D} [-] contrast of 12
99%	2.6	3.6
95%	1.8	2.2
90%	1.6	1.8

2.4.7 Effect of leakage length

The effect of the leakage length is investigated by using L2 values (representative of the leakage length) of 50 m, 130 m and 200 m. The effect is shown in the tables below. The effect is negligible for both contrasts. (note the contrast is varied by changing barrier hydraulic conductivity, not the conductivity of the aquifer as this would affect the leakage length).

Table 2.14 Effect of leakage length for partially developed pipe with length of 50 m and a contrast of 4 (depth 40 m, aquifer width 100 m, barrier depth 2 m)

%	F_{3D} [-] λ 50 m	F_{3D} [-] λ 130 m	F_{3D} [-] λ 200 m
99%	2.1	2.2	2.2
95%	1.5	1.5	1.5
90%	1.3	1.3	1.3

Table 2.15 Effect of leakage length for partially developed pipe with length of 50 m and a contrast of 12 (depth 40 m, aquifer width 100 m, barrier depth 2 m)

%	F_{3D} [-] λ 50 m	F_{3D} [-] λ 130 m	F_{3D} [-] λ 200 m
99%	2.8	2.9	2.9
95%	1.7	1.7	1.7
90%	1.4	1.4	1.4

It is noted here that the flow towards the hinterland is simulated using a boundary condition at the rear of the model (i.e. the distance L2). This results in a slightly different flow pattern than the simulation of a semi-permeable layer. It is recommended for phase 3 to simulate the blanket layer, as this represents reality better.

2.4.8 Effect of aquifer width

The effect of aquifer width is analysed in combination with the effect of floodplain length (L1) in phase 1b, as the combination of these is important for the convergence of flow. Plainly stated, with a longer floodplain flow can converge from a larger width upstream to the pipe, and then a larger width has more effect. Furthermore, the effect is larger at a higher contrast. This is summarised in the figure below which shows the effect of model width on the 3D factor relative to the 3D factor that is computed for a 100 m wide model.

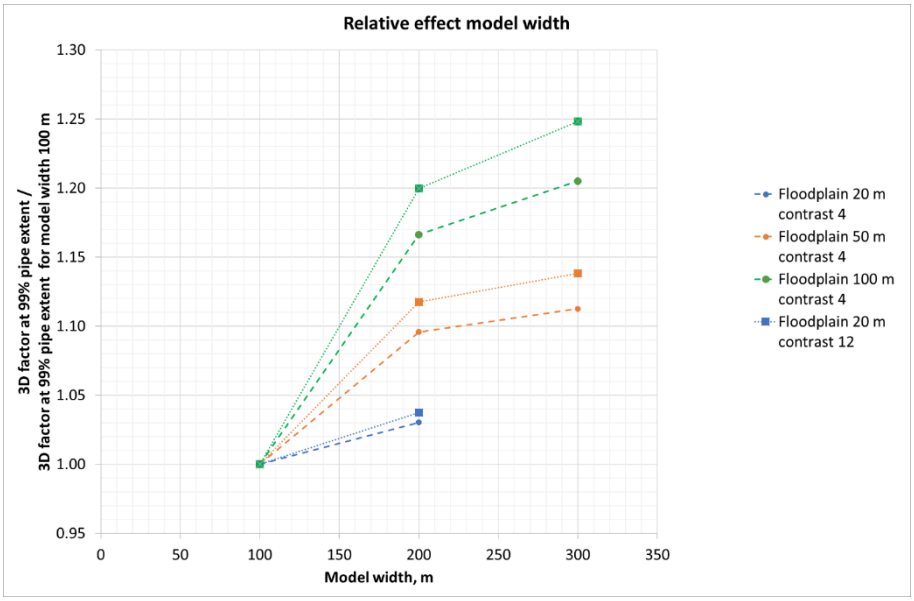

Figure 2.8 Effect of model width, refer to text for details

2.4.9 Effect of a perpendicular pipe running to the barrier

In the current models, only the pipe parallel to the barrier in the background sand is modelled for both the 2D version and the 3D versions of the computations.
In practice there will be one or more pipes that run to the barrier below the blanket, perpendicular to the barrier. This might possibly affect the magnitude of the 3D effect. The influence is investigated for a pipe that runs to the barrier in the centre of the model, this pipe has a width of 0.4 m (in a half space model, the pipe is modelled with 0.2 m). The pipe is modelled 50 m in front of the barrier in the model with a leakage length of 130 m.

It is noted that modelling this pipe requires significant mesh refinements (as the pipe is 0.2 m wide, the refinement is to 0.1 m elements in the pipe running up to the barrier but also in the

area upstream of the barrier). The model with the fine mesh is used as the mesh refinement was too large for the model with a coarser mesh.

The perpendicular pipe does reduce the modelled gradient in the barrier, and this effect is largest in the centre of the model as shown below for contrast 4.

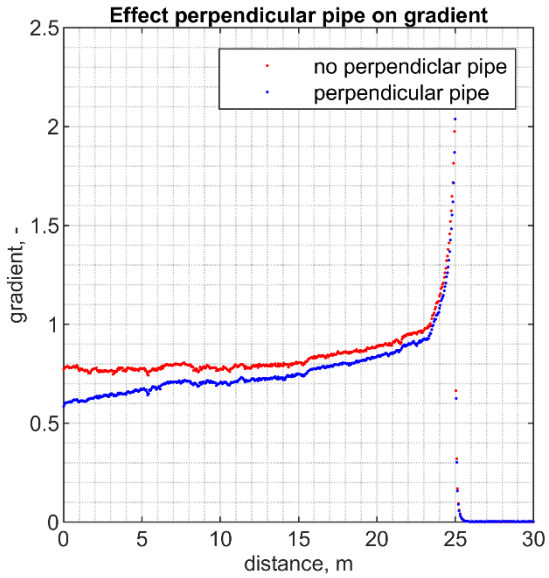

Figure 2.9 Illustration of horizontal gradients along the width of the aquifer for the case with a perpendicular pipe running to the barrier (blue) and the case where there is no perpendicular pipe (red)

The results are shown in the tables below for contrasts 4 and 12. The 3D effect is approximately 5-10% lower when the perpendicular pipe is modelled. This can be considered an insignificant effect as compared to the other uncertainties. Contrast doesn't affect the difference significantly.

Table 2.16 Effect of perpendicular pipe (50 m long and 0.2 m wide) for model with L 130 m, contrast 4, model width 100 m, pipe parallel to the barrier 50 m, aquifer depth 40 m and barrier depth 2 m with a fine mesh

%	F_{3D} [-] no perpendicular pipe	F_{3D} [-] with perpendicular pipe	$\frac{F_{3D}\,[-]\ \textit{with perpendicular pipe}}{F_{3D}\,[-]\ \textit{no perpendicular pipe}}$
99%	2.2	2.0	0.91
95%	1.5	1.4	0.93
90%	1.3	1.2	0.92

Table 2.17 Effect of perpendicular pipe (50 m long and 0.2 m wide) for model with L 130 m, contrast 12, model width 100 m, pipe parallel to the barrier 50 m, aquifer depth 40 m and barrier depth 2 m with a fine mesh

%	F_{3D} [-] no perpendicular pipe	F_{3D} [-] with perpendicular pipe	$\frac{F_{3D}\,[-]\ \textit{with perpendicular pipe}}{F_{3D}\,[-]\ \textit{no perpendicular pipe}}$
99%	2.9	2.7	0.93
95%	1.7	1.6	0.94
90%	1.4	1.3	0.93

2.4.10 Effect of anisotropic permeability

In naturally deposited sands, the hydraulic conductivity may be different (lower) in the vertical direction than in the horizontal direction. The ratio of the vertical to the horizontal hydraulic conductivity is expressed by the anisotropy ratio *A.* For river bed deposits, values in a range of 1-5 may be expected, and for floodplain deposits this value may even be higher, up to 10 (Van Beek et al. 2020). Measurements at the pilot location even indicate higher values could be possible (Rosenbrand & Koelewijn, 2020a) Therefore the effect of the factor 15 is investigated.

Note that the barrier remains isotropic as this is a man-made artefact. For the anisotropic calculations strictly speaking the leakage length will be affected as well, however, the effective leakage length is not modified in the model as this was found to have little effect on the results in the prior computations (i.e. the model length is not modified). The effect of the leakage length is discussed further in the summary. The contrast is expressed relative to the horizontal permeability. Thus, only the vertical hydraulic conductivity is reduced in order to model anisotropy.

Anisotropy results in lower heads along the top centreline of the model, and accordingly lower gradients in the barrier as shown in the figures below. Anisotropy controls the distribution of water towards the barrier and the downstream edge of the model: due to the lower vertical hydraulic conductivity in the anisotropic model, less flow will converge towards the pipe and more towards the downstream edge of the model, resulting in lower gradients in comparison with the isotropic case.

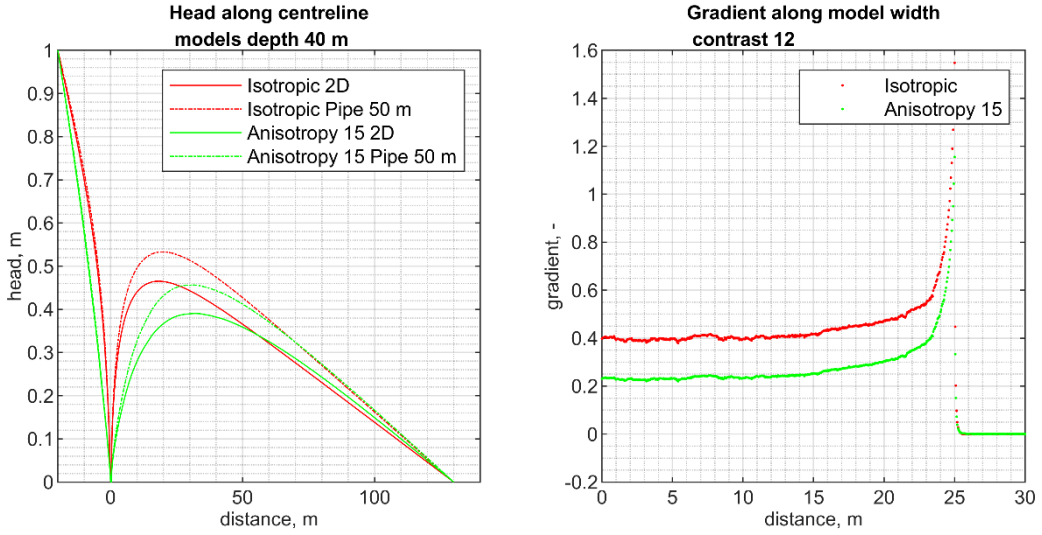

Figure 2.10 Illustration of head profile along the x axis at the centreline of the model (left hand side) and horizontal gradients over 0.1 m upstream of the tip of the pipe in the barrier along the width of the aquifer (right hand side)

The 3D effect is larger for the anisotropic case, as shown in the tables below. This is probably because the 3D effect is due to convergence of flow from the side, the z direction in these models, and the anisotropy affects the vertical (y direction). This is explained further in the summary.

Table 2.18 Effect of anisotropy of the aquifer (vertical aquifer permeability is 1/15 of horizontal aquifer permeability) for model with L 130 m, contrast 4, model width 100 m, pipe parallel to the barrier 50 m, aquifer depth 40 m and barrier depth 2 m with a fine mesh

%	F_{3D} [-] isotropic	F_{3D} [-] anisotropy 15	$\frac{F_{3D}\,[-]\,\boldsymbol{isotropic}}{F_{3D}\,[-]\boldsymbol{anisotropy15}}$
99%	2.2	2.6	1.20
95%	1.5	1.8	1.18
90%	1.3	1.5	1.14

Table 2.19 Effect of perpendicular pipe (50 m long and 0.2 m wide) for model with L 130 m, contrast 12, model width 100 m, pipe parallel to the barrier 50 m, aquifer depth 40 m and barrier depth 2 m with a fine mesh

%	F_{3D} [-] isotropic	F_{3D} [-] anisotropy 15	$\frac{F_{3D}\,[-]\,\boldsymbol{isotropic}}{F_{3D}\,[-]\boldsymbol{anisotropy15}}$
99%	2.9	3.7	1.29
95%	1.7	2.1	1.24
90%	1.4	1.7	1.18

2.5 Summary

The analysis in this section has demonstrated that the 3D effect is complex and that the relative importance of the effect of a given parameter depends on the other parameters in the model.

The parameter ranges investigated here are based on what might be expected at the pilot location. For those ranges the following effects are found:

- Barrier depth (between 1 or 2 m) has a negligible effect
- Leakage length has a relatively small effect
- The extent of the pipe along the barrier has a very strong effect:
  - *A shorter pipe gives a larger 3D effect*
- The effect of the depth of the aquifer plays a non-negligible role
  - *A shallower aquifer gives a larger 3D effect*
- The effect of the width of the aquifer plays a non-negligible role:
  - *A wider aquifer gives a larger 3D effect*
- The effect of the hydraulic conductivity contrast of the aquifer plays a non-negligible role:
  - *A higher contrast gives a larger 3D effect*
- The effect of the length of the floodplain of the aquifer plays a non-negligible role:
  - *A longer floodplain gives a larger 3D effect*
- The effect of modelling a pipe perpendicular to the barrier is relatively less important:
  - *Modelling this pipe slightly reduces the 3D effect*
- The effect of an anisotropic aquifer affects the 3D effect:
  - *The 3D effect increases with anisotropy, and the effect is larger for a higher contrast.*

2.5.1 Conceptual model

The influence of factors on the gradients inside the barrier and on the 3D, effect is complex and can be counter intuitive. A conceptual model aids in understanding the effect of individual parameters and the combination of parameters. This is described in this section.

The effect of parameters on the 3D effect is explained by first considering how parameters affect the flow field, and then how this affects the gradients in the barrier upstream of the pipe in 2D and in 3D. Note that this model explains the expected effects, the significance of these depends on the magnitude of the effect, which is not explained in the conceptual model as this is strongly dependent on the relative size of all other effects.

For simplification, we consider the flow field in terms of the flow entering the barrier from the upstream side; and inside the barrier the distribution between flow to the pipe and flow to the polder.

In the table below, a 3D situation is understood as a model where the pipe has only progressed a limited distance L_{lat} parallel to the barrier. A 2D situation is when the pipe has progressed along the entire width of the model, W.

Figure 2.11 Summary of effect of parameters on gradients and 3D effect

Parameter or cluster of parameters	Effect on flow entering the barrier	Effect on distribution of flow the flow inside the barrier between pipe and polder	Effect on gradients in 2D	Effect on gradients in 3D and 3D effect
Shape: **Length of upstream floodplain, L1** **Depth of aquifer, D** **Width of aquifer, W**	The width of the model is only relevant for 3D: in combination with a larger L1, flow converges from a larger area to the pipe for a larger W. Depth affects flow in 2D and 3D. With a larger depth more flow can converge to the barrier, the effect is larger with a larger L1. In 3D with a smaller D, the flow from the side forms a relatively larger component of the total flow into the barrier. This can result in a larger 3D effect. The magnitude of the effect depends on the shape (relation L1, W, D), and distribution of flow between the pipe and the polder.	D affects the leakage length; refer to leakage length. The effect of W can be seen in relation to L_{lat}; refer to L_{lat}	More flow into the barrier leads **to higher gradients for larger D, and larger W.** A **larger L1 increases** convergence flow to the barrier from D, but also causes a larger head drop in the aquifer. The net effect is typically **lower gradient**	A **smaller D** results in less total flow to the barrier, **and lower 3D gradients** but the contribution of flow from the side is relatively larger, giving a **larger 3D effect**. The magnitude of the effect also depends on the shape (relation L1, W, D). **A larger W gives a higher 3D gradient, and a larger 3D effect**. The magnitude of the effect also depends on the shape (relation L1, W, D).
Anisotropy of the aquifer, A.	Similar to D, anisotropy affects flow from the depth to the aquifer. **A larger A reduces flow to the barrier.** In 3D with a larger A, the flow from the side (W) forms a relatively larger component of the total flow into the barrier, refer to comment in shape.	A affects the leakage length; refer to leakage length.	Less flow leads to **lower gradients for higher A.**	Due to less flow with larger A, **gradients are lower, but the 3D effect is larger** due to a relatively larger contribution of flow from the side.
Contrast, C	With a higher C the head in the aquifer is relatively higher than in the barrier, i.e. more convergence of flow to the barrier.	With a higher C flow will converge more to the pipe and less to the polder.	A **higher C results in lower gradients** despite more convergence of flow, due to a higher head drop in the aquifer.	A **higher contrast** enhances concentration of flow to the pipe, although **3D gradients are lower, the 3D effect is larger.**
L_{lat} only relevant for 3D	A higher L_{lat} will drain more water from the barrier and increase convergence of flow to the barrier	With a larger L_{lat} more flow leaves the barrier through the pipe as opposed to the polder.		**A larger L_{lat}** increases the outflow area and spreads the flow leaving the barrier. Despite larger flow to the barrier and to the pipe this results

Parameter or cluster of parameters	Effect on flow entering the barrier	Effect on distribution of flow the flow inside the barrier between pipe and polder	Effect on gradients in 2D	Effect on gradients in 3D and 3D effect
				in **lower gradients and a lower 3D effect.**
L2: representative for leakage length	A larger L2 will result in more convergence of flow to the barrier due to higher heads in the aquifer close to the barrier.	With a larger L2 flow inside the barrier will concentrate more to the pipe due to the higher heads in the aquifer close to the barrier	A higher **L2 results in higher gradients**	A **higher L2 increases gradients and the 3D effect** due to more concentration of flow to the pipe.

2.5.2 Recommendations

Considering all these factors it is recommended to derive a location specific 3D factor for application. This implies that the aquifer width, depth, hydraulic conductivity contrast, length of the floodplain and to a lesser extent leakage length are represented as well as possible. For uncertain parameters, the sensitivity of the results can be investigated. It is noted that the leakage length appears to be least important of these parameters based on current calculations, however, this might be due to the simplification used in the approach used in the current sensitivity analysis. This simplification might possibly also affect the modelled influence of the pipe running perpendicular to the barrier. For a field situation it is recommended to model the permeable cover layer and obtain a better representation. However, considering the small effect of the perpendicular pipe and the requirements for mesh refinement associated with modelling this, it is not recommended to model a perpendicular pipe for the field case.
In such a model, the effect of the lateral pipe development can be varied to determine the range of 3D factors that can be expected, as this parameter is not known a priori.

3 Phase 2: Sensitivity analysis with protrusion

In the second phase a sensitivity analysis is conducted in which the protrusion is modelled, to be able to assess both the vertical gradient, for fluidisation at the upstream side of the slope, and the gradient perpendicular to the slope.

3.1 Geometry and parameters

In this phase a more detailed geometry is used, which includes the protrusion, to assess the effect of parameters on the 3D factor that are related to this configuration. The geometry is illustrated below, showing a top and side view of the aquifer and the barrier. The situation is modelled in half-space: in the text, all dimensions are reported in full space. This model provides some more detail with respect to the protrusion and presence of the pipe.

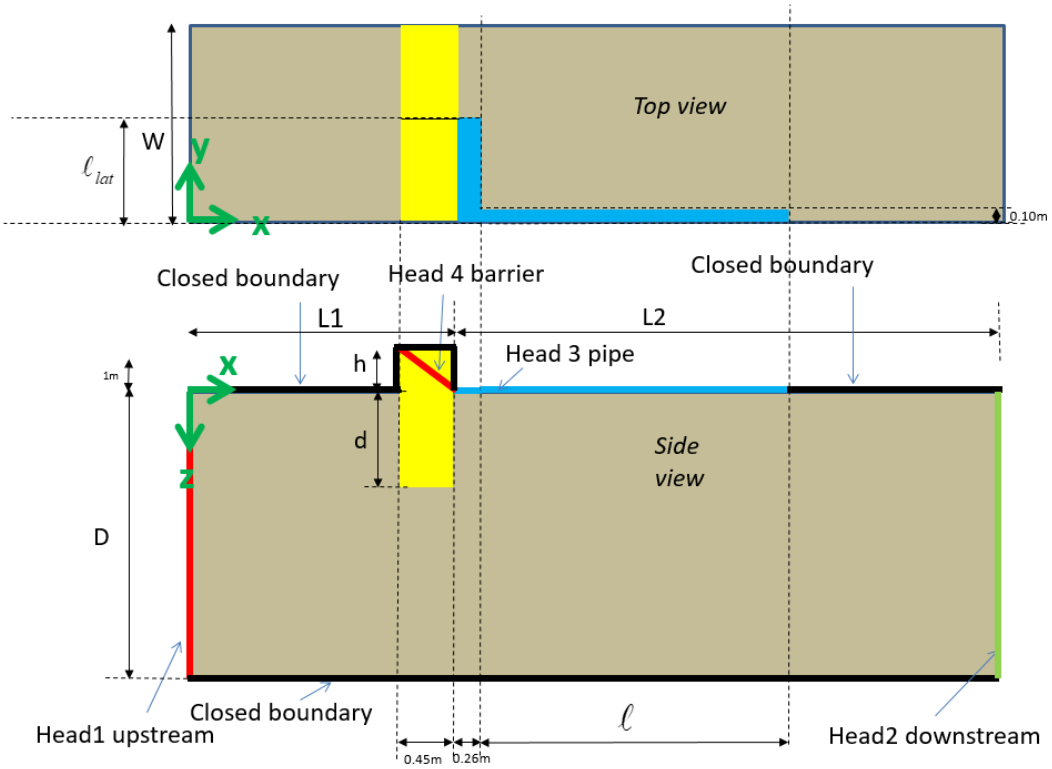

Figure 3.1 Axisymmetrical (half-space) geometry with protruding CSB (yellow) and pipe (blue)

The parameter variations that are applied are the lateral development and shape of the slope in the barrier and the pipe length ℓ. The geometry (L1, L2) is varied as well, as the sensitivity study indicated that geometry is relevant for the 3D effect. Details are provided in Table 3.1. The slope height is exactly 0.16 m. Given a width of 0.45 m this gives a slope angle of 19.57°.

Table 3.1 Parameter variation in phase 2 (full-space), the bold parameters are varied, non-bold are fixed, values that were used in the basis calculation are in Italics

Parameter	Symbol	Values
Thickness aquifer	D [m]	8, *20*, 40
Width aquifer	W [m]	100
Length CSB to downstream boundary	L2 [m]	110, *200*
Length CSB to upstream boundary	L1 [m]	20, 120
Width CSB	w [m]	0.45
Depth CSB	d [m]	1
Lateral pipe development	ℓ_{lat} [m]	1.2, 2.2, *3.2*, *100*
Height slope protrusion	h [m]	0.16
Slope angle	α [deg]	20
Side slope angle	β [deg]	20, *90*
Pipe zone downstream of CSB		0.26
Hydraulic conductivity CSB	k_{CSB} [m/s]	175
Hydraulic conductivity aquifer	k_s [m/s]	15
Hydraulic conductivity contrast CSB/aquifer	k_{CSB}/k_s [-]	11.7

The width of the barrier was increased to 0.45 m. The depth of the barrier was not varied, since it was found in phase 1, that its influence on the 3D factor was limited. The slope of the barrier may not be exactly 20 degrees, but since this parameter is difficult to vary in 3D numerical calculations, it is considered a reasonable starting point.

Most calculations are conducted with a vertical slide slope (Figure 2.3), although the sides of the slope will not be vertical in reality. To find out whether the concentration of flow is severely affected by vertical side slopes, the angle of the side slope was lowered to 20 degrees in some calculations.

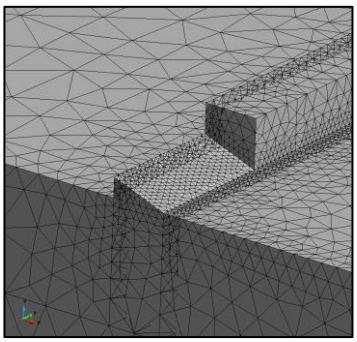

Figure 3.2 The basic configuration is with vertical side slopes

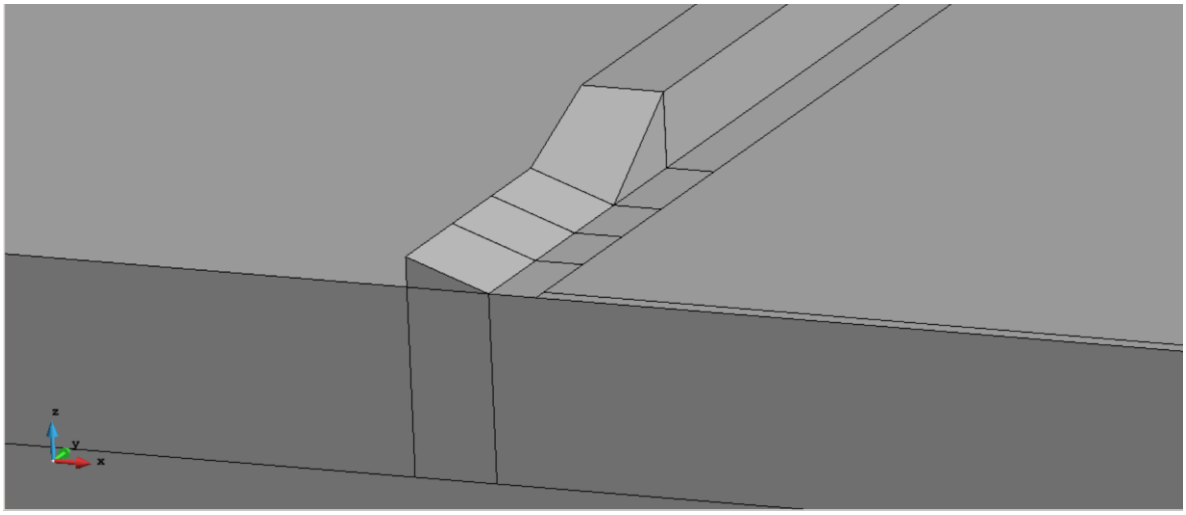

Figure 3.3 Erosion hole with inclined slope

For a barrier with a protrusion, two gradients are of importance: the vertical gradient at the upstream side of the barrier, that will lead to heave in the critical situation, and the gradient perpendicular to the slope (Figure 3.4). The vertical gradient was calculated as the average gradient over the protruding height of 0.16 m at the upstream side of the barrier, for each location along the width of the aquifer.
The gradient perpendicular to the slope was calculated halfway the slope over a distance of 0.10 m, for each location along the width of the aquifer. Analysis of this gradient is useful to check whether the slope angle used in 2D calculations is representative for practice.

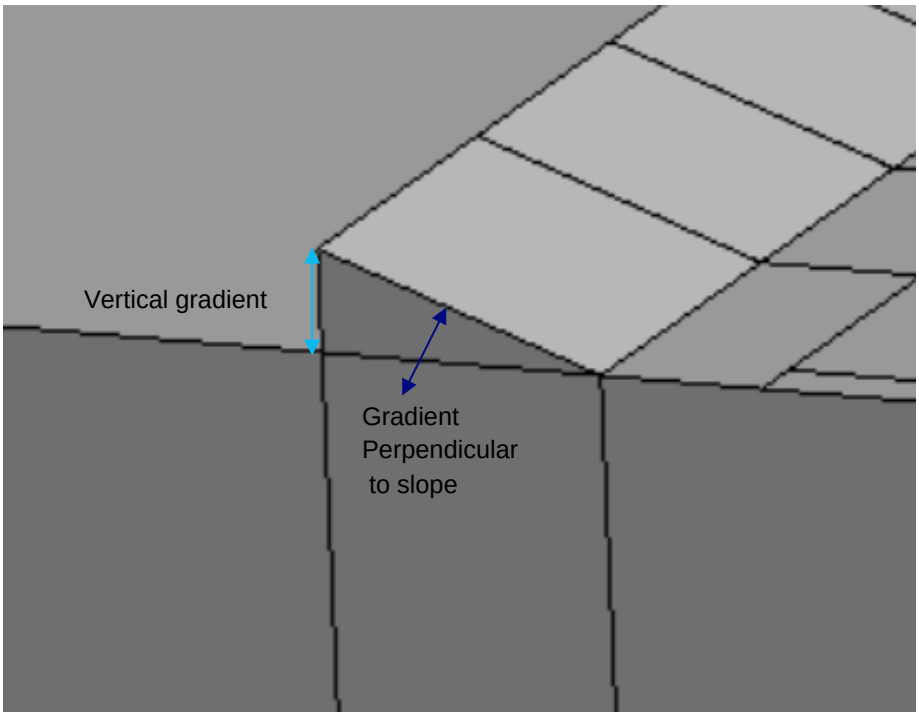

Figure 3.4 Relevant gradients for barrier with protrusion

The table below gives the computed scenarios.

Table 3.2 Overview computed scenarios (parameters are in full-space, computations in half-space)

Scenario	Width model	Thickness sand layer	Distance inflow-CSB	Distance CSB-outflow	Length normal pipe	Width erosion hole in protrusion	Width pipe parallel to inkassing	Width pipe perp. To CSB	Width CSB	Slope CSB	Height slope CSB	Side slope	k_CSB/ k_sand
	[m]	[m]	[m]	[m]	[m]	[m]	[m]	[m]	[m]	[deg]	[m]	[deg]	
1	100	20	20	200	200	100	100	50	0.45	20	0.16	nvt	11.7
2	100	20	20	200	200	100	100	0.1	0.45	20	0.16	nvt	11.7
2b	100	20	120	200	200	100	100	0.1	0.45	20	0.16	nvt	11.7
3	100	20	20	200	200	1.2	1.2	0.1	0.45	20	0.16	90	11.7
4	100	20	20	200	200	2.2	2.2	0.1	0.45	20	0.16	90	11.7
5	100	20	20	200	200	3.2	3.2	0.1	0.45	20	0.16	90	11.7
6	100	20	20	200	200	3.2	3.2	0.1	0.45	20	0.16	20	11.7
6b	100	20	120	200	200	3.2	3.2	0.1	0.45	20	0.16	20	11.7
G1	100	40	120	110	25	100	100	0.1	0.45	20	0.16	nvt	11.7
G2	100	40	120	110	25	3.2	3.2	0.1	0.45	20	0.16	20	11.7
G1b	100	8	120	110	25	100	100	0.1	0.45	20	0.16	nvt	11.7
G2b	100	8	120	110	25	3.2	3.2	0.1	0.45	20	0.16	20	11.7

3.2 Mesh

An unstructured mesh with quadratic elements was applied. A 5 m mesh was created with a mesh refinement of 0.05 m at the slope surface in the CSB.

It is noted that the effect of mesh size (mainly around the CSB and probably also the perpendicular pipe) on the results was not analysed.

3.3 Results

The figures below give examples of the gradients along the width of the aquifer (half-space results). Similar to the results for the horizontal gradient in phase 1, the vertical gradient is constant along the width of the aquifer for a fully developed lateral pipe. For a partially developed pipe, the gradients peak at the corner of the eroded zone. This peak value is reduced when the side slopes are modelled more realistically, which confirms the assumption in phase 1, that the peak value overestimates the 3D factor if the gradient at the extreme of the pipe is used.

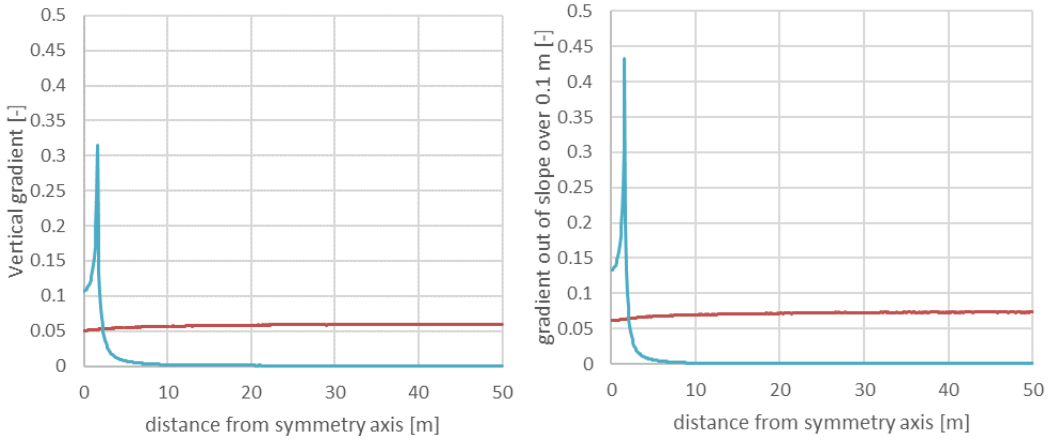

Figure 3.5 Vertical gradient at the upstream side of the slope (left figure) and gradient perpendicular to the slope (right figure), plotted as function of the distance from the symmetry axis, calculated for full lateral development – 2D (red) and partial lateral development (blue). Note that the gradients for the red line still vary due to the presence of a pipe towards the barrier

The figure below compares the results of a vertical and inclined side slope. This figure illustrates that the peak is indeed flattened. For a protrusion, it is expected that the slopes in the barrier will adjust until the gradient is in equilibrium with the slope angle, resulting in an elongated amphitheater, with slopes at the sides which are shallower than those in the middle. As a result of this development, it is expected that the peaks at the sides will flatten.

Considering longitudinal shape of the amphitheatre, the gradient will remain highest near the corners and the effect of the shape of the side wall and its effect on the local gradient is difficult to assess. Therefore, for the purpose of comparing vertical gradients to gradients out of the slope, the value along the central axis is selected here as representative for the 3D effect.
The gradient perpendicular to the slope was calculated to find out whether the load on the slope is increased in a 3D situation: for this gradient the centre gradient is selected as well, as representative for the 3D effect. Due to the presence of a pipe, the horizontal gradient is not constant along the width in the calculations in which the lateral pipe development equals the full width (‘2D equivalents’). For the calculation of the 3D factor, the center gradients in the calculation with partial lateral pipes are divided by the center gradients of their 2D equivalents.

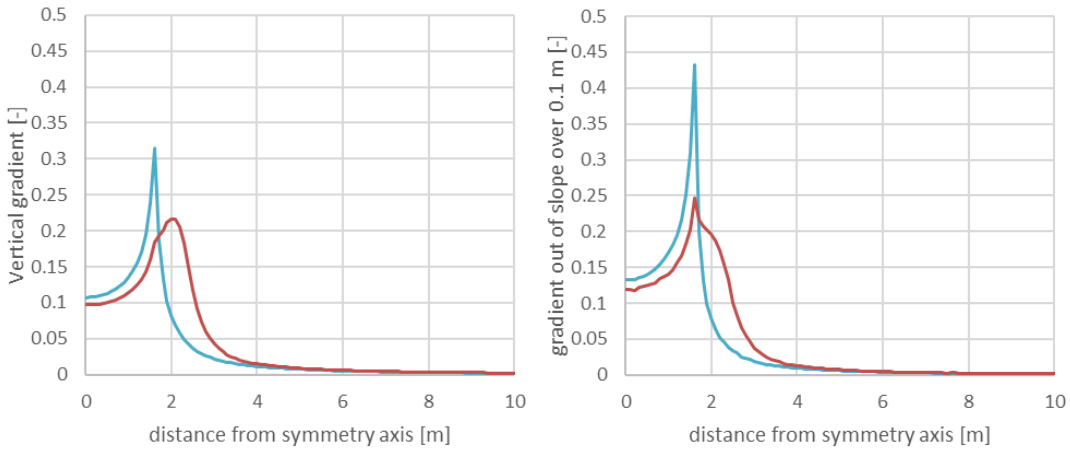

Figure 3.6 Vertical gradient at the upstream side of the slope (left) and gradient perpendicular to the slope (right) across the width of the aquifer, calculated for partial lateral development with vertical slope (blue) and inclined slope (red)

The table below gives a summary of calculated 3D factors per scenario.

Table 3.3 Summary of calculated 3D factor per scenario

3D scenario	Compared with 2D scenario	Width erosion hole [m]	Side wall erosion hole	Thickness aquifer [m]	Ratio inflow boundary-CSB and CSB-outflow boundary	3D factor outward gradient in centre hole	3D factor vertical gradient in centre hole
3	2	1.2	vertical	20	0.10	3.8	3.6
4	2	2.2	vertical	20	0.10	2.6	2.6
5	2	3.2	vertical	20	0.10	2.2	2.1
6	2	3.2	inclined	20	0.10	1.9	1.9
6b	2b	3.2	inclined	20	0.60	3.1	3.1
G2	G1	3.2	inclined	40	1.09	2.7	2.7
G2b	G1b	3.2	inclined	8	1.09	4.3	4.2

When the perpendicular and vertical gradients are compared, it is found that both respond in the same way to all variables (Figure 3-6). This confirms that the 3D effect is largely controlled by the flow towards the barrier and to a lesser extent by the location in the barrier. This also means that the simplification in phase 1 most likely represents the 3D effect well, at least in a qualitative manner.

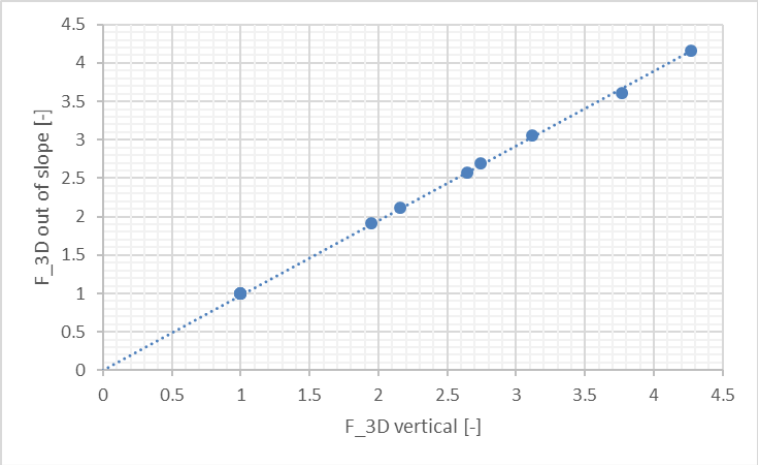

Figure 3.7 3D factors for gradients out of the slope plotted versus 3D factors for vertical gradients, for all simulations in phase 2

Since the 3D factors are essentially the same for vertical gradients and for gradients perpendicular to the slope, for all results only the vertical gradients are provided.

It is evident that the flattened side wall calculations provide more reliable values for the 3D factor. The flattening of the side wall eliminates the peak, and provides a decent estimate of the gradient in the corner of the elongated amphitheatre. However, the flattened side wall calculations are not suitable for deriving a 3D factor, since they are very complicated. Therefore a comparison is made between the vertical gradients of simulations with vertical and flattened side wall (simulations 5 and 6 respectively).

It is likely that vertical heave will occur at a location where the vertical distance is lowest: for the vertical side wall calculation, this can be anywhere along the slope; for the flattened side wall calculation, it is unlikely that the vertical fluidisation will take place along the flattened side wall.

Therefore the maximum representative vertical gradient in the situation with a flattened side wall, is at the point where the vertical distance is smallest. In simulation 6, in which the side wall is flattened, the maximum vertical gradient, which is found at a distance of 1.6 m from the symmetry axis, is equal to 0.18. For simulation 5, which is equivalent to 6, except for the side wall, which is vertical, the maximum vertical gradient is controlled by the peak. In this simulation, the vertical gradient equals 0.18 at a distance of 0.25 m from the side wall, which is about 84% of the half-space transverse length.

Part of the reduction in vertical gradient due to the flattened side wall is related to the additional transverse length that is created by the flattened side wall. This effect is relatively large for these simulations, since the lateral pipe development is rather short (3.2 m in full-space). Therefore, it can be expected that for larger lateral development of the pipe, as will be likely in practice, the reduction is somewhat smaller. The distance will not vary a lot though, since the gradient is quite steep in this area.

It can be questioned how to extrapolate this finding to larger lateral pipe lengths. If the distance at which the vertical gradient is comparable is an absolute distance, the observed distance of 0.25 m here is a minimum value. If a relative distance is more appropriate, a value of 90% is expected to be reasonable. Considering this, in the following chapters several relative distances are evaluated.

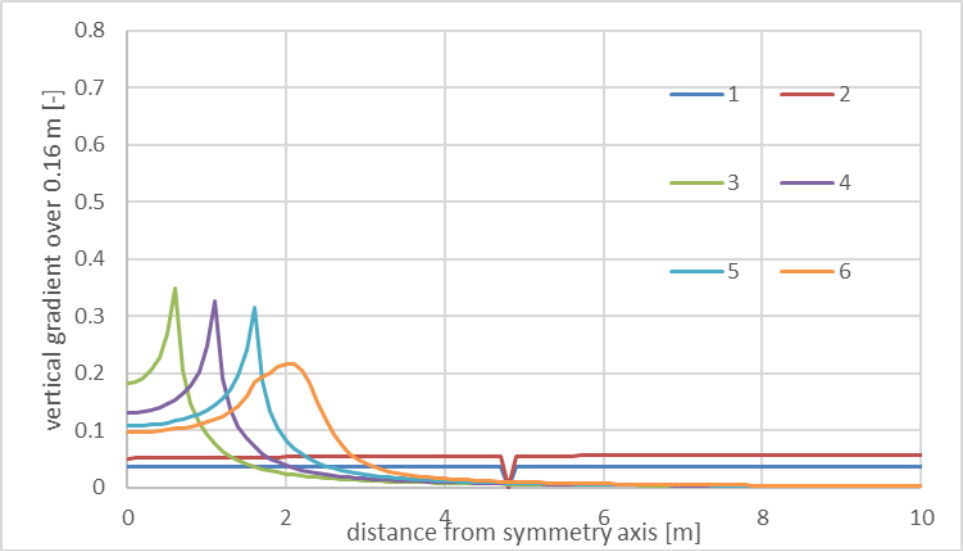

Figure 3.8 Vertical gradients for simulations 1-6 (1-5: vertical side wall and varying lateral pipe length, 6: as 5, but with flattened side wall)

3.3.1 Results aquifer depth

To confirm conclusions of Phase I, in which it was found that an increase of depth leads to a reduction of the 3D factor, the aquifer depth was varied in this phase too. Table 3.4 shows the results for an aquifer depth of 8 and 40, for both the second phase (vertical gradient) and the first phase (horizontal gradient – permeability contrast of 12).

Table 3.4 shows that the reduction in aquifer depth from 40 to 8 causes an increase of the 3D factor by over 50%. This effect is more severe than for the situation in phase I. Probably this is related to the length of the aquifer upstream of the barrier, which was larger for these calculations in phase II (120 m) than in phase I (20 m). Also the smaller lateral pipe development will have played a role.

Table 3.4 3D factors from phase I and II on the effect of aquifer depth

Phase		F_{3D} [-] aquifer depth of 40 m	F_{3D} [-] aquifer depth of 8 m	F_{3D_D8} / F_{3D_D40} [-]
II	i_vertical	2.7	4.2	1.5
I	i_hor - 99%	2.9	3.6	1.2
I	i_hor - 95%	1.7	2.2	1.3
I	i_hor - 90%	1.4	1.8	1.3

3.3.2 Results length upstream of the CSB

The length upstream of the barrier to the inflow controls the flow towards the barrier and is therefore expected to have some effect on the 3D factor. The upstream length was increased from 20 to 120 m (parameter values in full space: W=100 m, D=20 m, λ=200 m, ℓ_{lat} =3.2 m, pipe from downstream to upstream). The 3D factor for the vertical gradient increases from 1.9 to 3.1 as a result of the increase length upstream of the barrier. As such, the inflow length is an important parameter to estimate in practice.

3.3.3 Results lateral development

The effect of the lateral pipe development was studied for the standard parameters of (W=100 m, D=20 m, λ=200 m, upstream length of 20 m). The figure below illustrates that the 3D factor rapidly decreases with lateral development, as was already noted in chapter 2.

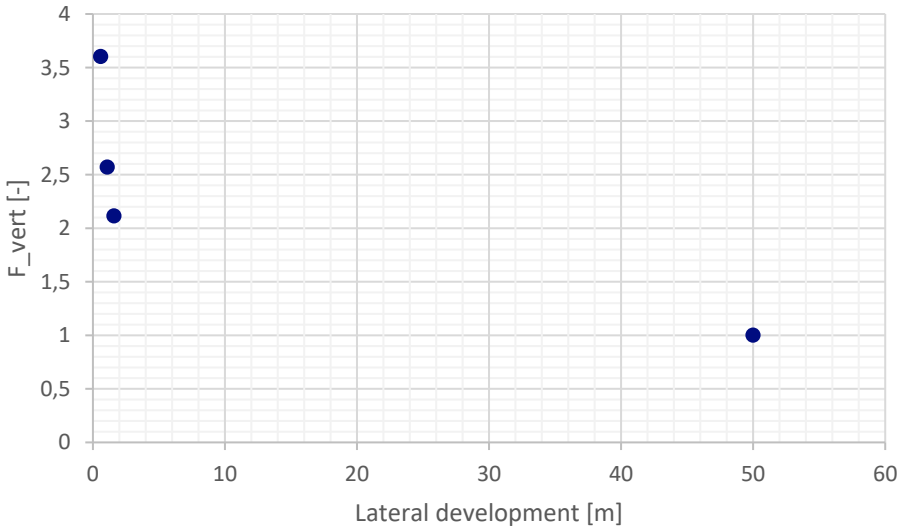

Figure 3.9 Effect of lateral pipe development on the 3D factor for the vertical gradient

3.4 Summary

The 3D effect is similar for the vertical gradients and the gradients perpendicular to the slope. This suggests that simple models, such as used in phase 1 in chapter 2, can be used to analyse the effect of parameters such as geometry and shape on the 3D effect, and the results are also applicable to other gradients in the barrier.

The simulations with vertical and flattened side walls of the slope illustrate that the peak in the corner of the slope is unrealistic. However, the flattened side wall calculations are too complex to be applied in practice. The comparison of flattened side wall and vertical side wall

calculations illustrates that the gradient at a distance of approximately 90% of the lateral half-space pipe length, or 0.25 m is representative for the determination of the vertical gradient, for this specific lateral pipe length. For longer lateral pipe lengths, it may also be 0.25 m or 90% of the lateral half-space pipe length. Considering the complexity of the calculations with protruding aquifer, only 1 slope angle is investigated. The location may be different for other slope angles. Therefore, in the following chapters different relative locations are evaluated.

4 Phase 3: 3D effect at Gameren

This chapter addresses the 3D effect for the pilot situation at Gameren. As the analysis in phase 1 indicated that location specific parameters affecting shape (length of floodplain, width, depth) as well as relating to permeability (permeability, leakage length, anisotropy, contrast), all affect the 3D effect the analysis is conducted by choosing values that are more or less representative for the pilot situation. A further analysis will therefore be required in order to establish a generic 3D effect.

The extent of the pipe along the barrier is an important unknown factor that has a very significant effect on the 3D effect as shown in phase 2. In this chapter, different lengths are used to determine a range of values for the 3D effect belonging to different lengths. The decision how to come to a design value based on these is part of the design philosophy.

Another important question to be addressed in the design philosophy is at which distance from the centre axis the 3D effect should be computed. In this chapter three options (90, 95, and 99%) are reported as well as the effect of integrating in between these distances.

4.1 Model description

The situation in Gameren is very heterogeneous, as described in Koelewijn et al. (2020). An aerial view of the area is shown below.

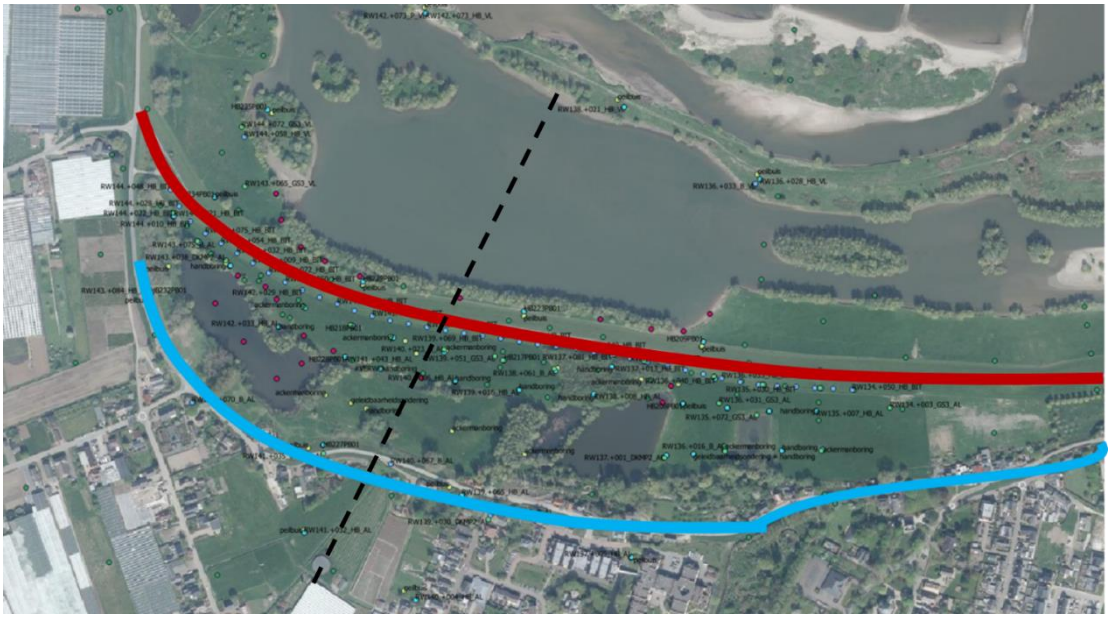

Figure 4.1 Areal view of the pilot location (modified after Koelewijn et al. 2020), red line indicates the embankment that will be reinforced, blue line indicates the former primary embankment. Dashed line indicates approximately the basis for the schematisation which is used

This indicates that the length of the floodplain on the river side, can vary. On the landside there are areas with water bodies making this variable as well. The subsurface schematisation for different profiles along the embankments is also variable. Based on descriptions in Koelewijn et al. (2020) and Rosenbrand and Koelewijn (2020a&b) the schematisations are selected in order to approximate the different situations.

Based on the findings in Section 2.5, the 3D effect is addressed for a configuration which is expected to be unfavourable for the 3D effect. This might not be unfavourable for the critical head drop. However, the intent is to determine a realistic 3D effect that provides a safe value for the whole spectrum of the 3D effect in this study. In the 2D cross sectional analyses, the critical head drop will be determined and corrected with the 3D effect. The current study addresses only determination of a 3D effect, not the safety philosophy associated with translating this to a 3D factor for design.

Characteristics for an unfavourable 3D effect are:

- A long floodplain: this allows for convergence of flow to the barrier over a larger area. This is the case for the profiles with an infilled sandpit in the floodplain
- A long leakage length in the polder, this causes more flow to the barrier. This is the case for the profiles without a clay pit in the polder.

These situations do occur together, so it is realistic to address these in this analysis.

For computational efficiency, half-space models are used. As shown in Figure 4.1 the area is not symmetrical, as is the assumption with half-space models. Also due to limitations of the numerical simulations with regards to mesh refinement, the model width has to be limited. Different models are used and the implications of this are discussed in Section 4.2 and 4.3 The basis schematisation used is shown in Figure 4.2, note that this is not an exact schematisation of a specific profile, but of a situation that is considered representative based on the available information. This model is referred to as the long model, as in subsequent steps shorter models were used in which the downstream boundary conditions were based on the results from the long model.

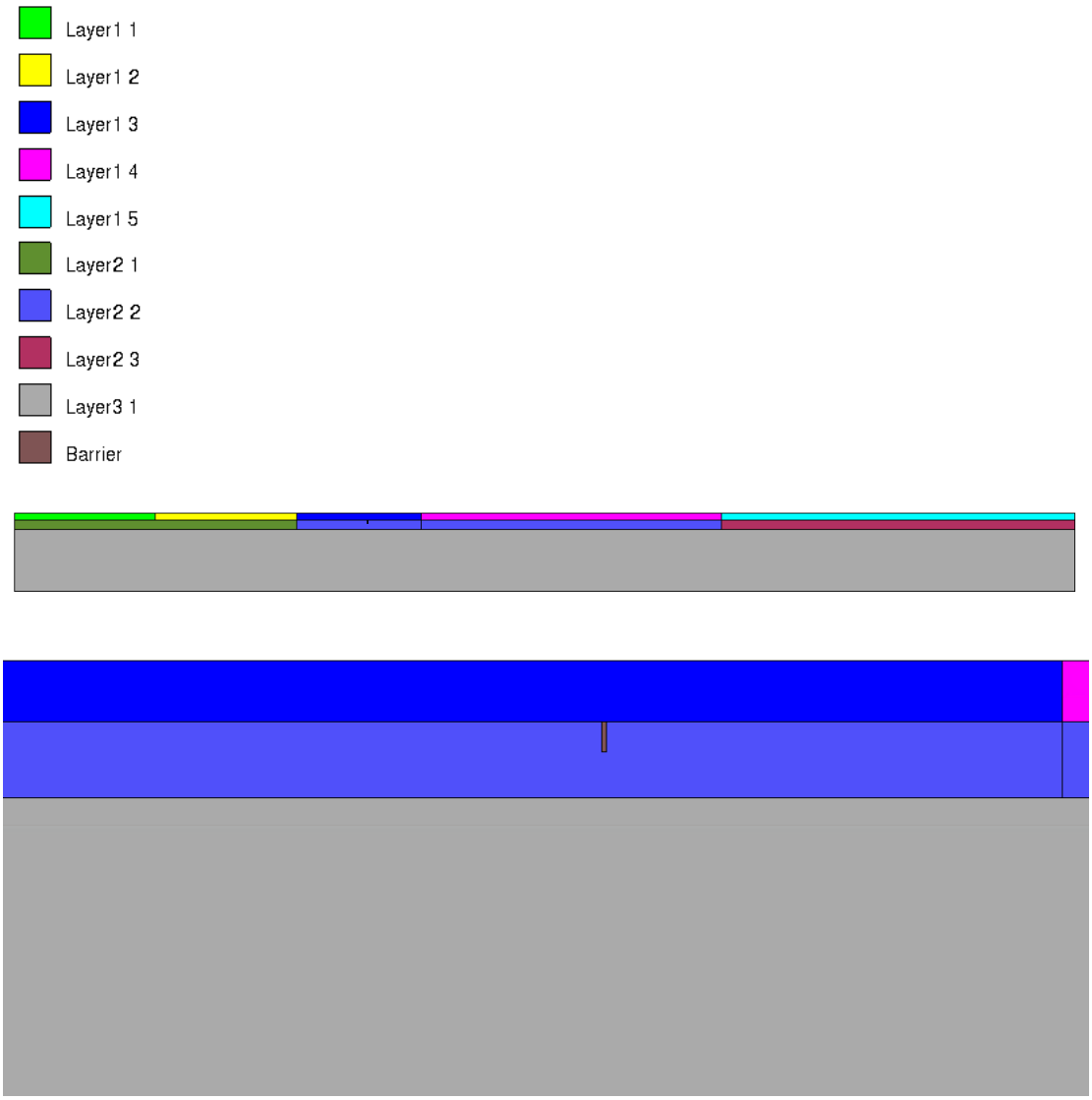

Figure 4.2 Long model & close up at the barrier, cross section (x-y plane). Layer 1 1, 1 2 and 2 1 are 'dredge', layer 1 3 and 1 4 are clay cover , layer 1 5 and 2 5 are clay cover Gameren, layer 2 2 is aquifer top and layer 3 1 is aquifer bottom. Left hand side is upstream, the embankments are not modelled as it will not contribute significantly to fluid flow. The model runs 200 m upstream of the barrier and 400 m downstream of the barrier. Refer to Figure 4.1 for indication of the location of the cross section

The half-space model shown above, with a width of 250 m was used to compute the head profiles for a pipe along the entire barrier (2D situation) and for a pipe of only 5 m (corresponding to a model width of 0.5 km with a 10 m pipe in a 'symmetrical model').
As the mesh refinement was an issue (discussed in Section 4.2), these models were used in order to determine the head in the aquifer at 60 m downstream of the barrier. Then 'short models' as shown below were used as well to assess the 3D effect. Note that in the short models the length of the floodplain (upstream of the barrier) is not reduced as this distance affects concentration of flow to the pipe.

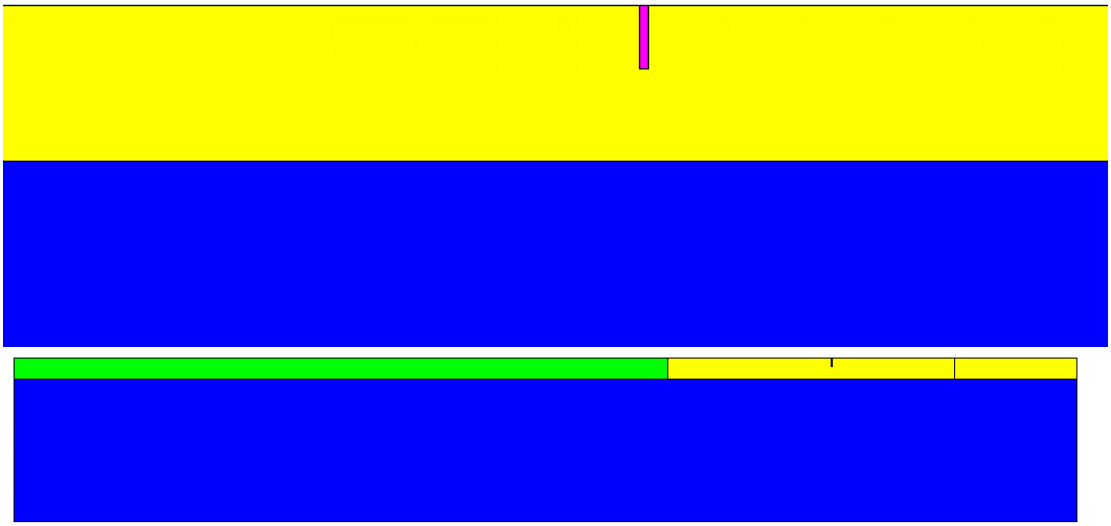

Figure 4.3 Short model, cross section (x-y plane). Green is 'dredge' layer yellow is aquifer top and blue is aquifer bottom, pink is barrier

In these short models, the cover layer below the embankment and in the polder are not modelled. Because the leakage length is long (ca. 240 m), and leakage along the part of the model that is cut off is accounted for by shortening the model and applying the head boundary, the leakage to the surface over the shorter distance can be neglected (as shown in Section 4.2)

Even in these models mesh effects played a role. This is an important limitation in the analysis of 3D effects with the current modelling approach. Various combinations of model width and mesh refinement were therefore used in order to assess the bandwidth of the uncertainty for the 3D effect that is associated with modelling choices.

The short models shown above, with a width of 250 m and with a width of 150 m ('small short') were used to compute the head profiles for a pipe along the entire barrier and for a pipe of only 5 m (corresponding to a model width of 0.5 km with a 10 m pipe, and a model width of 0.3 km with a 10 m pipe, in a 'symmetrical model').

4.1.1 Mesh

The program GiD, version 14 was used to generate meshes. In order to determine a 3D effect and gradients inside the barrier, local mesh refinement is essential. Note that many options for mesh refinement resulted in either an inability of the mesh generator to construct a mesh or resulted in meshes that were too large to compute in DgFlow. This limitation is considered significant for the feasibility of defining a 3D effect.

The local mesh refinement resulted in strong mesh refinement effects at specific locations in the model. This means that even in a '' 2D version' i.e. a 3D model where the pipe is developed along the entire width of the model , there are fluctuations in the modelled head profile (which would be expected to be constant, and serve as the basis to compare 3D effects as discussed in Section 4.2).
This problem was more notable in these models due to the larger size and more complex geometry than in the models in Phase 1.

Not all variations are reported, only the best variation for the ‘long model’ and the two best variations for the short and small short models. These are detailed in Appendix 7B.1.

4.1.2 Materials

The soil permeabilities are based on Koelewijn et al. (2020). The table below shows the materials and the hydraulic conductivity, in the short models, as the cover layer is not modelled the dredge layer has only 5/9ths the thickness of the thickness it has in the long models. Therefore, the hydraulic conductivity is also scaled by 5/9. Only the top aquifer is anisotropic with a 5 times higher horizontal permeability.

Table 4.1 material properties

Soil name	Hydraulic conductivity m/s	Hydraulic conductivity m^2
Top aquifer	3.69e-4 horizontal 7.38e-5 vertical	4.93e-11 9.86e-12
Bottom aquifer	3.69e-4	4.93e-11
Barrier	3.52e-3	4.71e-10
Clay cover	1.15e-6	1.54e-13
Clay cover Gameren	1.73e-5	2.31e-12
Dredge layer (in long model)	1.15e-6	1.54e-13
Dredge layer (in short model)	6.40e-7	8.56e-14

4.1.3 Boundary conditions

In the long models boundary conditions are shown below. The vertical left hand side boundary, and the top surface of the dredge layer have a river head as is also the case in the models Koelewijn et al. 2021).

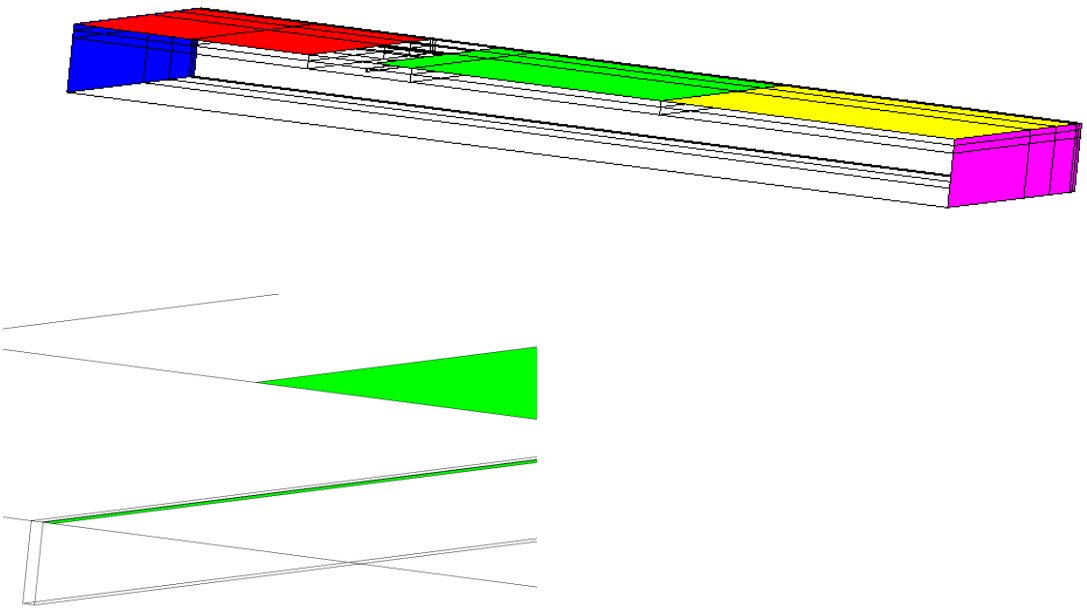

Figure 4.4 Boundary conditions for the long model (top entire model, bottom close-up at the barrier), blue and red are both river boundary (9 m + NAP). Green is the polder level 1.8 m + NAP, Yellow and Pink are the polder level at Gameren (1.8 m + NAP). The pipe in front of and 0.04 m inside the barrier (bottom figure) also has the green polder level boundary

For the short models, the river head boundary condition cannot be assigned over the entire floodplain (dredge layer), as this would involve a hydraulic short-cut with the aquifer at the outer toe of the dike (as the blanket below the dike and in the polder is not modelled see also Figure 4.3. However, due to the low hydraulic conductivity of the material that fills the former sand pit, this does not affect the head profile (as shown in Section 4.2).

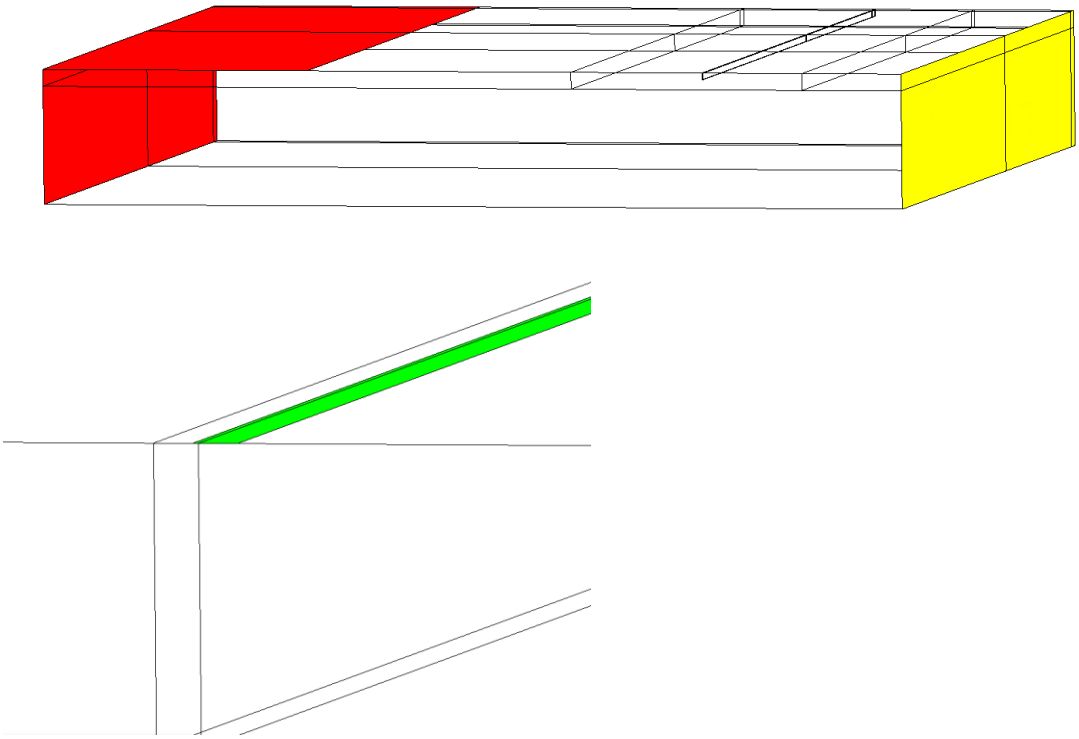

Figure 4.5 Boundary conditions for the short models (top entire model, bottom close-up at the barrier). Red is the river boundary (9 m + NAP). Green is the pipe boundary 1.8 m + NAP, Yellow is the polder level computed using the long models at this location (2.66 m for the 2D models with a complete pipe, 4.21 m for the models with a 5 m wide pipe in half space)

The pipe is modelled as a constant head boundary with the same water level as the polder (1.8 m +NAP), i.e. no head drop in the sand boil as it is uncertain whether there will be a suspension in the boil at the high flow rates associated with the critical head drop for the CSB. The pipe is 0.26 m wide in front of the barrier and 0.04 m inside the barrier. In the 2D-equivalent models the pipe extends along the entire width of the model. In the 3D models the pipe has a length of 5 m in the half space (i.e. 10 m in a symmetrical situation).

The polder boundary conditions in the long model are based on Koelewijn et al. (2021), i.e. 1.8 m +NAP (Figure 4.4). In the short models, the polder boundary is already at x= 60 m, the value assigned is obtained from the modelled head in the aquifer at that location from the large models. The figures below show that the head in the aquifer is relatively constant in a slice through the plane at x= 60 m. For the 2D situation, with a pipe parallel to the entire barrier the head is 2.66 m. For the 3D situation with a 5 m wide pipe (in half space) the head is 4.21 m.

Figure 4.6 Head at x=60 m in the long model, top model with pipe along entire barrier, bottom model with 5 m pipe (in half space)

Table 4.2 Summary of boundary conditions

Boundary name	**Value m + NAP**
River	9
Polder in long model	1.8
Polder Gameren in long model	1.8
Pipe	1.8
Polder short models 2D situation	2.66
Polder short models 5 m pipe (in half space)	4.21

4.1.4 Overview of calculations

Model name	Pipe extent half space m (full-space)	Model width half space m (in full space)	Comments
Long model 2D	250 (500)	250 (500)	Model includes the area behind the former primary dike
Long model pipe 5 m	5 (10)	250 (500)	Model includes the area behind the former primary dike
Short 2D f2	250 (500)	250 (500)	On polder side the model is 60 m (with BC, from Long model)
Short Pipe 5 m f2	5 (10)	250 (500)	On polder side the model is 60 m (with BC, from Long model)
Small Short 2D	250 (500)	150 (300)	On polder side the model is 60 m (with BC, from Long model)
Small Short Pipe 5 m	5 (10)	150 (300)	On polder side the model is 60 m (with BC, from Long model)
Long model 2D DeklaagVar	250 (500)	250 (500)	Model includes the area behind the former primary dike. Permeability of the cover layer is higher than in basis model
Long model pipe 5 m DeklaagVar	5 (10)	250 (500)	Model includes the area behind the former primary dike. Permeability of the cover layer is higher than in basis model
Small Short 2D	250 (500)	150 (300)	On polder side the model is 60 m (with BC, from Long model). Permeability of the cover layer is higher than in basis model
Small Short Pipe 5 m	5 (10)	150 (300)	On polder side the model is 60 m (with BC, from Long model). Permeability of the cover layer is higher than in basis model

4.2 Results and discussion 2D models

The head distribution in the long model shown below indicates that there is little flow to the polder area behind the former primary embankment and through the cover layer in the area between the current and former embankments. Inside the aquifer upstream of the barrier contour lines are approximately vertical and they curve towards the barrier.

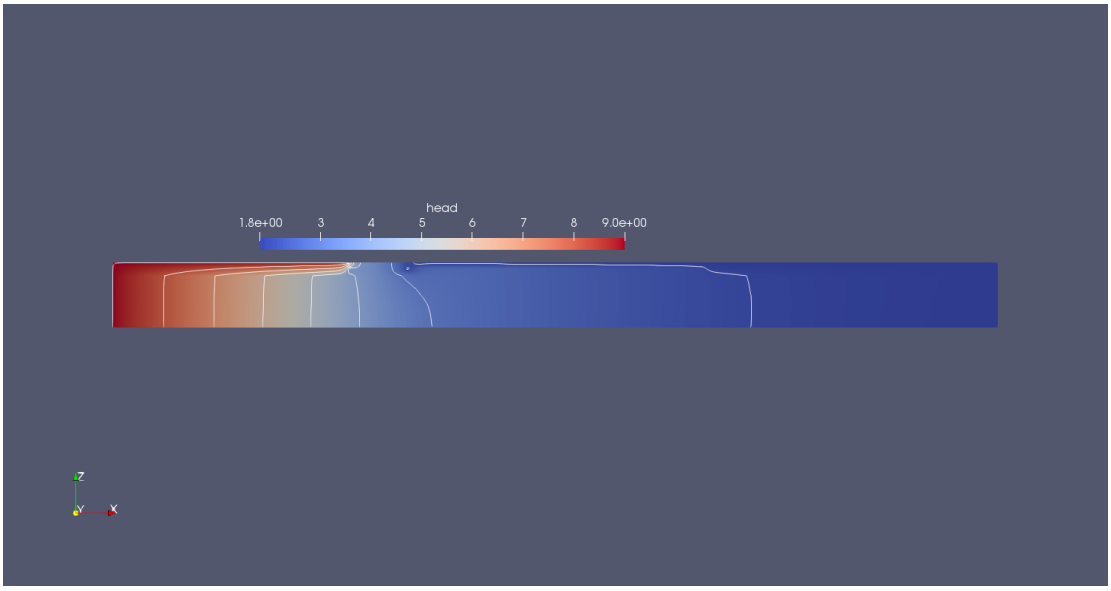

Figure 4.7 Head profile for long 2D model. Head contours spaced 1 m

In the short model contour lines in the aquifer upstream of the embankment are similar to the long model and the same holds for the curvature at the barrier.
These qualitative observations are confirmed by the head profiles in the next sections.

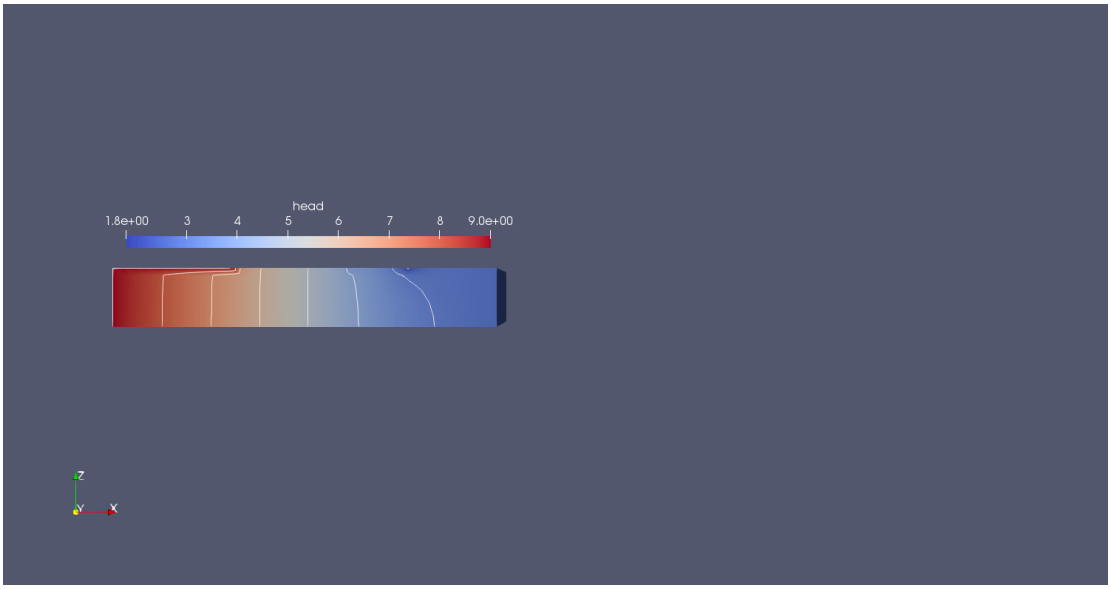

Figure 4.8 Head profile for long 2D model. Head contours spaced 1 m

4.2.1 Head profiles along x-axis

The head profile along the X axis at the elevation 0 m NAP (top of the barrier) is shown below. The similar profiles for the long and the short models shows that simplifications in the short models do not affect the groundwater profile in the aquifer close to the barrier. The difference in the head profiles between distance x = -200 and x = -40 m in the long model is due to the application of the boundary conditions as described in Section 4.1.3.

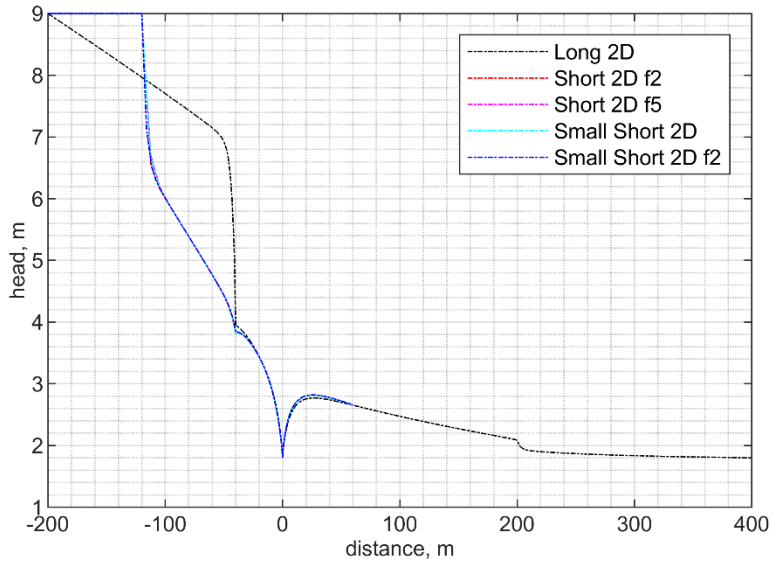

Figure 4.9 Head profiles along the centre of the models (along the x-axis in the plane y = 0 m). Note that the four short models head profiles overly therefore only small short 2D f2 is visible. (the distance 0 corresponds to the top downstream end of the barrier)

A close up of the head profiles inside the barrier is shown below

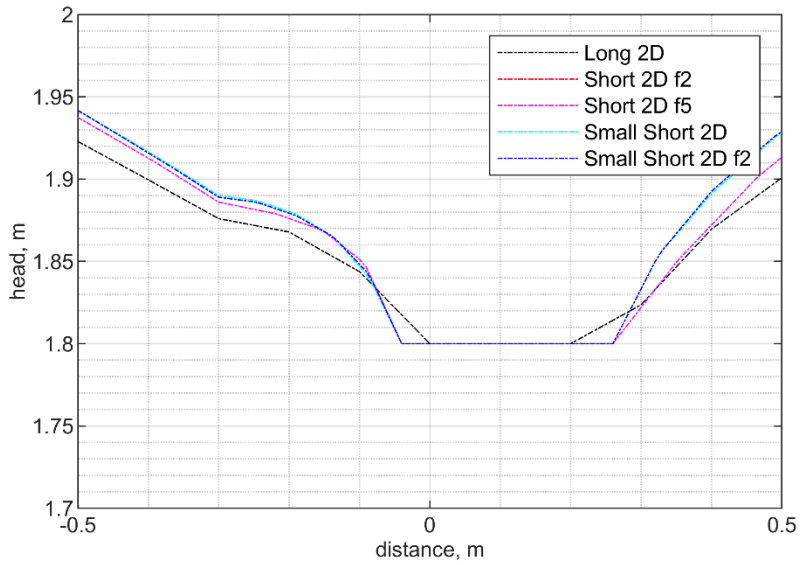

Figure 4.10 Head profiles along the centre of the models close up inside the barrier (along the x-axis in the plane y = 0 m)

These profiles show that the head in the longer model is slightly lower than in the short models. This is due to a lower level of mesh refinement in the long model, in which the base elements are 10 m large (refer to Appendix C for mesh refinement settings). This illustrates the need for a high level of mesh refinement, and the limitations of this approach for practice.

4.2.2 Head profiles inside the barrier (along model width) in 2D models

The 2D models (with a pipe developed fully along the barrier width should show a head profile that is approximately constant. This serves as the basis for assessing the 3D effect, as was also the case in Phases 1 and 2.

However, variation along the model width in head can be seen. The head profile at the location used to compute the gradient (0.1 m upstream of the pipe tip) is shown along the entire width of the models below.

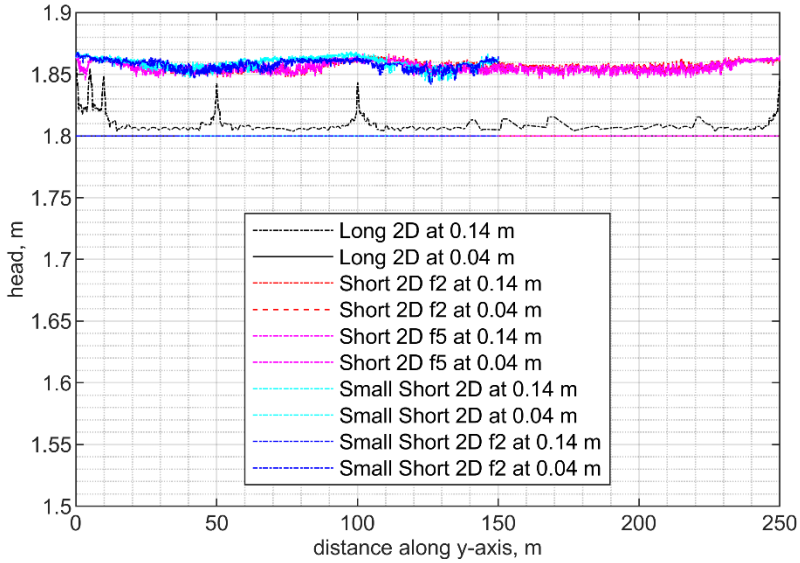

Figure 4.11 Modelled head along the width of the barrier

Here there is a clear difference between the head in the long and shorter models, due to the lower mesh refinement of the latter. Note however that the difference in absolute terms is in the order of ca. 5 cm. The impact on the computed gradients is large as shown in the next section.
The head at the pipe tip is equal in all models, showing that the boundary condition is applied as specified.

A problem is that in order to model the 3D models with a limited pipe extent, the location of the edge of the pipe (even if the boundary condition is assigned along the entire width for the 2D calculations) results in a surface inside the model at that location. This causes local refinements that lead to locally higher gradients at those locations. This is shown in the two figures below which zoom in on a smaller portion of the barrier width. Especially in the long model, there are clear spikes corresponding with surfaces whether the end of the pipe might be modelled. (note that in the models the pipe is modelled along the entire width, however in order to compare models with the same mesh the locations of the edge of the pipe must already be present in the geometry).

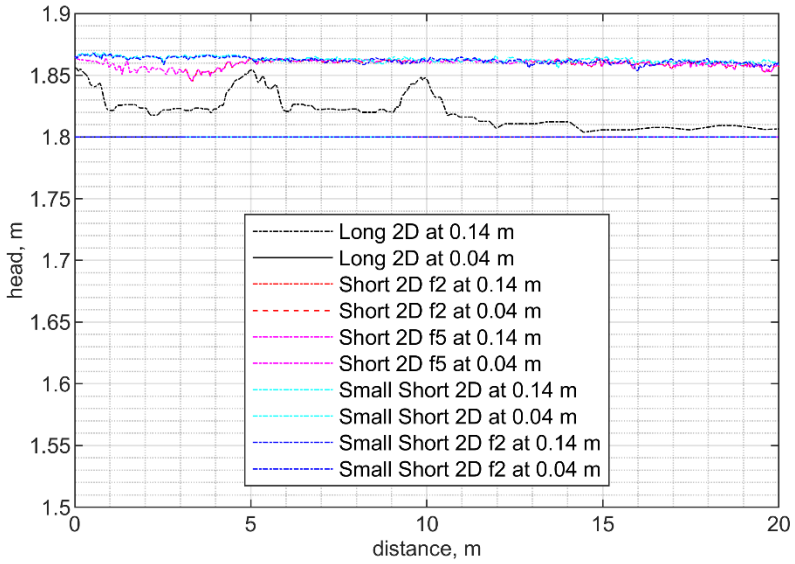

Figure 4.12 Heads modelled inside the barrier along the model width (close up along first 20 m from the centre of the model)

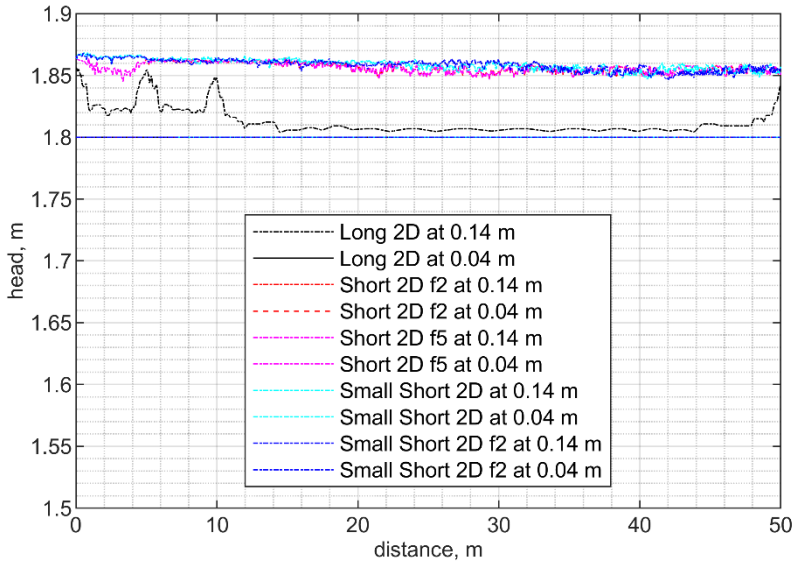

Figure 4.13 Heads modelled inside the barrier along the model width (close up along first 50 m from the centre of the model)

4.2.3 Modelled gradients over 0.1 m upstream of the pipe inside the barrier (along model width) in 2D models

The effect of the relatively small variations in the head, caused by local mesh refinements, on the computed gradients is significant as shown below.

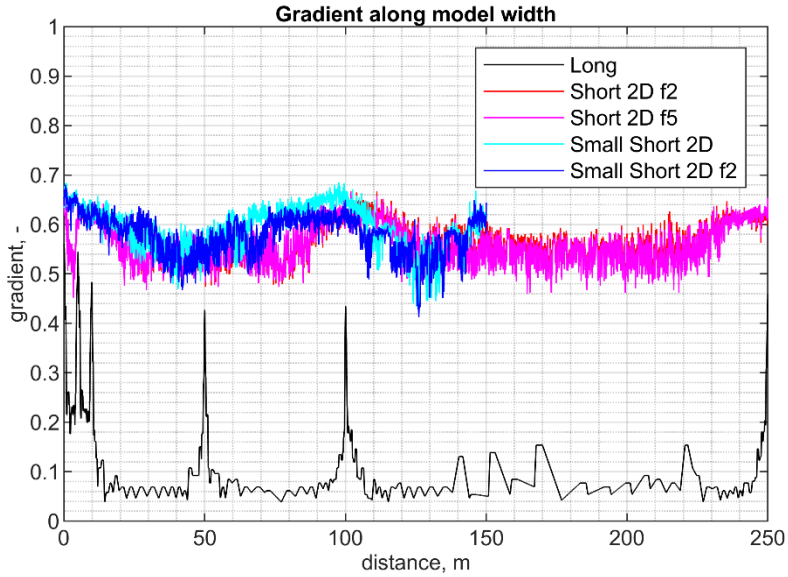

Figure 4.14 Modelled gradient over 0.1 m upstream of the pipe tip along the width of the model

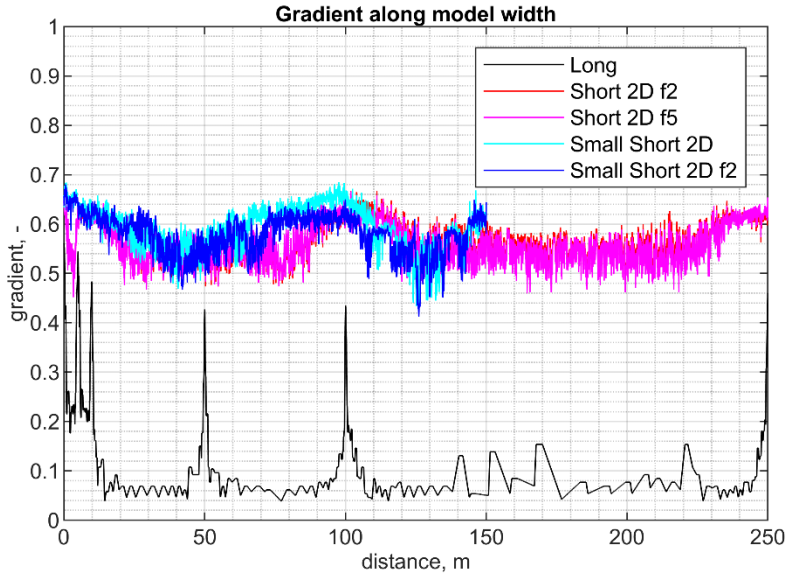

Figure 4.15 Modelled gradient over 0.1 m upstream of the pipe tip along the width of the model

Below the scale is enlarged in order to focus on only the short models. As the intent is to analyse 3D effects for a pipe of 5 m wide (in half space), we zoom in on this area.

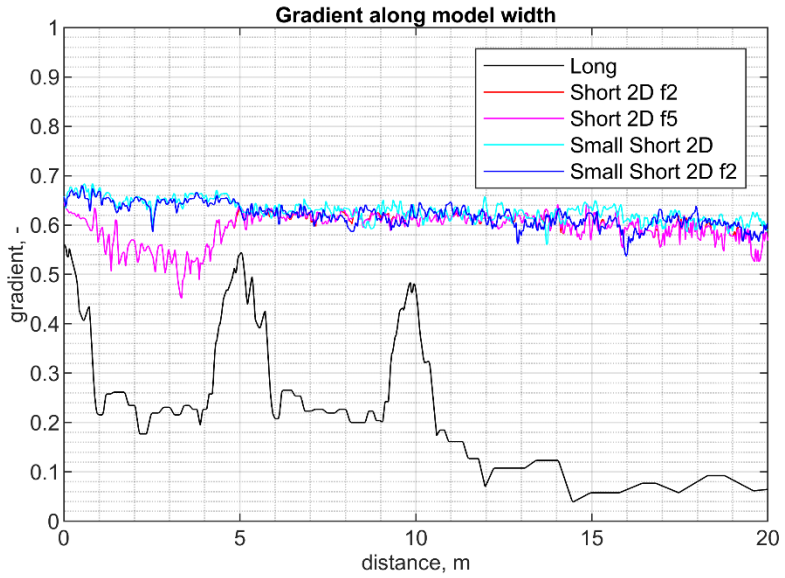

Figure 4.16 Modelled gradient over 0.1 m upstream of the pipe tip along the width of the model

The table below shows statistics for the computed gradient in the barrier along the entire model width.

Table 4.3 Overview of modelled gradients over 0.1 m upstream of the pipe tip in the barrier along the width of different 2D models

Model name	Minimum gradient	Maximum gradient	Mean gradient	Range of gradients	Range / mean, %
Long BaseVar1_2D	0.04	0.56	0.09	0.52	584%
Short2D_f2	0.45	0.67	0.56	0.22	38%
Short2D_f5	0.45	0.67	0.56	0.21	38%
Small Short 2D	0.43	0.69	0.59	0.25	43%
Small Short 2D f2	0.41	0.68	0.58	0.27	46%

4.2.3.1 Discussion for assessing 3D effect

Considering the gradients shown in Figure 4.16, and the statistics shown in Table 4.3 models Short f2 and Short f5 can be considered equivalent. Similarly, the difference between models Small Short and Small Short f2 is small. The long model clearly performs worst, due to the limited possibilities for mesh refinement.

We see also that although the variation (range/mean) of the gradient along the entire width of the model is largest (Figure 4.16) in model Small Short, the variation is not random. When we consider only the variation in the modelled gradient in the area which would be considered for the 3D effect, the gradient variation for the small short models is less than for the short models. Thus, a most appropriate model to determine the 3D affect appears to be the small short model. The next Section investigates how the models perform for a 5 m long pipe (in half space).

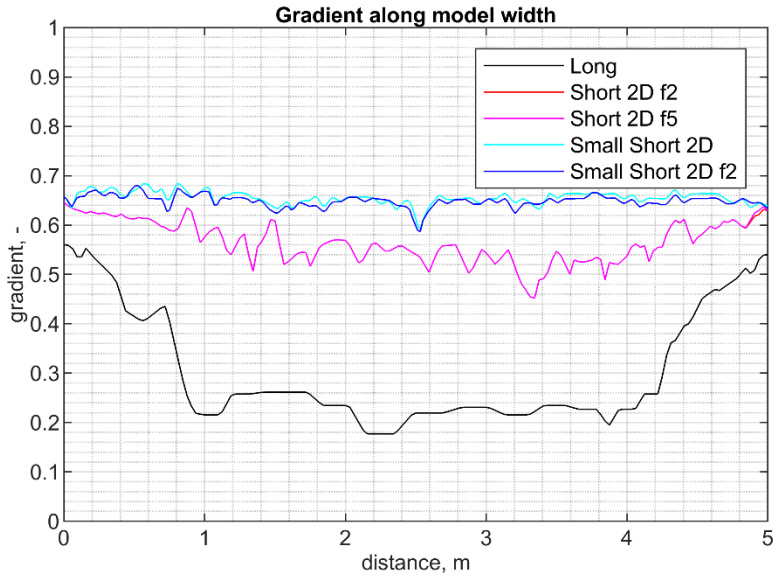

Figure 4.17 Modelled gradient over 0.1 m upstream of the pipe tip along the width of the model

4.3 Results and discussion 3D models

In the 3D models the pipe extends only 5 m parallel to the barrier (in half space). Since there was little difference between the mesh effects in the two short models and the two small short models, this section continues with results from models: Long, Short f2 and Small Short.

The head profiles in the long and short models are shown below. As noted for the 2D models, the head distributions in these figures suggest that the head distribution in the aquifer is approximated well enough using the short models (with the polder boundary that was based on the long model). This is confirmed by the head profiles in the next sections.

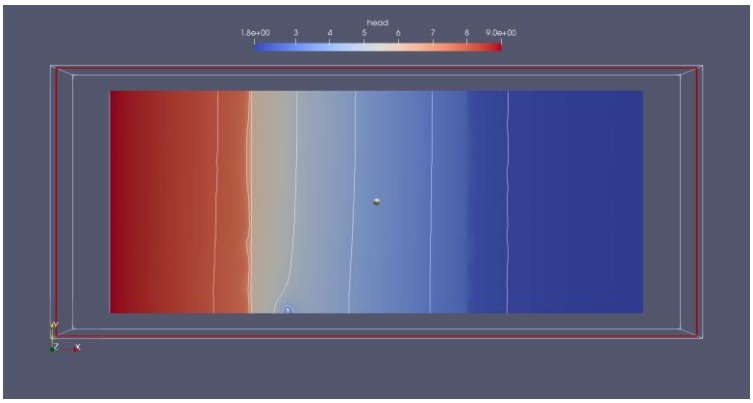

a)Long, top view at elevation z = 0 m

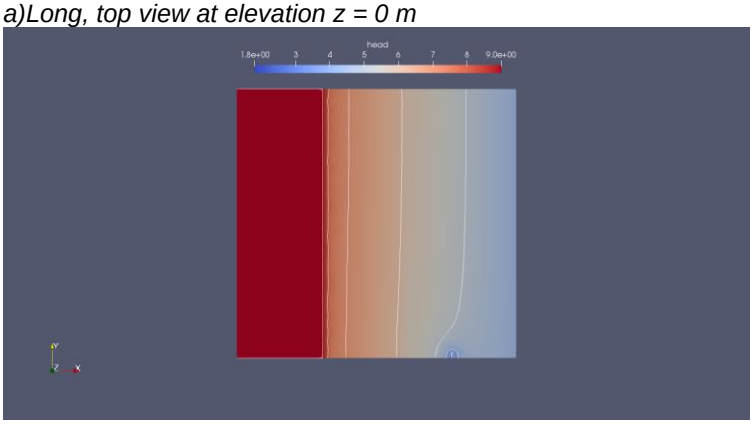

b) Short

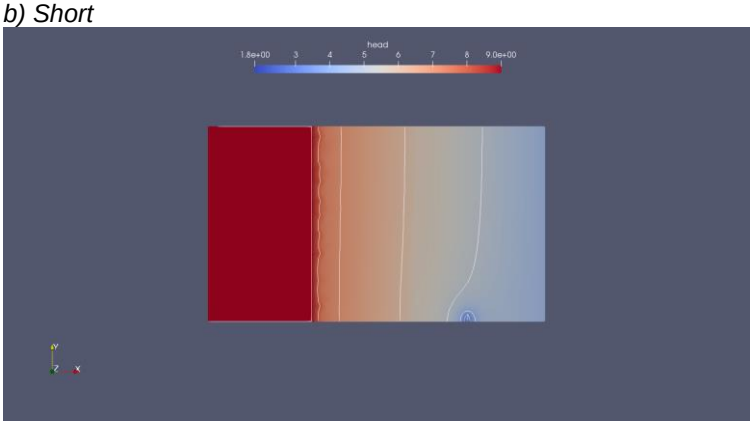

c) Small Short

Figure 4.18Plan view of head distribution in the models at the elevation 0 m NAP (top of the barrier) for models with 5 m wide pipe (in half space). Head contours are spaced 1 m

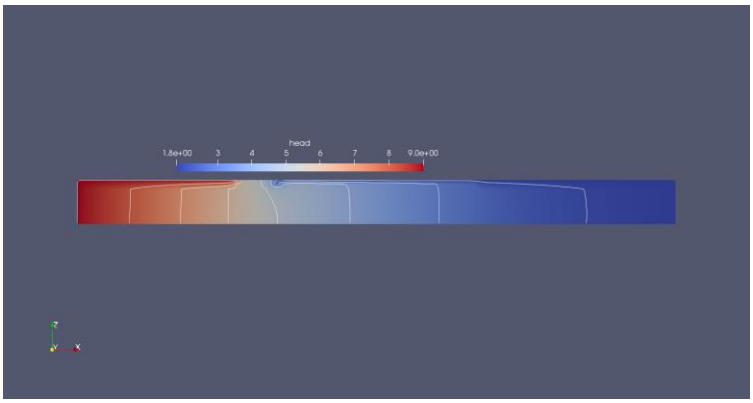

a)Long

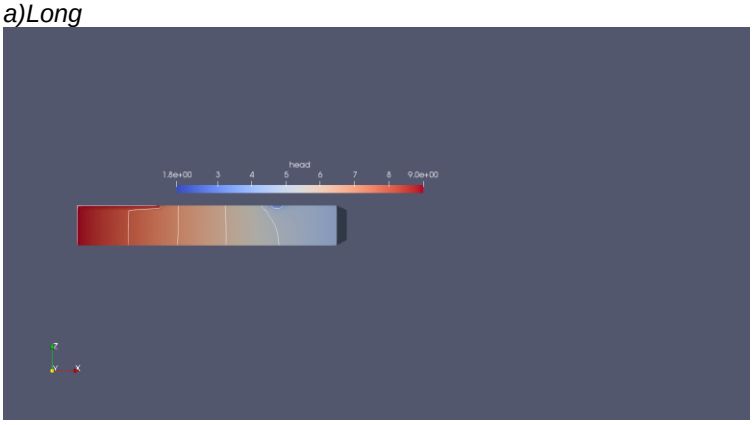

b) Short

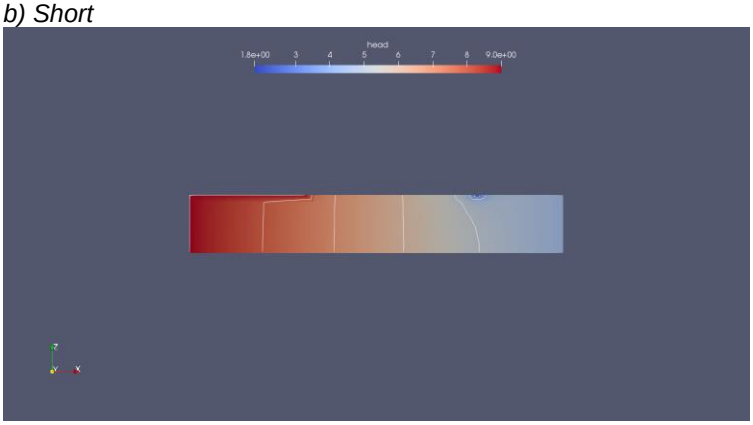

c) Small Short

Figure 4.19 Profile view of head distribution in the models at the centre of the model (y=0 m) for models with 5 m wide pipe (in half space), top long model, bottom short model

By zooming in on the pipe in the plan view we have an indication of the distance over which water converges to the pipe. The contour shown where the flow still curves to the pipe is approximately at y = 11.5 m in the long model and around y = 11 m in the short model and in the small short model. On the one hand this suggests that the approach of using a shorter model to approximate the field situation is valid (comparing the long and short models) but it also indicates that for this specific situation with limited parallel pipe development a model width of 150 m is sufficient to capture the 3D effect. This is further analysed in the sections below.

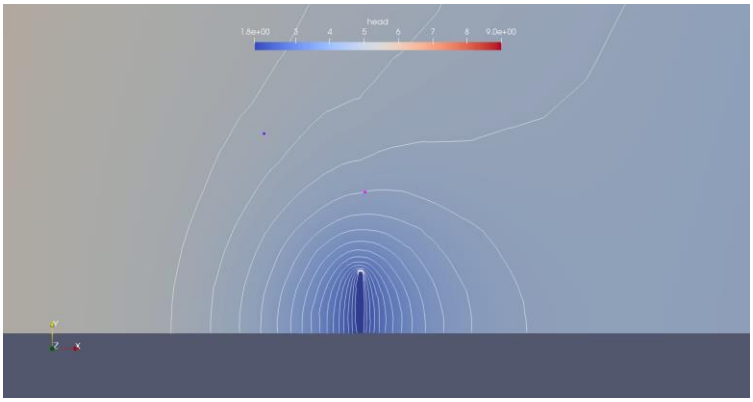

Figure 4.20 Plan view of head distribution in the long model at the elevation 0 m NAP (top of the barrier) close up at the barrier. Head contours only shown between 1.8 m NAP (the pipe boundary) and 5 m NAP, contours spaced 0.2 m

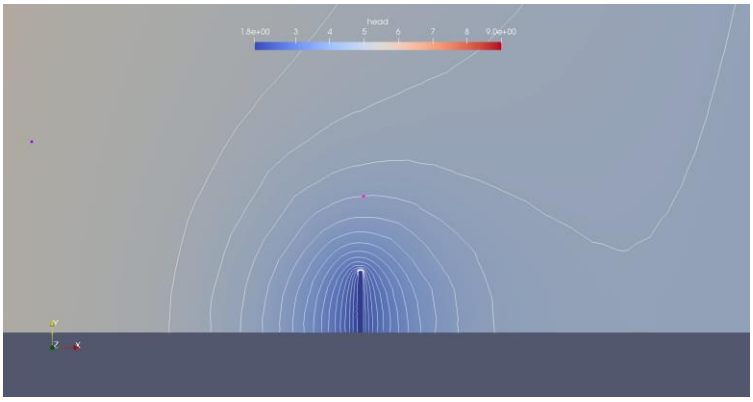

Figure 4.21 Plan view of head distribution in the short model at the elevation 0 m NAP (top of the barrier) close up at the barrier. Head contours only shown between 1.8 m NAP (the pipe boundary) and 5 m NAP, contours spaced 0.2 m

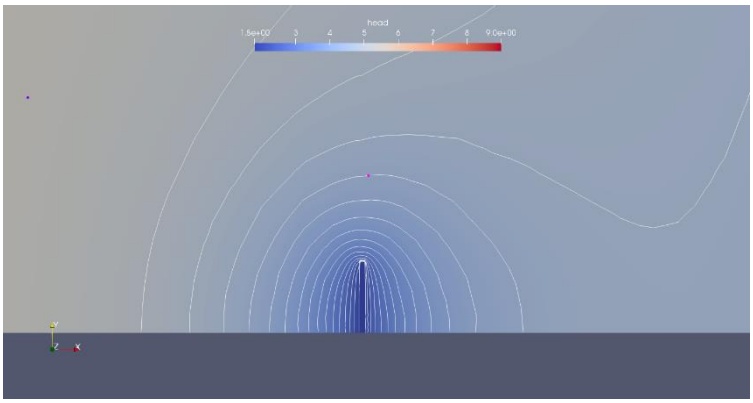

Figure 4.22 Plan view of head distribution in the small short model at the elevation 0 m NAP (top of the barrier) close up at the barrier. Head contours only shown between 1.8 m NAP (the pipe boundary) and 5 m NAP, contours spaced 0.2 m

4.3.1 Head profiles along x-axis

The head profile along the X axis at the elevation 0 m NAP (top of the barrier) is shown below. The similar profiles for the long and the short models shows that simplifications in the short models do not affect the groundwater profile in the aquifer close to the barrier as was also noted for the 2D models. The difference in the head profiles between distance x = -200 and x = -40 m in the long model is due to the application of the boundary conditions as described in Section 4.1.3.

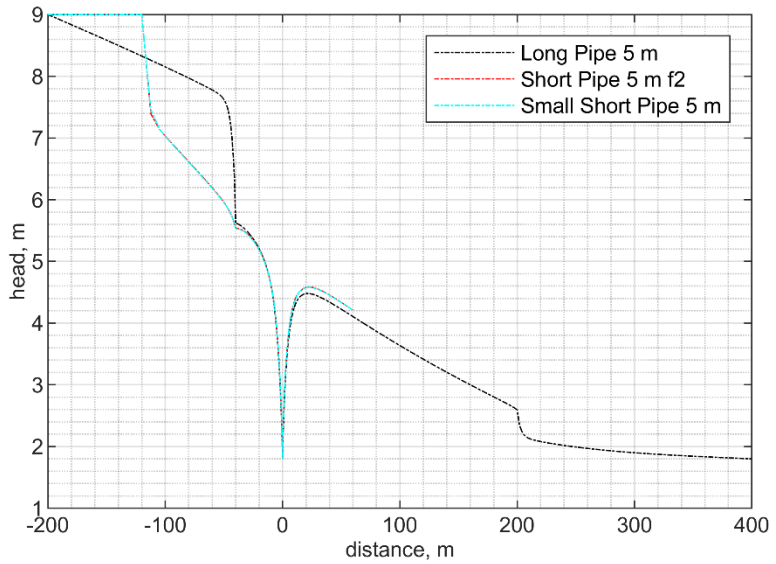

Figure 4.23 Head profiles along the centre of the models (along the x-axis in the plane y = 0 m (the distance 0 corresponds to the top downstream end of the barrier)

A close up of the head profiles inside the barrier is shown below.

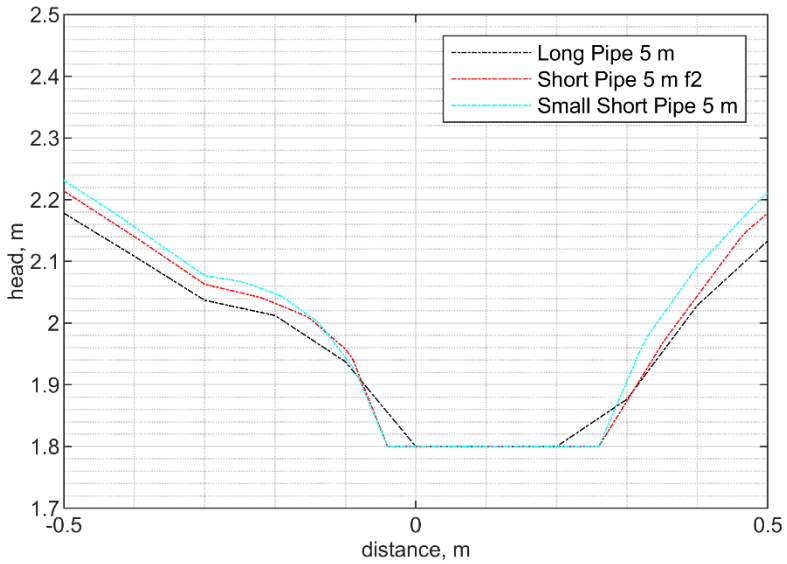

Figure 4.24 Head profiles along the centre of the models close up inside the barrier (along the x-axis in the plane y = 0 m)

These profiles show that the head in the longer model is slightly lower than in the short models as also noted for the 2D models in Section 4.2.

4.3.2 Head profiles inside the barrier (along model width)

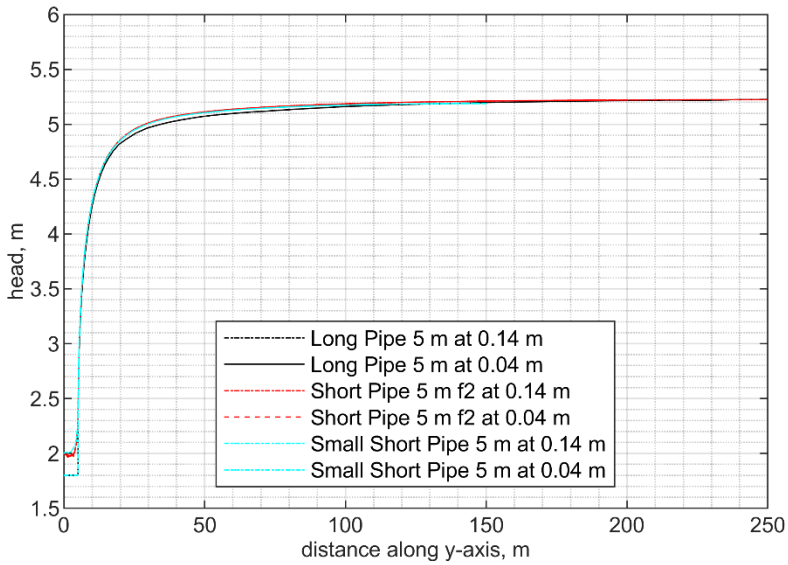

Figure 4.25 Modelled head along the width of the barrier, the pipe is until 0.04 m in the barrier, therefore the head at 0.04 m is the head in the pipe and the head at 0.14 m is the head 0.1 m upstream of the pipe tip

As the pipe is only present along the first 5 m of the model (in half space), the head increases sharply beyond this distance and levels off between 50 and 100 m. This confirms the observation in Section 4.3 that model widths greater than 150 m don't significantly affect the results at the end of the pipe in the barrier, i.e. a 150 m wide model is also representative for a 250 m wide situation (or wider).

In order to look more closely at the head profile in the first meters, a close up view is shown below.

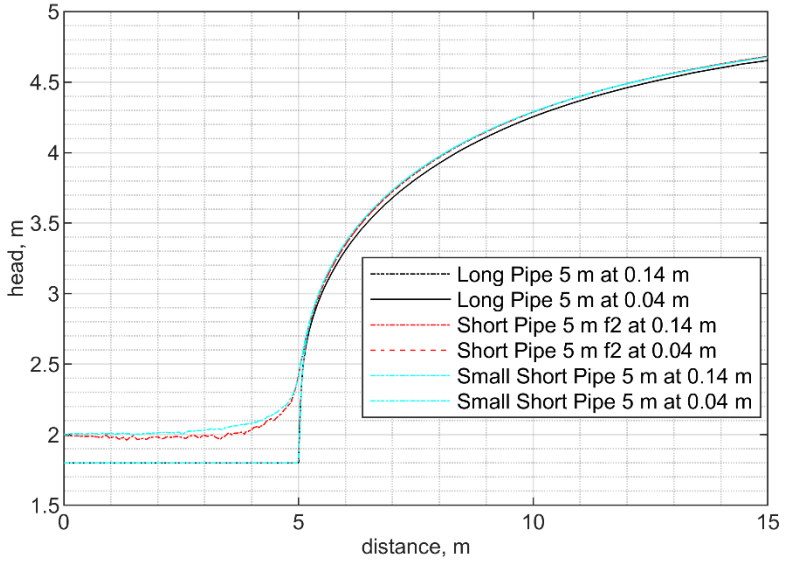

Figure 4.26 Heads modelled inside the barrier along the model width (close up along first 15 m from the centre of the model)

4.3.3 Modelled gradients over 0.1 m upstream of the pipe inside the barrier (along model width) in 2D models

The gradients in the barrier are shown below. These peak sharply at the end of the pipe, and beyond this quickly fall to approximately 0. The similar profiles for the Short and the Small Short models confirm that increasing the model width in this situation does not affect the computed gradient significantly.

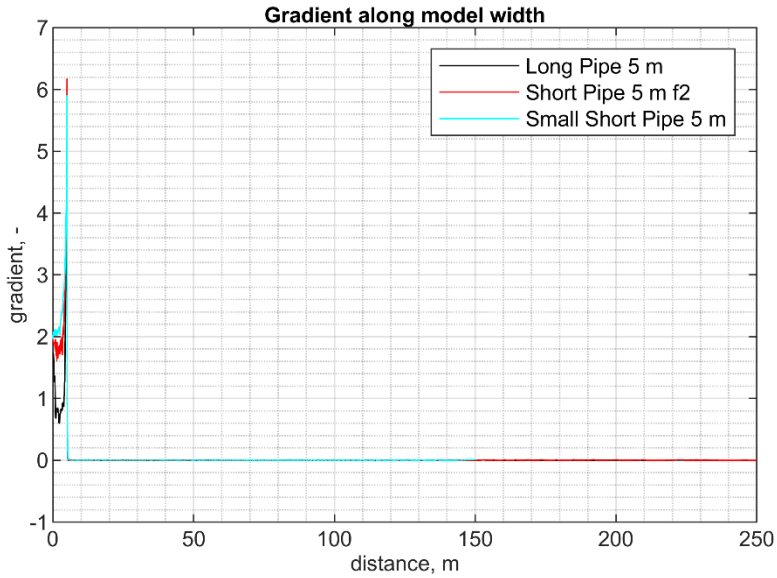

Figure 4.27 Modelled gradient over 0.1 m upstream of the pipe tip along the width of the model

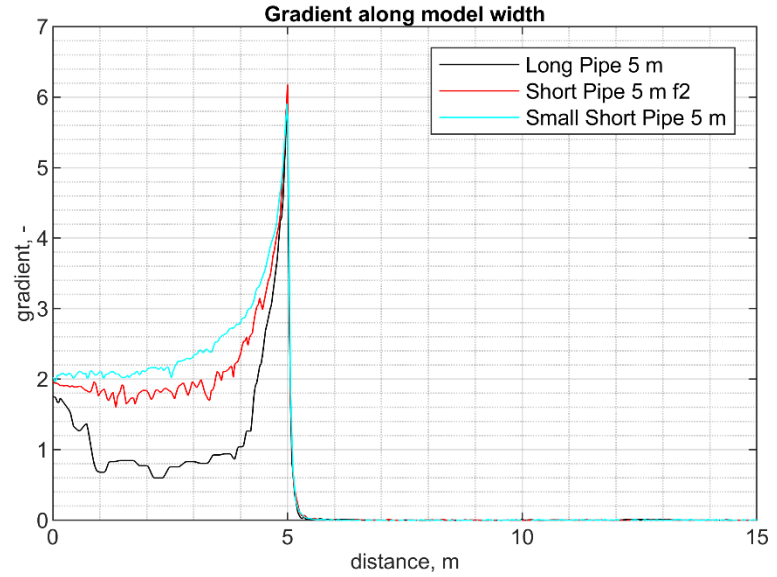

Figure 4.28 Modelled gradient over 0.1 m upstream of the pipe tip along the width of the model close up along first 15 m

4.4 Comparison of 2D and 3D models.

The effect of the pipe parallel to the entire barrier in the '2D model' on the head in the aquifer downstream is very large in comparison with a pipe that has only developed over 5 m in half space (see below). This is confirmed by the head profiles in the next section.

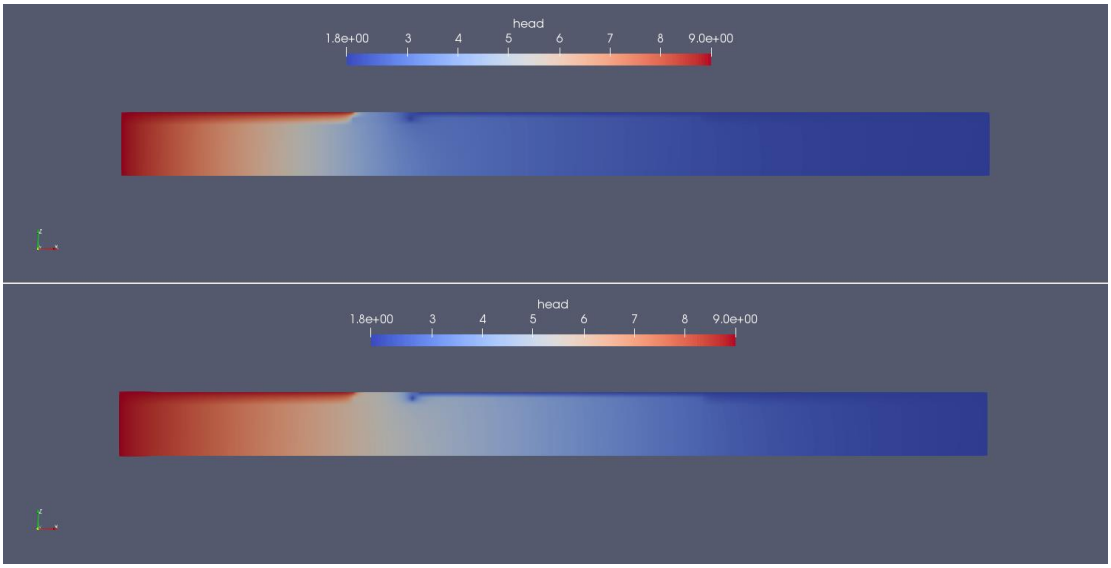

Figure 4.29 Head in profile of 2D model (top) and model with 5 m pipe along the barrier (bottom)

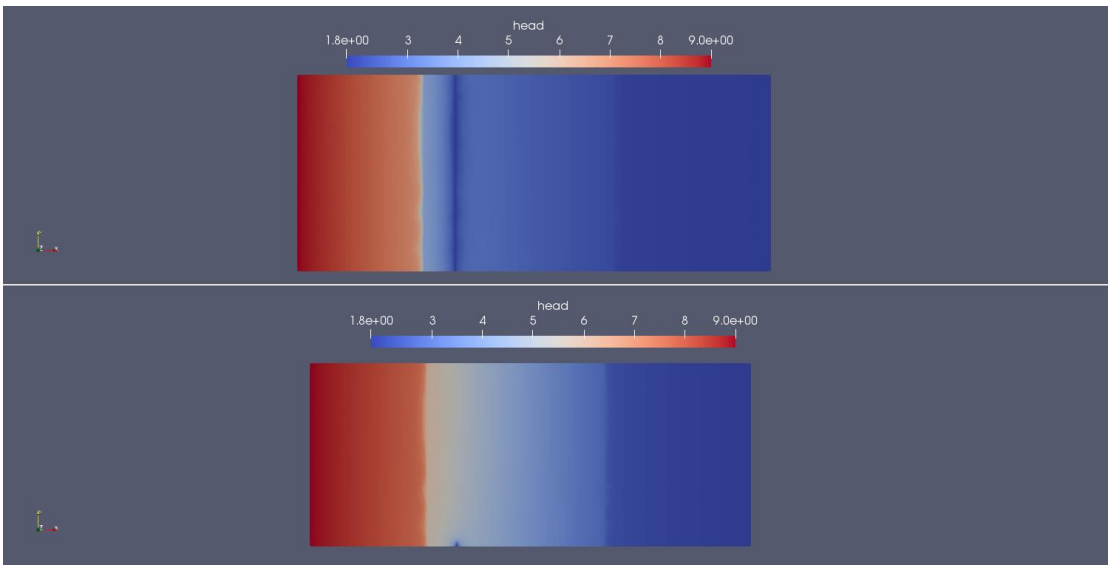

Figure 4.30 Head in plan view of 2D model (top) and model with 5 m pipe along the barrier (bottom)

4.4.1 Head profiles along x-axis

This section compares the head profiles along the model for the 2D and 3D models. The small drop in the head profiles of the long models at 200 m distance occurs where the subsurface changes from the top aquifer, to the cover layer at Gameren (refer also to Section 4.1 for the model description). This occurs at the location of the former primary embankment. The higher head in the aquifer between the two embankments (ca. 0 m and ca. 200 m) in the 3D models indicates that during a high water event significant seepage can be expected due to the high heads in the aquifer (which is also observed, e.g. Koelewijn et al. (2020)).

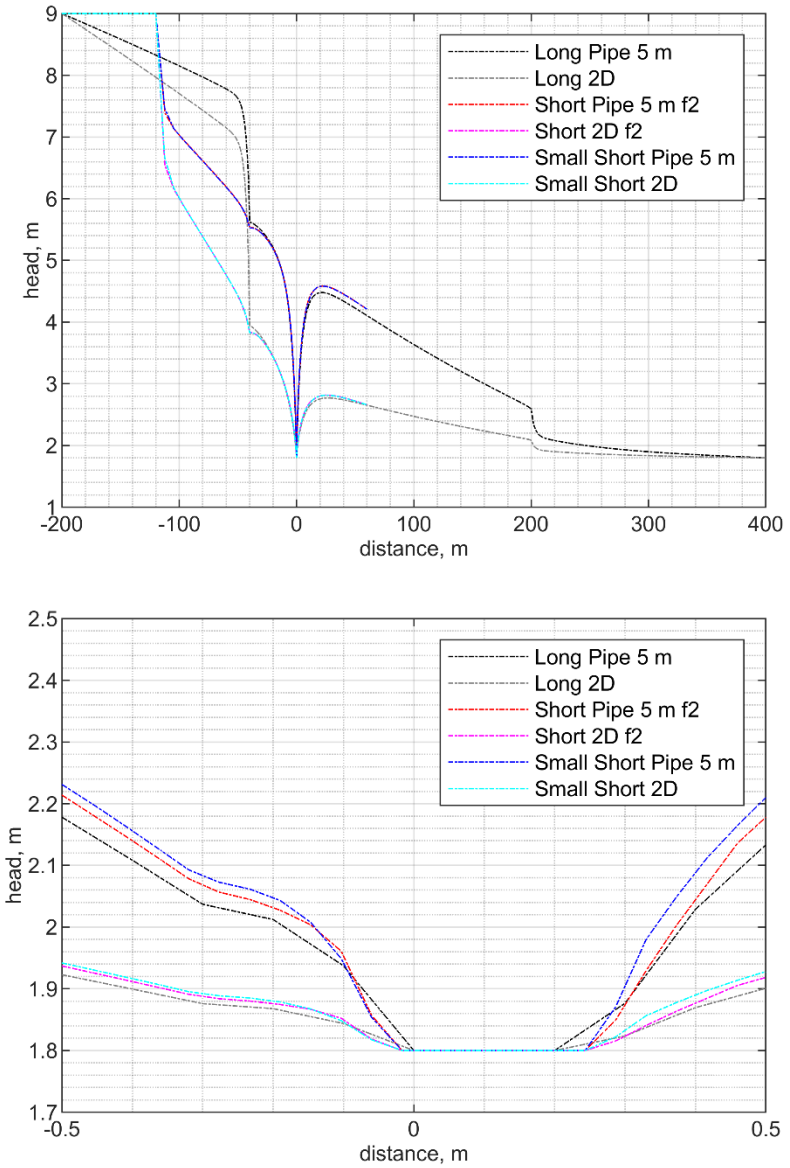

Figure 4.31 Head profile along x axis at 0 m NAP (height of the top of the barrier), top entire model, bottom close up at the barrier

4.4.2 Head profiles inside the barrier (along the model width)

In the 3D model the head in the barrier rises strongly beyond the end of the pipe.

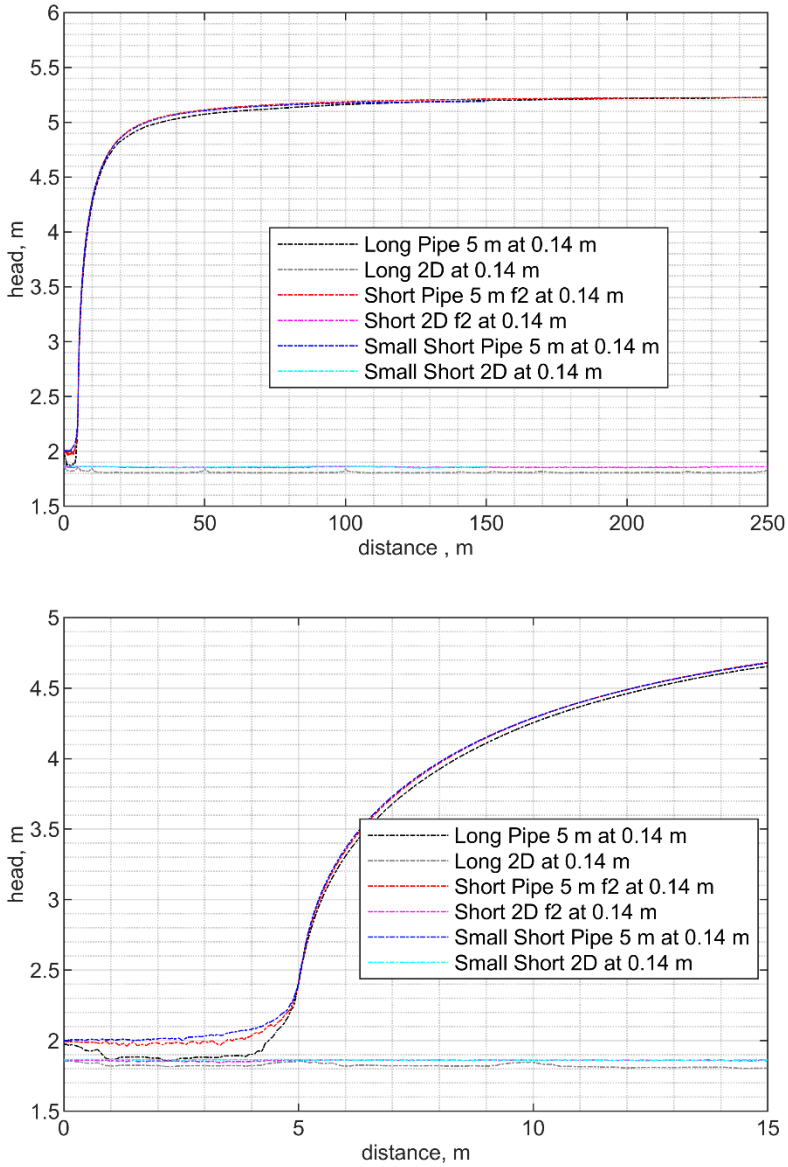

Figure 4.32 Head profile along model width at 0 m elevation, top entire model, bottom close up at the barrier

The head in the barrier in the long model is clearly lower in the 2D and 3D models therefore only the gradients for the short models are assessed (as the head profiles for both 2D and 3D short models show a good match with the long models).

4.4.3 Modelled gradients over 0.1 m upstream of the pipe inside the barrier (along model width)

The modelled gradients in the 3D models are significantly higher than in the 2D models. This is not only the case at the end of the pipe, but along the entire width of the pipe.

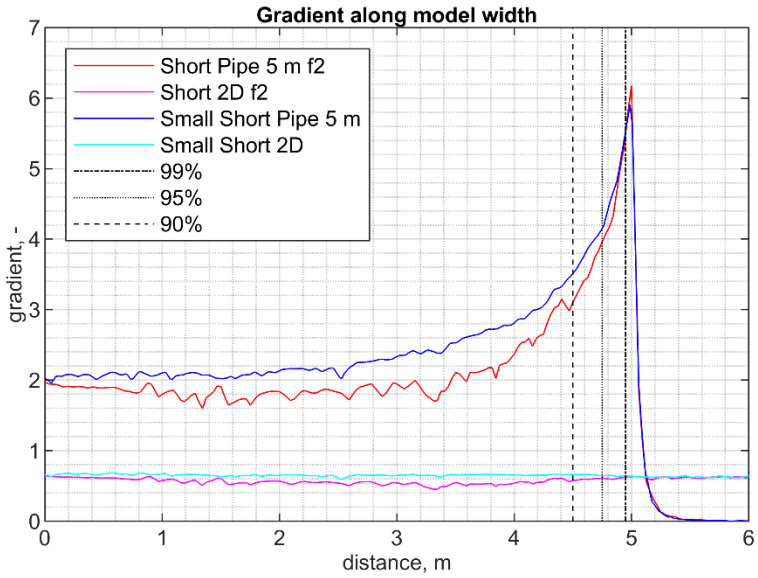

Figure 4.33 Modelled gradient over 0.1 m upstream of the pipe tip along the width of the model close up along first 15 m

4.4.3.1 Discussion for assessing 3D effect

The analyses in chapters 1 and 2 show that the 3D effect increases sharply with decreasing distance to the end of the pipe. Therefore, 3D effects at 99%, 95% and 90% from the centre axis were shown. In the models in this chapter mesh effect also affect the determined '2D gradient' and therefore the basis for the comparison of the 3D gradient.

By using only the gradients that are computed at an exact location, such as 99% etc. the computed 2D gradient is more sensitive to mesh variations. An average gradient over an interval might therefore be more suitable.
For a 5 m long pipe (in half space), 99% from the centre axis is only 0.05 m from the end of the pipe. Considering the meshes of the short and small short models (below) in which the elements close to the edge of the pipe have a size of approximately 0.05 to 0.08 m. This distance does not seem like a logical choice to determine averaged gradients (as this will not be an average but a gradient over 1 element). Therefore, the average gradients between 95% distance and 99% and between 90% and 99%, and between 90 and 95% are computed for both the 2D and the 3D models, as well as the 'point' gradients at 99%, 95% and 90% for comparison.

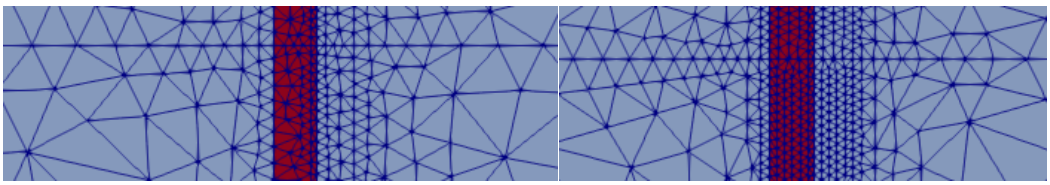

Figure 4.34 Left hand side model short f2, right hand side small short. Blue is aquifer, red is barrier

Table 4.4 Modelled gradients over 0.1 m upstream of the pipe tip

Model name	Point gradients (at % of distance from centre axis)			Average gradients (average between specified ranges of distance from centre axis)		
	99%	95%	90%	95-99%	90-99%	90-95%
Short 2D f2	0.63	0.61	0.57	0.61	0.60	0.60
Short Pipe 5 f2	5.54	3.96	3.10	4.67	4.06	3.51
Small Short 2D	0.65	0.64	0.66	0.64	0.65	0.66
Small Short Pipe 5	5.53	4.16	3.51	4.73	4.25	3.85

The 2D models show that there is some variation in the computed gradients at the point locations especially in the model Short as compared to Small Short. This is probably due to the coarser mesh in model Short than in model Small Short.

In the 3D models the gradients fall sharply with increasing distance from the pipe tip. The 3D effect is computed by the ratio of the gradient in the 3D model to the gradient in the 2D model.

Table 4.5 Ratio of 3D/2D gradients

Model name	Ratio 3D/2D gradient (at % of distance from centre axis)			Ratio 3D/2D gradient (average between specified ranges of distance from centre axis)		
	99%	95%	90%	95-99%	90-99%	90-95%
Short f2	8.8	6.5	5.4	7.6	6.7	5.9
Small Short	8.6	6.5	5.3	7.3	6.5	5.9

These results show a very strong 3D effect, stronger than in many of the previous analyses in phase 1. Also the effect of model width is negligible, but this is probably because the models are already very wide relative to the lateral pipe extent, the difference between 250 m and 150 m (in half space) may be negligible for this configuration but the difference between 20 and 100 m would probably be larger.

The larger 3D effect is probably related to the leakage length. Although one of the conclusions in phase 1 was that the leakage length does not have a significant effect on the 3D effect, a closer consideration of the head profiles and head distributions in the current chapter suggests that for the current combination of a shorter pipe and a longer leakage length the leakage length is important. The parameters are shown below (note that the leakage length is computed for the horizontal hydraulic conductivity of the top aquifer). The effect of the leakage length is investigated in the next section by increasing the hydraulic conductivity of the cover layer from 0.1 m to 1.5 m (reducing the leakage length from 240 to 60 m).

Table 4.6 Comparison of parameters for analysis in phase 1 and phase 3 of this report

Parameter	Analysis in phase 1	Analysis in phase 3
Model width, m (full space)	100	500, 300 (width doesn't matter)
Pipe progression parallel to barrier, m (full space)	50	10
Leakage length (s), m	50, 130, 200	240
Ratio pipe length/model width	0.5	0.02, 0.03

4.4.3.2 Sensitivity to leakage length: analysis and discussion

This analysis is done with the Long model in order to compute the head at a distance of 60 m from the barrier in the polder, which is the boundary condition for the Small Short models. Refer to Section 4.1 for model details.

If clay cover is also 1.5 m/d (like clay cover Gameren) instead of 0.1 m/day this would result in more seepage to the polder in between the two embankments. This is confirmed by the head profiles below for the long models.

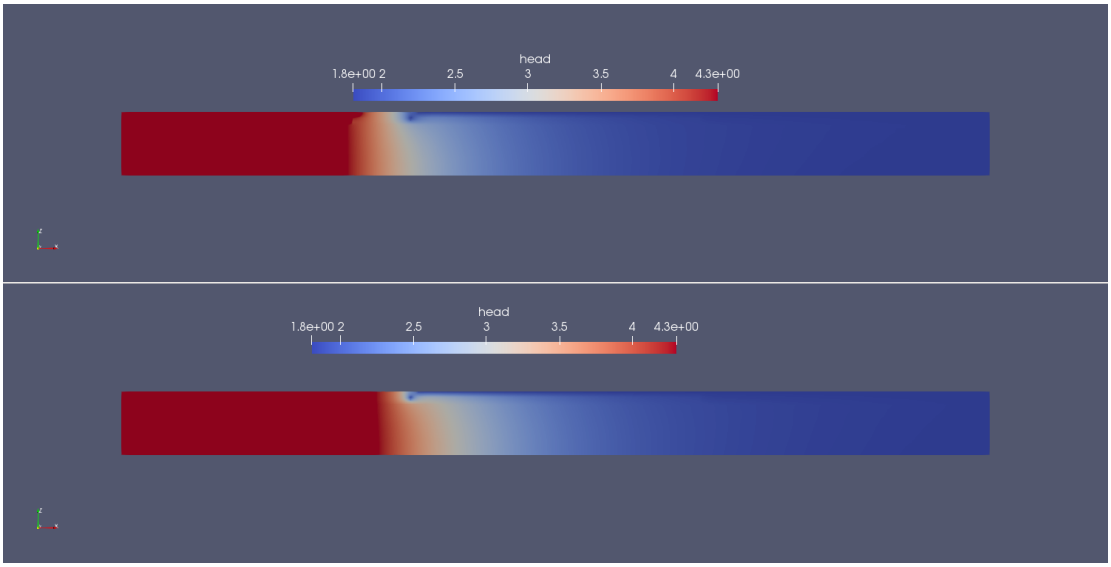

Figure 4.35 Head distribution in long models with a higher permeability for the clay cover layer. Top model with a pipe along the entire model width, 2D model, and bottom model with a 5 m pipe

The computed heads at 60 m are 2.22 m for the '2D situation' and 2.55 m for the 5 m pipe. Note the difference with the basis schematisation where these heads were 2.66 m for 2D and 4.21 for 3D.

The head profiles along the centre axis are shown below for the long and short models. As opposed to the analysis with a less permeable clay blanket, in this analysis there is a larger difference between the two models. This is the consequence of the shorter leakage length, ca. 60 m. This means that in the long model there is seepage to the polder through the surface which is not accounted for in the short models with a closed boundary condition. Evidence of this is the head profile downstream of the barrier which is higher for the small short models than in the long models. Inside the barrier, the small short models also give somewhat higher head profiles.

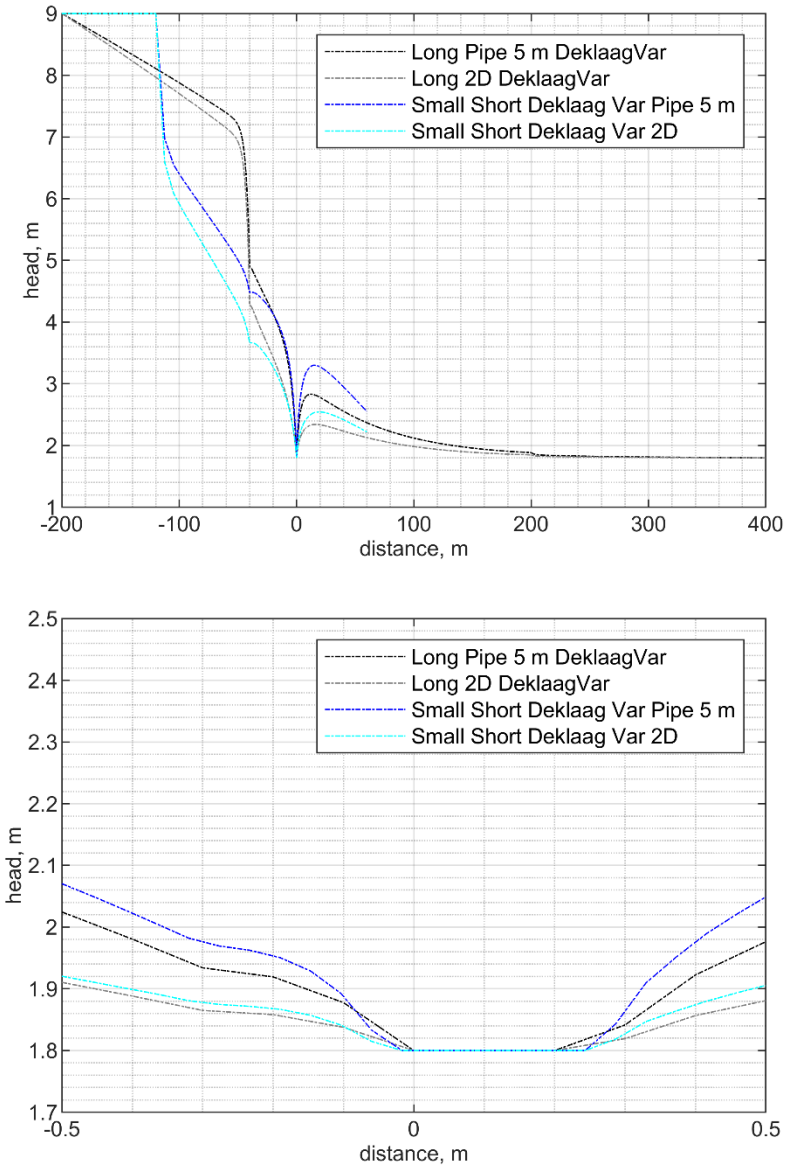

Figure 4.36 Modelled head profiles along the centre axis in the Long and Small Short models with a more permeable clay blanket (Deklaag Var)

The head profiles inside the barrier along the model width are shown below. These show that the influence of the pipe in the 3D model is smaller than in the models with a less permeable blanket clay layer. In the current model the influence on the heads already appears to level off after ca. 50 m.

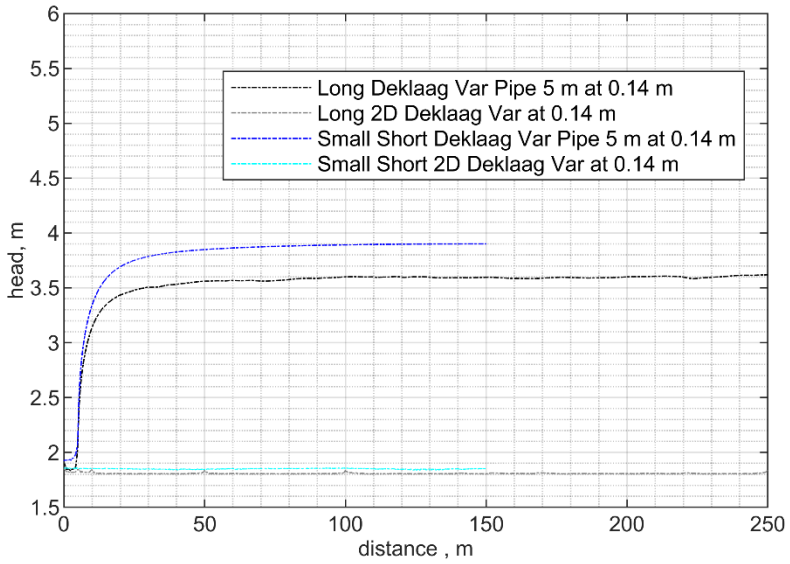

Figure 4.37 Modelled head profiles along the model width in the Long and Small Short models with a more permeable clay blanket (Deklaag Var)

The head contours indicating from which distance flow still converges to the pipe in the barrier below also show a slightly shorter distance than for the basis model. The last contour line that curves to the pipe is at 8 m along the model width.

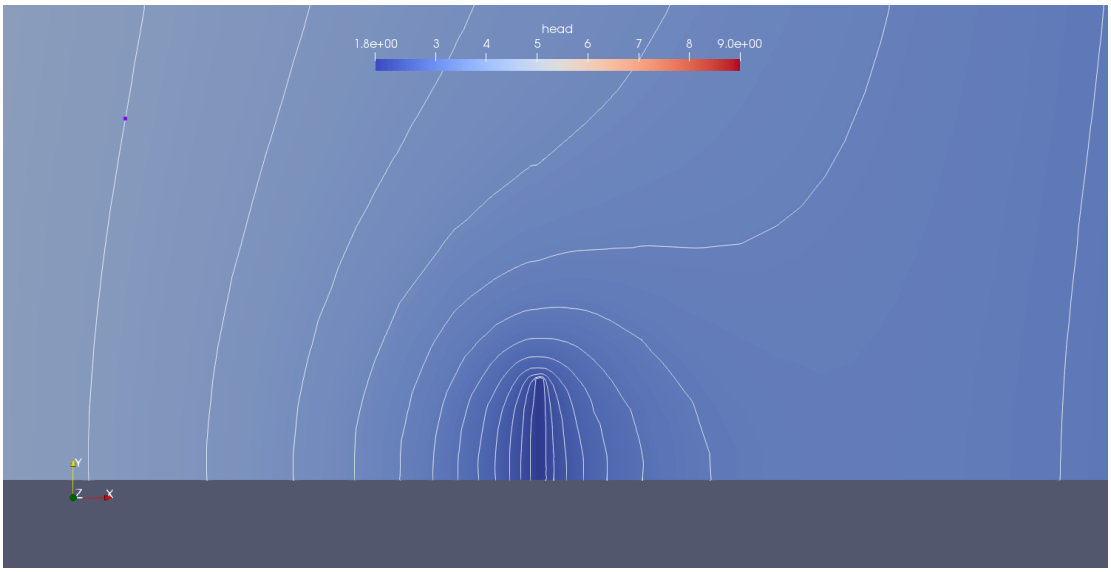

Figure 4.38 Plan view of head distribution in the small short model with a more permeable blanket at the elevation 0 m NAP (top of the barrier) close up at the barrier. Head contours only shown between 1.8 m NAP (the pipe boundary) and 5 m NAP, contours spaced 0.2 m

The modelled gradients in the small short model are shown below for the more and less permeable blankets. Although the shape of the curves is similar, the gradients for the more permeable clay cover are significantly lower.

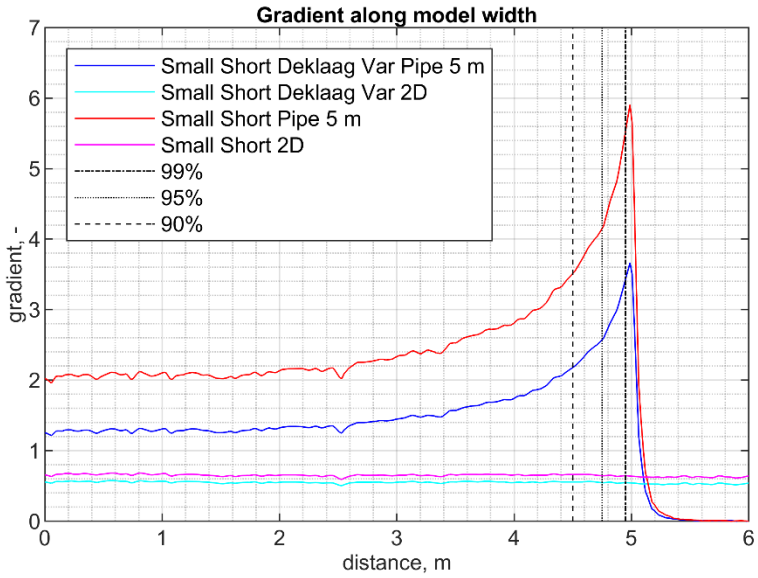

Figure 4.39 Modelled gradient over 0.1 m upstream of the pipe tip along the first 6 m width of the model for analysis with a clay cover layer with 0.1 m/day permeability and with 1.5 m/day permeability (Deklaag Var)

The modelled gradients at different locations along the extent of the pipe are shown below.

Table 4.7 Modelled gradients over 0.1 m upstream of the pipe tip

Model name	Point gradients (at % of distance from centre axis)			Average gradients (average between specified ranges of distance from centre axis)		
	99%	95%	90%	95-99%	90-99%	90-95%
Small Short 2D	0.65	0.64	0.66	0.64	0.65	0.66
Small Short Pipe 5	5.53	4.16	3.51	4.73	4.25	3.85
Small Short 2D Deklaag Var	0.55	0.55	0.56	0.55	0.55	0.56
Small Short Pipe 5 Deklaag Var	3.43	2.58	2.18	2.93	2.64	2.39

The 2D models show that there is some variation in the computed gradients at the point locations especially in the model Short as compared to Small Short. This is probably due to the coarser mesh in model Short than in model Small Short.

In the 3D models the gradients fall sharply with increasing distance from the pipe tip. The 3D effect is computed by the ratio of the gradient in the 3D model to the gradient in the 2D model.

Model name	Ratio 3D/2D gradient (at % of distance from centre axis)			Ratio 3D/2D gradient (average between specified ranges of distance from centre axis)		
	99%	95%	90%	95-99%	90-99%	90-95%
Small Short	8.6	6.5	5.3	7.3	6.5	5.9
Small Short Deklaag Var	6.3	4.7	3.9	5.4	4.8	4.3

The gradients are significantly lower with a more permeable blanket, and the 3D effect is also smaller. This makes the hydraulic conductivity (and thickness) of the blanket in the polder

(and other factors which affect the head level there, such as drainage) especially significant for assessing the strength of a CSB.

A view of the head contours at the surface level shows the effect of the hydraulic conductivity of the blanket.

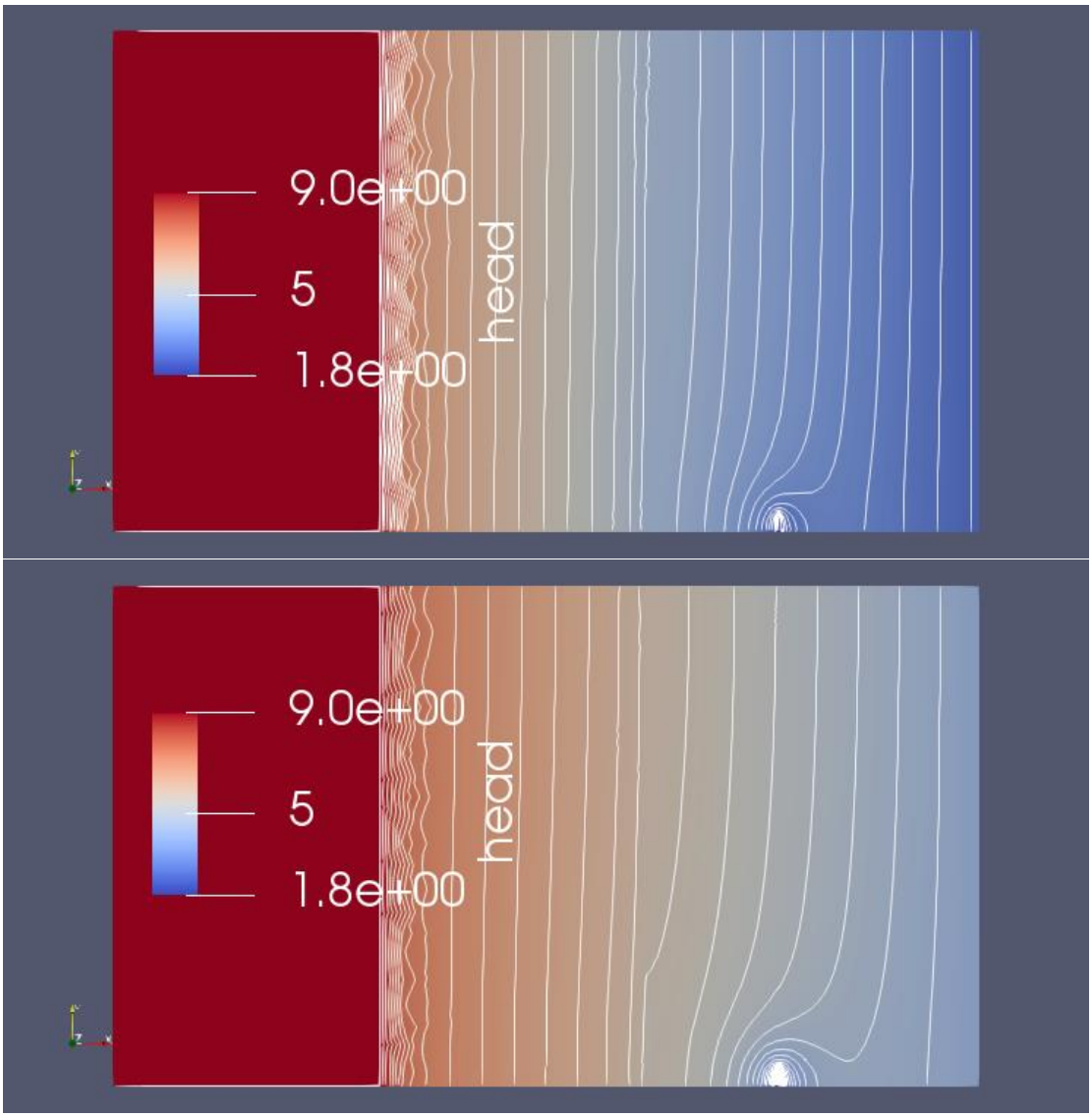

Figure 4.40 Plan view of head distribution in the small short model at the elevation 0 m NAP (top of the barrier) Top basis model, bottom model with a more permeable cover layer. Head contours shown between 1.8 m NAP (the pipe boundary) and 9 m NAP, contours spaced 0.2 m

A close up, where the barrier is red and the aquifer is blue, is shown below.

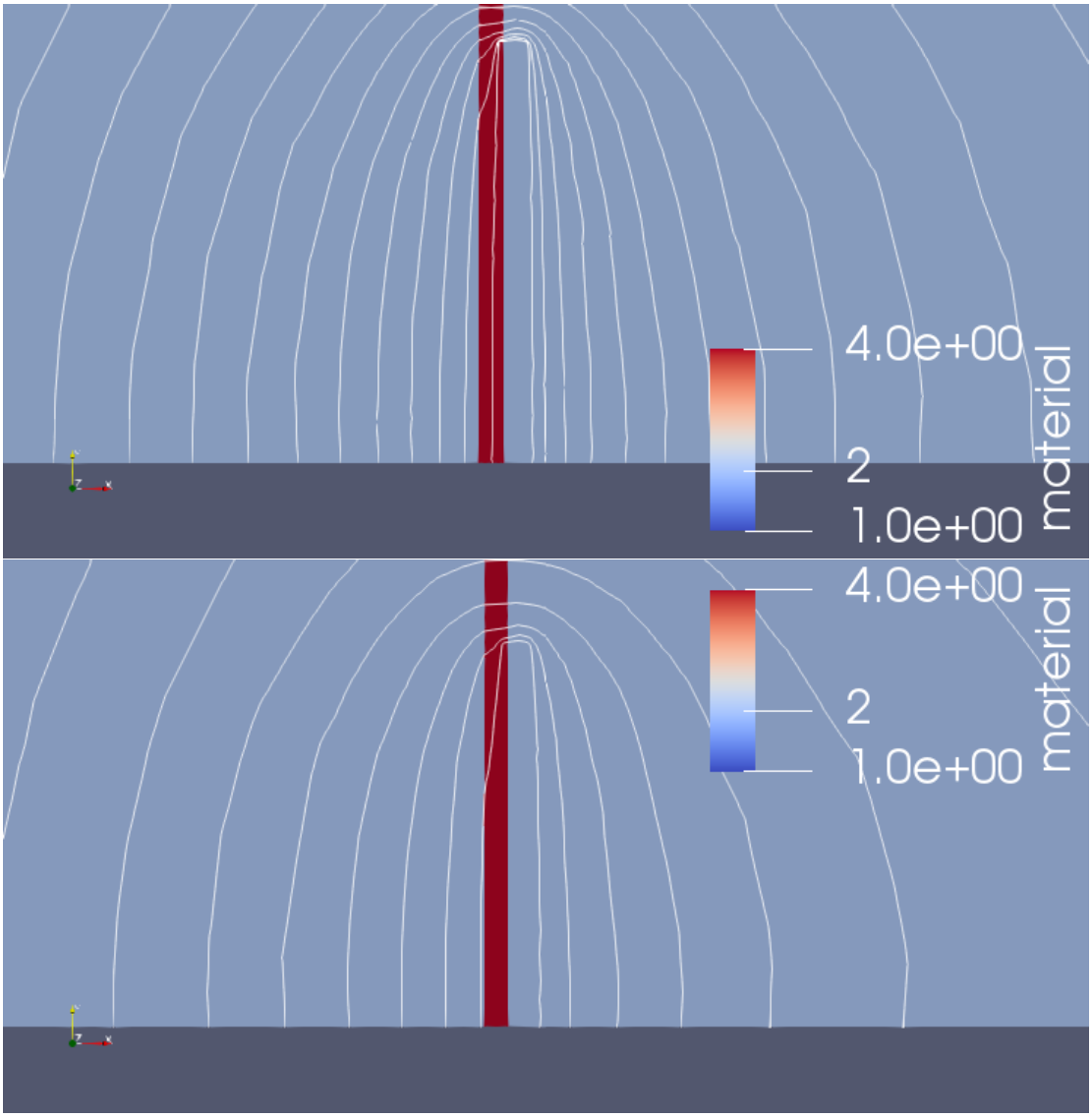

Figure 4.41 Plan view of head contours in the small short model at the elevation 0 m NAP (top of the barrier) Top basis model, bottom model with a more permeable cover layer. Head contours shown between 1.8 m NAP (the pipe boundary) and 9 m NAP, contours spaced 0.2 m. Red is barrier blue is aquifer

4.4.3.3 Fluxes

The modelled fluxes are computed for the inflow, the pipe and the right-hand side outflow barrier in order to compare the effect of the cover on the concentration of flow to the pipe. The table below shows that in the '2D' equivalent models the majority of the flow exits the model though the pipe, whereas in the models with a 5 m pipe most flow leaves through the polder boundary. With a more permeable blanket, there is less concentration of flow to the pipe. This effect is relatively larger for the models with a 5 m pipe than for the '2D models' resulting in a weaker 3D effect with a more permeable blanket.

Table 4.8 Modelled fluxes in the 150 m wide small short models

Model name	Flux in m^3/s	Flux pipe m^3/s	Flux right hand side boundary (polder) m^3/s	Flow balance (in – pipe – polder) m^3/s	% of flow to pipe
SmallShort2D	0.0595	0.045	0.0145	0.00	76%
SmallShort2D_DeklaagVar	0.0614	0.0379	0.0235	0.00	62%
SmallShortPip5	0.0389	0.0059	0.0331	0.00	15%
SmallShortPip5_DeklaagVar	0.0515	0.0037	0.0479	0.00	7%

4.5 Summary

This section addressed the size of the models that is required in order to analyse the 3D effect for the Gameren situation. The combined use of a larger, coarser meshed, model to compute the head in the polder at a given distance downstream of the barrier, and a finer meshed shorter model was found effective. This approach worked best for the situation where the leakage length was substantially longer than the length of the shorter model.

There is a limit to the required width of the model that is needed to assess the 3D effect. The required width depends on the lateral pipe extent and the hydraulic conductivity of the blanket layer in the polder. For the current situation, a width of 150 m (in half space) appears sufficient.

This section showed that the 3D effect for the Gameren situation is sensitive to the leakage length. In earlier Chapters the effect of different factors was investigated. Chapter 5 discusses how to combine these insights to assess the 3D factor.

5 Discussion

The previous chapter illustrated that the 3D factor can vary significantly, even if the soil conditions are known and well represented. The main uncertainties are related to the *lateral development of the pipe* at the barrier and the selection of the *location* in the pipe that provides a *representative gradient*. The reasons this location is important is because the sides of the pipe in the barrier will be sloping as opposed to the straight cut off in the models. A sloping side reduces the peak gradient that is numerically computed, therefore the numerically computed gradient at some distance from the pipe end is more realistic than the numerical gradient at the pipe end. The lateral development of the pipe reduces the 3D factor, but it is unknown to which extent this will take place in practice.

The 3D factor is largely controlled by these two uncertainties. However, the calculations, and their inherent assumptions, and knowledge of the piping phenomenon allow for an evaluation of these uncertainties.

Various factors affect the 3D effect. This chapter provides a brief summary of the main assumptions that are used in the modelling approach in Chapter 4, and the influence these have on the 3D effect.

5.1 Assumptions in the modelling approach for the 3D effect:

1. **Shape of the end of the pipe in the barrier, a straight cut off as opposed to an amphi-theatre or a sloping side**
   a. The peak 3D gradients for the schematization with straight ends would not be so severe in reality if an amphitheatre, or sloping side forms as shown in Chapter 3. The sloping sides reduce the gradients at the ends of the pipe in the barrier significantly. Using a gradient at a distance from the end of the lateral pipe in the model reduces the effect of these ends on the modelled gradient. The question is at which distance from the pipe end is reasonable modelled.

2. **Distance of progression of pipe parallel to the barrier**
   In order to model and compute a 3D effect, an assumption has to be made for the distance that the pipe progresses parallel to the barrier. As explained in detail for Gameren in Section 5.3, the pipe may stop progressing parallel to the barrier due to heterogeneities such as clay lenses. In the models for Gameren a relatively short distance is used, more parallel progression reduces the 3D effects significantly as shown in Chapter 2. It is unknown to which distance the pipe will grow in practice. Conceptually, in a homogeneous model the pipe would progress parallel to the entire length of the barrier, and there would be no 3D effect. However, heterogeneities in the subsurface may cause the pipe to stop.

3. **The pipe is a drain with unlimited capacity only along the barrier width (parallel to the barrier):**
   a. Neglecting the physical presence of a perpendicular pipe running to the barrier. The pipe which runs from the sand boil to the barrier will also have a lower head than the surrounding aquifer, and therefore will also drain some of the flow. Therefore, this perpendicular pipe will reduce the concentration of flow to the pipe inside the barrier to some extent.

      This has more effect for shorter parallel pipes as the size of the pipe running towards the barrier relative to the pipe parallel to the barrier increases.

b. No head loss in the pipe running perpendicular to the barrier

This has more effect with a longer perpendicular pipe running to the barrier. The head loss depends on the flow in the pipe, with higher flow rates (i.e. higher head drops) the pipe deepens, and resistance decreases. And as in a) it is more important for a shorter parallel pipe.

c. No head loss in the pipe parallel to the barrier

The pipe depth will be deepest in the center, where the pipe initially meets the barrier, and shallower at the tips of the lateral pipe, giving a larger resistance to flow at the tips which will limit the 3D effect. It will reduce the peak at the corner of the pipe zone, for a barrier level with the aquifer. For an amphitheatre the shape inside the barrier will differ as discussed in point 1: in that situation no head loss is expected in the pipe parallel to the barrier since the pipe is connected to the open space in the barrier resulting from the formation of the slope.

d. No head loss in the sand boil at the end of the pipe

5.2 Qualification of the effects of assumptions for the Gameren situation

A first indication of the relative effects for the situation at Gameren as is discussed below, based on the analyses in the previous chapters and in Koelewijn et al. (2021).

1. **Shape of the end of the pipe in the barrier, a straight cut off as opposed to an amphi-theatre or sloping sides**
   The location at which the gradients are used to compute the 3D factors in the models for Gameren has a strong effect on the 3D factor.

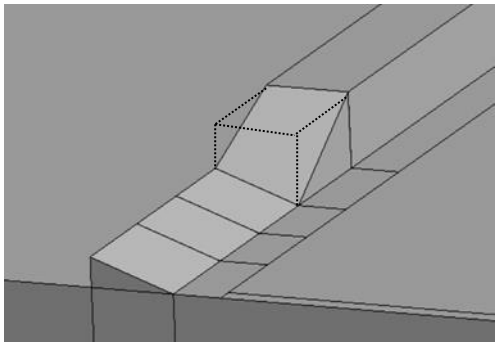

Figure 5.1Illustration of straight cut off and sloping sides

The table below shows the 3D factor in the Gameren model (with the basis cover layer using model Small Short) at different distances from the centre of the model.

As an amphitheatre shape, or sloping sides is considered a likely scenario, the very high modelled gradients closer to the pipe end are considered less likely. However, this will depend on the total lateral extent of the pipe as well.

For a 5 m lateral pipe, 99% distance from the centre axis would mean 2.5 cm from the end of the pipe in the model. This means that the modelled gradient at this distance is highly unlikely to occur in reality if a sloping side forms. Given the findings in chapter 3, a gradient at 25 cm from the end of the pipe might be more likely, i.e. at 90% from the centre axis.

For a 50 m lateral pipe 99% from the centre axis would be 2.5 m from the end of the pipe. Larger distances from the end of the pipe might be less realistic and even smaller distances might be possible, given the findings in chapter 3.

The analysis for Gameren was done with a 10 m lateral pipe. Here gradients at 90% or 95% from the centre axis are 50 or 25 cm from the end of the pipe, which might be realistic.

This section shows the 3D factors at different distances from the centre axis expressed as % from the centre axis.

Table 5.1 3D factor (gradient in 3D model/ gradient in 2D equivalent model) at different distances from the centre of the half-space model (i.e. the centre of the pipe) for the model for Gameren (with the basis cover layer and the refined mesh, and a 5 m lateral pipe (half-space), model SmallShort)

Distance from centre of half space model, m							
0 (0% of distance from centre axis)	**1 (20% of distance from centre axis)**	**2(40% of distance from centre axis)**	**3 (60% of distance from centre axis)**	**4 (80% of distance from centre axis)**	**4.5 (90% of distance from centre axis)**	**4.75 (95% of distance from centre axis)**	**4.95 (99% of distance from centre axis)**
3.1	3.1	3.1	3.3	3.6	5.3	6.5	8.6

2. Distance of progression of pipe parallel to the barrier

If parallel progression is along a longer distance, this reduces the 3D factor due to a larger outflow area from the barrier. Chapter 2 showed that increasing the lateral pipe extent reduces the 3D factor significantly. The effect of lateral pipe extent on the 3D factor is affected by the hydraulic conductivity contrast, as well as shape factors.

For a 40 m deep aquifer with contrast 4 (models phase 1a, Chapter 2), the 3D effect was computed for pipe extents of 1 m, 5 m, and 50 m, along the barrier width (in the 100 m wide model). The table below shows the effect of the parallel pipe lengths for the different models at 90% of the parallel pipe width.

Table 5.2 Effect of changes in lateral pipe length on the 3D effect i.e when the pipe increases in lateral extent from 1 m to 5 m, the 3D effect decreases by a factor of approximately 0.56 based on the models from phase 1a. This is a factor by which the 3D factor is scaled to account for the effect of lateral pipe progression

Effect of change of lateral pipe extent (full-space, in m) on 3D factor at 90% of lateral pipe extent **from phase 1a for a 40 m deep aquifer with contrast 4 (models phase 1a) and a 100 m wide model.**				**Effect of change of lateral pipe extent (full-space, in m) on 3D factor at 90% of lateral pipe extent** **from phase 1b for a 8 m deep aquifer with contrast 4 (models phase 1a) and a 100 m wide model.**	**Effect of change of lateral pipe extent (full-space, in m) on 3D factor at 90% of lateral pipe extent** **from phase 1b for a 8 m deep aquifer with contrast 12 (models phase 1a) and a 100 m wide model**
1 to 5	5 to 50	1 to 50	5 to 1	8 to 50	8 to 50
0.56	0.56	0.31	1.79	0.43	0.34

Based on these computations, for Gameren which is a deep model where the basis pipe has a lateral extent of 10 m (i.e. the 5 m in half space). The table below shows some first

estimates of the change in the 3D factor based on the values above based on expert judgement (i.e. a factor by which the 3D factor changes). Note that this is a rough estimate of the factor of reduction of the 3D effect. However, considering the uncertainty in the possible pipe extent it does not seem that a detailed numerical analysis will reduce the overall uncertainty with regards to this matter.

Considerations are:

- The contrast in Gameren is modelled as approx. 10 therefore effects will be somewhat stronger than modelled for contrast 4. For the field situation for Gameren a contrast of around 20 is expected now, so the effects will be even stronger
- The lateral pipe extension could be more or less than the 10 m modelled, therefore an estimate is given for both scenarios. The likelihood of the scenarios is discussed separately.

Table 5.3 Estimated effect of changes in lateral pipe length on the 3D effect i.e when the pipe decreases in lateral extent from 10 m to 5 m the 3D effect increases by a factor of approximately 1.3 to 1.8, this bandwidth is an estimate based on expert judgement, the minimal effect that the decrease of the lateral pipe extent is expected to have is 1.3, the maximal effect is 1.8. This is a factor by which the 3D factor is scaled to account for the effect of lateral pipe progression

Estimated factors for the change of the 3D effect for Gameren when the lateral pipe extent (m) changes			
10 to 5 estimate of strongest effect	**10 to 5** estimate of **weakest effect**	**10 to 50** estimate of **strongest effect**	**10 to 50** estimate of **weakest effect**
1.8	1.3	0.4	0.7

The effect on the 3D factors from table 5.1 is shown below (i.e. the values in table 5.1 are multiplied by the factors that account for different pipe extents). Note that it is assumed here that the effect at 90% is representative for shorter distances as well. It appears probable that the effect will be less for shorter pipe extents.

Table 5.4 Estimated 3D factors for different lateral pipe extents

	Estimated 3D factor for Gameren when the lateral pipe extent (m) changes			
	10 to 5 strongest effect	**10 to 5 weakest effect**	**10 to 50 strongest effect**	**10 to 50 weakest effect**
At 0% of distance from centre axis	5.6	4.0	1.2	2.2
At 20% of distance from centre axis	5.6	4.0	1.2	2.2
At 40% of distance from centre axis	5.6	4.0	1.2	2.2
At 60% of distance from centre axis	5.9	4.3	1.3	2.3

At 80% of distance from centre axis	6.5	4.7	1.4	2.5
At 90% of distance from centre axis	9.5	6.9	2.1	3.7
At 95% of distance from centre axis	11.7	8.5	2.6	4.6
At 99% of distance from centre axis	15.5	11.2	3.4	6.0

3. The pipe is a drain with unlimited capacity only along the barrier width (parallel to the barrier):

a) Neglecting the physical presence of a perpendicular pipe running to the barrier

The presence of a perpendicular pipe running to the barrier was considered in Chapter 2 for a situation with a 50 m pipe lateral to the barrier (100 m wide model). The effect on the gradient close to the centre of the model is greater than at the extent of the lateral pipe. Whereas in Chapter 2 the focus was on gradients at 90 to 99% of the pipe extent, this section focusses on different distances. The table below shows the modelled effects of the perpendicular pipe on the 3D factors.

Table 5.5 Factor of the effect of perpendicular pipe on the 3D factor (gradient in 3D model without perpendicular pipe/ gradient in 3D model with pipe) at different distances from the centre of the half-space model (i.e. the centre of the pipe) for models from phase 1b with aquifer width 100 m, depth 40 m, contrast 4 and a 50 m lateral pipe. (i.e. these are factors by which the 3D factor can be multiplied in order to account for the effect of a perpendicular pipe at the centre of the model)

Distance from centre of half space model, m							
0 (0% of distance from centre axis)	**1 (20% of distance from centre axis)**	**2(40% of distance from centre axis)**	**3 (60% of distance from centre axis)**	**4 (80% of distance from centre axis)**	**4.5 (90% of distance from centre axis)**	**4.75 (95% of distance from centre axis)**	**4.95 (99% of distance from centre axis)**
0.76	0.87	0.91	0.93	0.94	0.94	0.94	0.94

The effect on the 3D factors from table 5-1 is shown below (i.e. multiplication of table 5.1 by table 5.5).

Table 5.6 Calculated 3D factor for the Gameren model incorporating factor for perpendicular pipe.

Distance from centre of half space model, m							
0 (0% of distance from centre axis)	**1 (20% of distance from centre axis)**	**2(40% of distance from centre axis)**	**3 (60% of distance from centre axis)**	**4 (80% of distance from centre axis)**	**4.5 (90% of distance from centre axis)**	**4.75 (95% of distance from centre axis)**	**4.95 (99% of distance from centre axis)**
2.4	2.7	2.8	3.1	3.4	5.0	6.1	8.1

The effect of the perpendicular pipe on the 3D factor would be larger with a shorter pipe. In Gameren a 10 m pipe was modelled instead of 50 m. This effect is therefore not yet fully included.

The combined effects of 2) a perpendicular pipe (Table 5.5) and 3a) the different lateral extents of the pipe (Table 5.4) is shown below. Note that the assumption is that the effect of the perpendicular pipe is the same for the different levels of parallel pipe extent and this is based on the parallel extent of 50 m. For shorter lateral pipe extents, the effect of the perpendicular pipe might be larger, which would further reduce the factors.

Table 5.7 Estimated 3D factors for different lateral pipe extents, incorporating effects of a perpendicular pipe to the barrier

	Estimated 3D factor for Gameren when the lateral pipe extent (m) changes including effect of perpendicular pipe.			
	10 to 5 strongest effect	**10 to 5 weakest effect**	**10 to 50 strongest effect**	**10 to 50 weakest effect**
At 0% of distance from centre axis	4.2	3.1	0.9*	1.7
At 20% of distance from centre axis	4.8	3.5	1.1	1.9
At 40% of distance from centre axis	5.1	3.7	1.1	2.0
At 60% of distance from centre axis	5.5	4.0	1.2	2.1
At 80% of distance from centre axis	6.1	4.4	1.3	2.4
At 90% of distance from centre axis	9.0	6.5	2.0	3.5
At 95% of distance from centre axis	11.0	7.9	2.4	4.3
At 99% of distance from centre axis	14.6	10.5	3.2	5.7

* This is an unrealistic value, the 3D effect would not result in a factor less than 1. This indicates that the strongest estimated effect here is probably overestimating the effect of increasing the lateral pipe extent

b through d) The head loss in the pipe running perpendicular to, and parallel to the barrier as well as the head loss in the sand boil are neglected in the Gameren model for the 3D effect. These head losses can be accounted for even in 2D models.
The 3D factor affects what the critical head drop will be. If the critical head drop is low due to a strong 3D effect, this means that there will be less flow, resulting in shallower pipes and a lower velocity in the sand boil, increasing the resistance in these. This will have a positive effect, i.e. reduce the 3D factor, increasing the head drop that could be withstood.

5.3 Qualification of scenarios and associated 3D factors

This Section assesses the computed 3D effects and based on expert judgement summarizes these to likely 3D effects for Gameren, combining the qualitative aspects in 5.1 and quantitative results of section 5.2.

All scenarios assume that only one pipe will form towards the barrier, resulting in lateral development parallel to the barrier. In situations with thin or locally absent blankets, such as in Gameren, it is likely that more pipes will form. The assumption in this study is therefore conservative.
The transverse pipe is always expected to form, therefore this effect is applied in all scenarios. Causes for a limited pipe progression might be heterogeneity in the subsurface.

This could be in the form of different grainsize. However due to the much coarser grains of the barrier, this is expected not to have a significant effect on the lateral pipe progression.

Variation in the level of the cover layer is another factor that could limit the parallel progression. It might be expected that the pipe can follow the interface of the cover layer for situations where this slopes gently. However, if there is a more abrupt transition between the background sand and the cover layer, for instance in the case of an ancient channel that has incised into the cover layer, that might possibly cause the pipe to stop creating. The stopping of the pipe at a certain point gives rise to the 3D effect.

When the barrier protrudes above the sand layer into the blanket layer, a slope will form in the barrier material, reaching from the pipe towards the upstream edge of the barrier. In the case of a heterogeneity in the background sand, such as a clay lens, the slope will extend towards the side as well. This slightly reduces the strong concentration of flow at the edge of the slope.

For the situation at Gameren, a significant amount of variation in the level of the cover layer can be expected, and there can be heterogeneity even on shortly spaced distances as due to the depositional environment (Hijma, 2020). In some locations there may also be a more gradual transition from the aquifer to the cover layer, in which case it might be questionable at what elevation the pipe forms. Experience at IJzendoorn shows that in a situation of a CSB, a pipe may also form in the diffuse zone between cover layer and actual aquifer (van Beek et al, 2020)[1]. Thus, if the transition from aquifer to cover layer is more gradual along the barrier width, the pipe might not actually stop but continue in a transition layer. That would result in a more 2D situation, or at least a longer distance of lateral development.
In order to qualify the potential of a 3D flow situation occurring at Gameren, and the lateral pipe extent in such a case, both the likelihood of the pipe stopping at a heterogeneity and the spacing among such heterogeneities is relevant.

In this report, numerical models were used to compute the magnitude of the 3D effect for a given lateral pipe extent parallel to the barrier. The effect of various parameters was investigated, and in Section 4, the 3D effect for an assumed pipe extent of 10 m was computed for a schematisation of the situation at Gameren. However, the lateral pipe extent that will occur in the field at the critical situation is unknown, and might be larger or smaller than 10 m. Therefore, different scenarios have been developed which might occur in Gameren, where the lateral pipe extent is larger of smaller than 10 m. The 3D effect for those scenarios is quantified in Section 5.2. By combining the assessment of the likelihood of occurrence of the scenario itself with the estimated 3D factor for the scenario, an overall qualification of the most probable 3D effect in Gameren can established. These scenarios can also be used to derive a bandwidth for the 3D effect at Gameren.

[1] This aspect could also affect the filter stability of the barrier, which is a separate issue considered in the safety philosophy.

Table 5.8 Scenarios for possible lateral pipe extents

Lateral pipe extent (full-space)	Likelihood & explanation
5 m	A 5 m lateral pipe extent appears **unlikely**, this would imply there are two quite abrupt heterogeneities at very short spacing which both cause the pipe to stop. .
10 m	**Somewhat more likely**
50 m	**Most likely.**
2D situation, entire width of the barrier	**Less likely,** it is quite plausible that the heterogeneities will at some point limit pipe growth.

The computed 3D effects for a 5 m parallel pipe, a 10 m parallel pipe and a 50 m parallel pipe, including a compensation for the transverse pipe are then relevant. The table below shows the estimated 3D effects for these three situations.
As it can be considered likely that the 3D effect is best modelled at a certain distance from the pipe end (due to the formation of sloping sides) the 3D factors which correspond to a distance of ca. 0.5 m to 1 m from the end of the pipe are more likely than those which are much closer or further away. For the 5 and 50 m pipe, there is an upper and lower limit to the probable 3D effects as the Gameren situation was only modelled with a 10 m pipe as discussed in the previous chapter.

Based on the likelihood of the lateral pipe extent and likelihood of the location where the gradient is evaluated, the 3D factors are colored, ranging from unlikely (dark red) to most likely (green) and have a size (small is unlikely, large is likely).

Table 5.9 Estimated 3D factors for different lateral pipe extents (full-space) and a perpendicular pipe. The green larger values are considered more likely to occur, the red smaller values less likely

		Estimated 3D factors for Gameren all with correction for perpendicular pipe				
	Increase to 5 m parallel pipe **Upper limit effect of a shorter lateral pipe**	**Increase to 5 m parallel pipe weakest effect** **Lower limit effect of a shorter lateral pipe**	**Basis model, 10 m parallel pipe,**	**Increase to 50 m parallel pipe** **Upper limit effect of a longer lateral pipe,**	**Increase to 50 m parallel pipe** **Lower limit effect of a longer lateral pipe**	**2D situation**
At 0% of distance from centre axis	4.2	3.1	2.4	0.9	1.7	1
At 20% of distance from centre axis	4.8	3.5	2.7	1.1	1.9	1
At 40% of distance from centre axis	5.1	3.7	2.8	1.1	2.0	1
At 60% of distance from centre axis	5.5	4.0	3.1	1.2	2.1	1
At 80% of distance from centre axis	6.1	4.4	3.4	1.3	2.4	1
At 90% of distance from centre axis	9.0	6.5	5.0	2.0	3.5	1
At 95% of distance from centre axis	11.0	7.9	6.1	2.4	4.3	1
At 99% of distance from centre axis	14.6	10.5	8.1	3.2	5.7	1

In the most likely scenarios (green in table above) the 3D factor still varies from 2.4 – 6.1. For these situations it is evaluated how reliable the estimates of the 3D factor are:

Scenario 1: 10 m lateral pipe and location 90-95%, 3D factor of 5 – 6.1:

- In this situation the lateral pipe extent is relatively short. The short length means that the perpendicular pipe most likely has more influence
- Considering these high 3D factors, the critical head will be relatively close to the Sellmeijer equation. This means that there will be likely head loss in the perpendicular pipe from the sand boil to the barrier, which is not yet taken into account. This will reduce the load on the barrier, as noted later this is to be taken into account in the design calculations
- Considering these high 3D factors, it is more likely that the slope in the barrier will continue to develop sideward, or will further reduce the slope angle of the side wall (which was set to 20 degrees in this study)
- It is rather conservative to assume that the pipe will precisely develop between two heterogeneities and will not develop in other places along the barrier
- It is a conservative assumption that the pipe will only develop across 10 m, since the slope in the barrier will develop further sideward than the location of the heterogeneity. How much further is unknown, but it is expected that the slope will flatten considerably due to the high inflow. As an example, a protrusion of 0.50 m and an estimated slope of 10 degrees will result in an extension of the pipe length of about 3 m beyond the heterogeneity. When pipes form along the roof of the barrier, this will further decrease the 3D effect.

Scenario 2: 50 m lateral pipe and location 95-99%, 3D factor of 2.4 – 5.7:

- The range from ‘lower limit’ to ‘upper limit’ is rather large, the estimated lower and upper limits of the effect could possibly be refined with more modeling. The current estimated 2.4 factor might be too low indeed, this relies on the maximum estimated effect of lateral pipe development. However, for shorter distances along the model this leads to factors smaller than 1 which is unlikely.
- As in scenario 1, the higher the 3D factor, the more head loss in the pipe is expected, since the Sellmeijer critical head is approached. This reduces the load on the barrier, as noted later this is to be taken into account in the design calculations.
- For the higher 3D factors it is more likely that the barrier will continue to develop sideward, or will further reduce the slope angle of the side wall (which was set to 20 degrees in this study). A further reduction of the slope angle will soften the peak

For both scenarios, these values reflect the 3D factors for the cover layer permeability as expected in Gameren. However, with a more permeable cover layer, or a shorter leakage length due to the clay pits, the 3D effect would be less severe.

Calculations are performed for only one erosion pipe that developed perpendicular (from the sand boil) to the barrier. Depending on the configuration more erosion pipe can occur, reducing the 3D effect.

6 Conclusions & recommendations

The coarse sand barrier (CSB) is an innovative method to reinforce existing dikes against the process of backward erosion piping (BEP). The CSB consists of a trench filled with coarse sand in the path of the pipe, below the blanket layer, which prevents the pipe from progressing upstream due to the higher resistance of the barrier against BEP. The top of the CSB can be level with the top of the aquifer, or the CSB can protrude into the cover layer. In practice the second option is most likely to be applied.
Experiments in the laboratory at different scales where the top of the CSB is level with the top of the aquifer show that when a pipe encounters the CSB, it progresses parallel to the barrier in the aquifer sand. This parallel progression of the pipe along the barrier will continue as long as the resistance to pipe formation parallel to the barrier is smaller than the resistance to breach through the barrier. Continued erosion results in an effectively 2D flow field in the barrier. Ideally, in a homogeneous situation, this also occurs in the field (Fig 6-1., l.h.s.). However, in the field the progression of the pipe parallel to the barrier may be limited, for instance by the presence of heterogeneity in the path of the pipe (Fig 6-1. r.h.s.). This could result in a strong concentration of flow at the edge of the pipe along the barrier increasing the load on the barrier grains. The 3D factor is defined as the ratio of the gradient that occurs due to the concentration of flow in a 3D situation, over the gradient that would occur in a 2D situation.

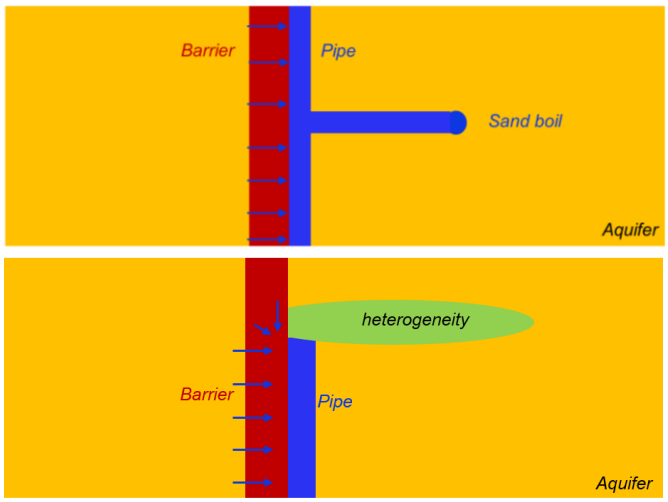

Figure 6.1 Plan view of the top of the aquifer with a CSB for a situation where the top of the CSB is level with the top of the aquifer, left hand side ideal homogeneous situation, right hand side situation with heterogeneity (not to scale)

When the barrier protrudes above the sand layer into the blanket layer, a slope will form in the barrier material, reaching from the pipe towards the upstream edge of the barrier. In the case of a heterogeneity in the background sand, such as a clay lens, the pipe in front of the barrier stops progressing. As with the previous case there is concentration of flow from the side in the barrier, but now this causes the slope to extend to the side, resulting in an elongated amphitheatre shape in the barrier. The slope to the side will flatten to some extent, the equilibrium slope angle to the side will depend on the configuration. This situation could not be observed in experiments due to the limited width, however, it appears probable that this will result in an equilibrium situation, whereby the exact slope that forms from the end of the pipe in front of the barrier to the side parallel to the barrier edge, is dependent on the configuration and the critical gradient for a particular location. The 3D effect for such a situation will be less

due to the formation of this slope, but it will still be present due to the inflow from the side. It is even possible that horizontal pipes form at the top of the barrier.

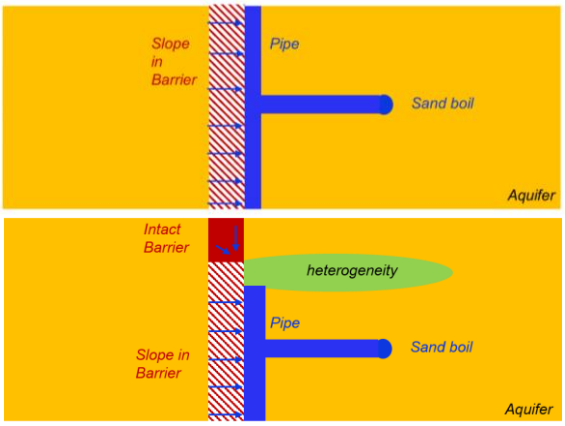

Figure 6.2 Plan view of the top of the aquifer with a CSB for a situation where the CSB protrudes into the cover layer, left hand side ideal homogeneous situation, right hand side situation with heterogeneity (not to scale)

The design approach for a CSB is based on numerical modelling in 2D finite element groundwater flow models in order to compute the local gradient inside the barrier $i_{barrier}$ (Fig. 6-2). This local gradient is compared to the maximum local gradient inside the barrier that the barrier can retain $i_{c,\ barrier}$. The value of $i_{c,barrier}$ is specific to the CSB material and dependent on the relative density of the barrier and can be determined based on laboratory experiments. However, the local gradient in the barrier will be underestimated in 2D models if the pipe is stopped at some distance along the barrier.

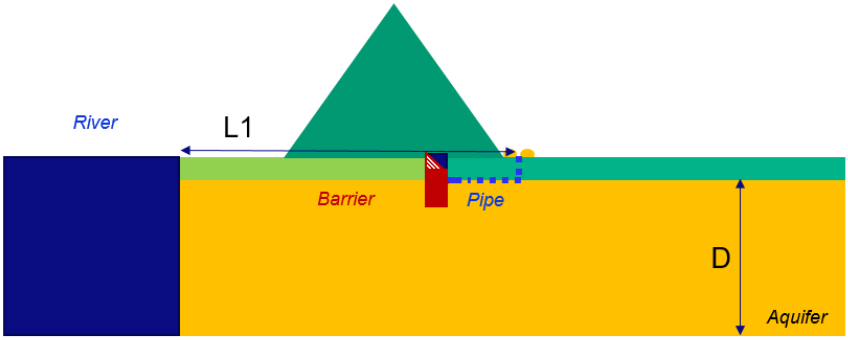

Figure 6.3 2D model in cross section used for design of CSB. The pipe runs from the sand boil to the barrier (dotted blue line) and subsequently progresses parallel to the barrier interface (solid blue line). Dashed triangle indicates situation with a CSB protruding into the cover layer, blue is eroded barrier

This report addresses the 3D effect for the CSB based on finite element 3D computations. The 3D effect is defined as the ratio of the gradient inside the barrier in a situation where the pipe has only developed a limited distance parallel to the barrier along the width of the model, $i_{barrier,\ 3D}$ to the gradient in the situation where the pipe has progressed along the entire width of the barrier $i_{barrier,\ 2D}$.
In the report, first a sensitivity analysis was performed to assess which factors affect the 3D effect. Subsequently the effect of the shape of the barrier, whether this protrudes into the cover layer or not, was investigated. Finally, the situation for the pilot application at Gameren was modelled.
In this report, for the purpose of studying the 3D factor in the sensitivity analysis, the slope is replaced by a pipe without head loss that has partly penetrated the barrier. This assumption is

allowed, since the flow towards the barrier largely controls the 3D effect, for which the precise geometry is not relevant. An exception to this, is the presence of a slope towards the sides (amphitheatre), which softens the 3D effect at the edges.

Main results
Parameters which affect the 3D effect strongly are listed below:

- The leakage length on the polder side of the levee, a long leakage length causes stronger concentration of flow to the pipe and a higher 3D effect
- The shape of the situation, aquifer depth *D*, aquifer width (model width) *W*, length of the floodplain and the base of the embankment *L1*:
  - A smaller *D* gives a higher 3D effect
  - A larger *W* increases the 3D effect, up to a certain limit which is situation specific
  - A larger *L1* increases the effect of the two components above
- The extent that the pipe progresses along the barrier width, the further the pipe progresses, the smaller the 3D effect
- The anisotropy (ratio of horizontal to vertical hydraulic conductivity $A = k_h/k_v$) of the aquifer, a higher *A* increases the 3D effect
- The hydraulic conductivity contrast between the CSB and the aquifer. A higher contrast increases the 3D effect.

The complexity resides in the fact that the relative effect of these parameters differs depending on the value of the other parameters. This means that no generic 3D factor exists that can be applied to all situations. A 3D factor should therefore be derived in 3D models that represent the design situations. This was done for the field situation in Gameren using a model without a protruding barrier. The numerical complexity of modelling a protruding barrier is such that it prohibits modelling the entire field situation, and the important geohydrological factors such as leakage length, multiple layers, and sufficient width of the model to the required extent. Analysis of the gradients in the protruding barrier for a simplified situation suggests that the 3D effect will be comparable for a protruding barrier, allowing for this form of analysis. Hereby it is important to note that the formation of a slope inside the barrier to the side will reduce the 3D effect as opposed to the modelled 3D effect. To account for the effect of the slope to the side starting at the pipe extent, the 3D effect is best evaluated at some distance from the furthest extent of the pipe as detailed below.
The situation specific model has two strong remaining uncertainties, namely:

1. The lateral extent of the pipe parallel to the barrier, which will not be known in advance
2. The modelled effect of 3D concentration of flow is strongest at the very furthest extent of the parallel pipe. However, as noted above, for a protruding barrier the peak modelled gradients are unlikely to occur due to the formation of a slope to the side.

The first uncertainty can be addressed by considering the degree of heterogeneity along the barrier width. Geological insight into the subsurface, and site investigation can be used to assess the likely spacing between heterogeneities, and the nature of the heterogeneity and the extent to which it is likely that the pipe will stop progressing. In case of a protruding barrier, the pipe may stop, but the slope will still form sideward in the barrier, which is homogeneous. It is expected that the slope will flatten and reach until the top of the protrusion, from where horizontal pipes may start to form. These pipes will reduce the 3D factor.
The second uncertainty is more difficult to assess and is based on an analysis of the effect of different options for modelling the ends of the pipe in the barrier.
For the situation at Gameren, a qualitative assessment of the local geology, the type of heterogeneity that might occur and the spacing among heterogeneities, in combination with qualitative evaluation of the effect of different parameters, was used to map out the likely 3D effects shown in Table 1. The most likely values range from ca. 3 to 6, however, the scenario of a 2D situation is not entirely ruled out. It is also noted that the higher the 3D effect becomes, the higher the loading from the side on the pipe is. That makes it more likely that the slope to the side in the protruding barrier will level off further, reducing the 3D effect. However, there is a limit to this, as the toe of that slope remains at the end of the pipe parallel to the barrier.

Finally, it is important to note that in situations with a high 3D effect, the critical head drop will be lower which results in a lower flow rate in the pipe downstream of the barrier, resulting in a shallower pipe and more resistance. That additional resistance could be accounted for in the design calculations for specific cross sections, as it will also depend on the length of the pipe downstream of the barrier.

Table 6.1 Estimated 3D factors for different lateral pipe extents (full-space) and a perpendicular pipe. The green larger values are considered more likely to occur, the red smaller values less likely

		Estimated 3D factors for Gameren all with correction for perpendicular pipe				
	Increase to 5 m parallel pipe **Upper limit effect of a shorter lateral pipe**	**Increase to 5 m parallel pipe weakest effect** **Lower limit effect of a shorter lateral pipe**	**Basis model, 10 m parallel pipe,**	**Increase to 50 m parallel pipe** **Upper limit effect of a longer lateral pipe,**	**Increase to 50 m parallel pipe** **Lower limit effect of a longer lateral pipe**	**2D situation**
At 0% of distance from centre axis	4.2	3.1	2.4	0.9	1.7	1
At 20% of distance from centre axis	4.8	3.5	2.7	1.1	1.9	1
At 40% of distance from centre axis	5.1	3.7	2.8	1.1	2.0	1
At 60% of distance from centre axis	5.5	4.0	3.1	1.2	2.1	1
At 80% of distance from centre axis	6.1	4.4	3.4	1.3	2.4	1
At 90% of distance from centre axis	9.0	6.5	5.0	2.0	3.5	1
At 95% of distance from centre axis	11.0	7.9	6.1	2.4	4.3	1
At 99% of distance from centre axis	14.6	10.5	8.1	3.2	5.7	1

6.1 Recommendations

Based on this study we come to the following recommendations:

1. Calculations were run in sensitivity analyses and for a situation as expected in Gameren. To be able to estimate the 3D effect for different situations, it is recommended to develop analytical models to make a first estimate of the 3D effect. Simple analytical models show what parameters are important and can significantly reduce the amount numerical calculations necessary for a different location
2. The slope at the ends of a pipe in de barrier parallel to the barrier has a significant influence on the maximum gradients in the CSB at the ends of the pipe. In this study, it was only possible to investigate this effect for one slope. It is recommended to investigate this influence for different slopes
3. This study shows that there are 2 types of 3D effects:
    - For a limited pipe length parallel to the barrier, water concentrates from the sides without pipe resulting in an average flow in the pipe in the barrier that is higher in a 3D situation than in a 2D situation. This depends mainly on the length of the pipe parallel to the barrier and the geometry and permeabilities of the soils and around the CSB
    - Also, for a very long pipe there will be an increase in gradients at the ends of the pipe, due to the change in boundary conditions. This change in boundary conditions depends on the slopes at the ends of the pipe
    - In further study, it may be worthwhile to study these effects separately to develop a better idea what effect is most important for a certain situation.

7 References

Hijma, M. 2020 Variatie in hoogteligging grens deklaag/zandlaag langs en over de GZB. Deltares Memo nr 11200952-000-GEO-0007.

Koelewijn, A.R., van der Kolk, B.J., Noordam, A. 2020. Toepasbaarheid grofzandbarrière bij Gameren. Deltares rapport 11200952-058-GEO-0001.

Rosenbrand E., Koelewijn, A.R., 2020a. Uitgangspunten her-kalibratie Gameren profiel 136+050. Deltares Memo 11200952-067-GEO-0001

Rosenbrand E., Koelewijn, A.R., 2020b. Analyse aanvullend grondonderzoek Gameren. Deltares Memo 11200952-067-GEO-0002

Van Beek, V.M., Hoogendoorn, R., Rosenbrand, E., Hijma, M. 2020. KvK Piping deelproject 019: Syntheserapport. Deltares Rapport 112-3719-019GEO-000

A Mesh analysis

A.1 Introduction

This memorandum concerns the mesh sensitivity of the computations performed in the analysis of the 3D effect for phase 1. The model description and main results are shown in the main report.
The results presented in the report are based on two stages of modelling, and different models were used. In the analysis of the results it was observed that apparently minor differences between models from the two stages concerning the mesh size had effects on the results that were of the same order of magnitude as the effects of the parameters analysed in the sensitivity analysis.

This has implications for the interpretation of the results, and in particular limits the extent to which results can be compared between the two stages.

A.2 Mesh effects

In the first series of models: a 5 m mesh was created with a mesh refinement to 0.05 m around the CSB, this results in 6 elements inside the barrier, which means that the critical gradient is calculated from the 2nd node upstream of the boundary condition of the pipe. A side views is shown below.

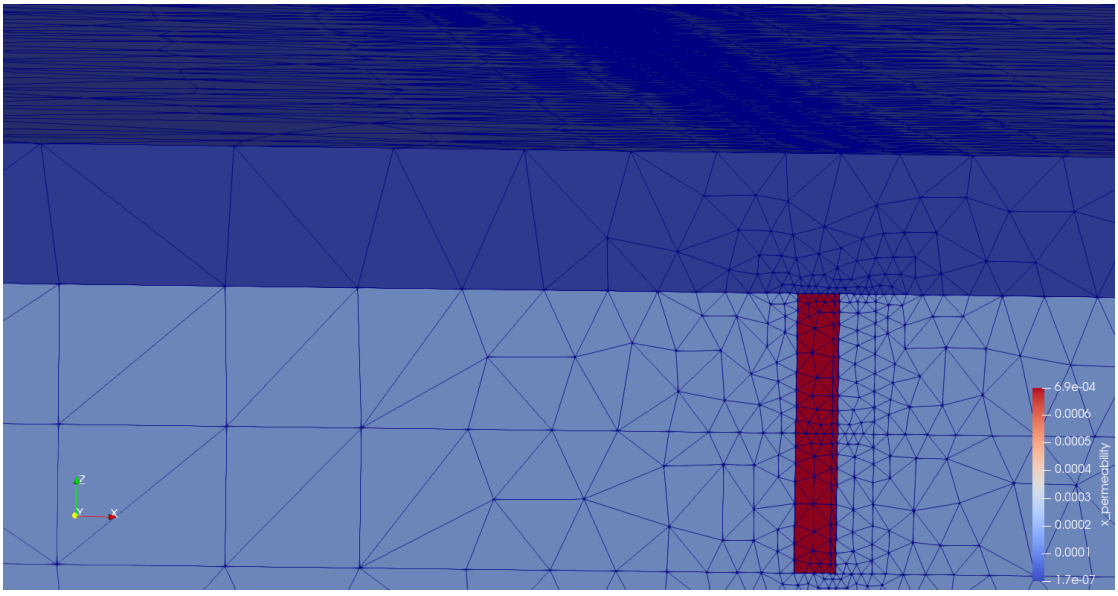

Figure A.1 Side view of mesh used in first stage of computations. Dark blue is cover, red is barrier and light blue is background sand. The depth of the barrier is 2 m

In the additional models, for models with a width of 100 m, a 2 m mesh was created close to the barrier (5 m in the hinterland), and the mesh in the barrier had an element size of 0.04 m resulting in 8 elements inside the barrier and the critical gradient is calculated from the 3rd node upstream of the boundary condition. A top view of the barrier and the locations used to calculate the gradient is shown below. These models are referred to as mesh fine in this memo.

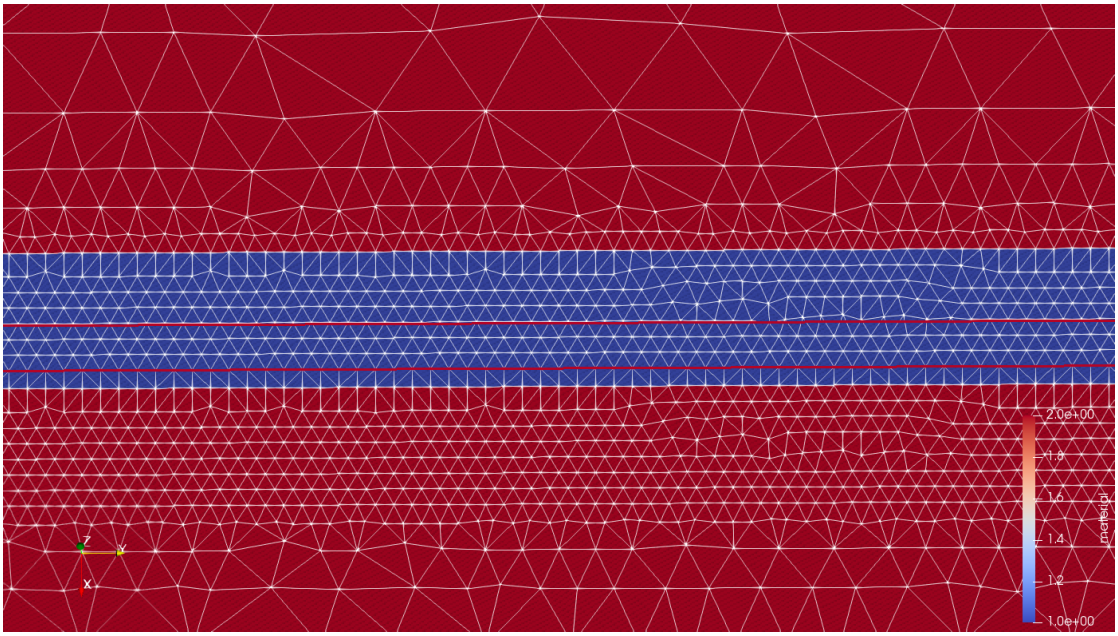

Figure A.2 Top view of mesh used in second batch of computations for models with width 100 m (mesh fine). Blue is barrier, red is background sand, red lines indicate distance over which the gradient is computed. (the width of the barrier (the blue area is 0.3 m)

Models with a width of 200 m could not be meshed so finely and therefore had a mesh size of 0.06 m inside the barrier (and 6 m elements). This resulted in 6 elements inside the barrier and the gradient computation was over 2 elements, similar to the first stage models. A model with a width of 100 m was also made with this coarser mesh, referred to as mesh coarse in this memo. The comparison of the results from the finer and the coarser mesh are important to be able to distinguish the effects due to a larger width of the models (200 m wide vs 100 m wide) from the effects of the mesh.

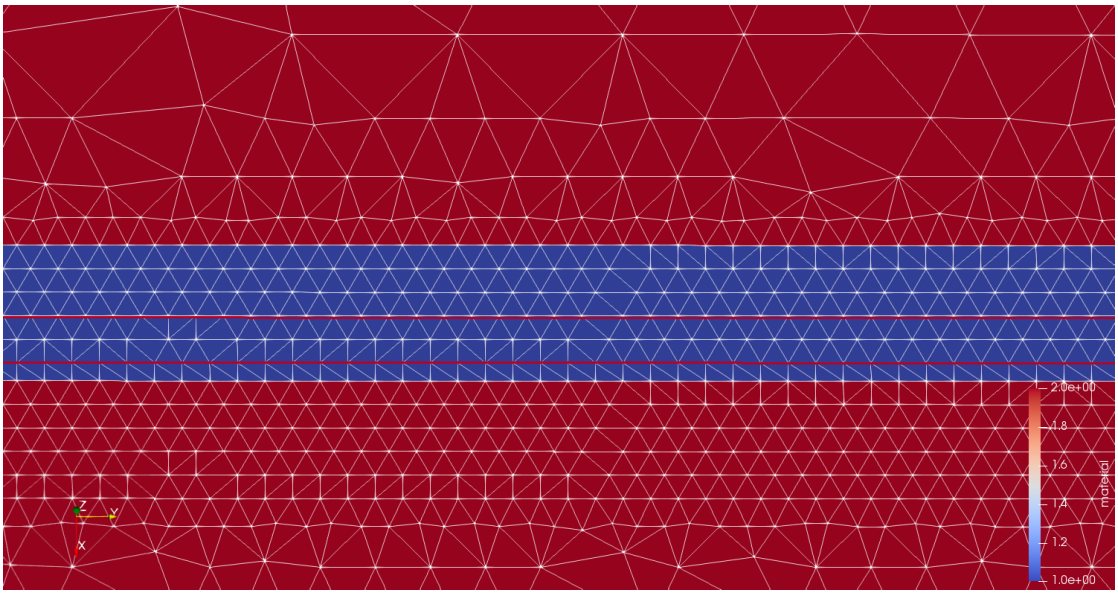

Figure A.3 Top view of mesh used in second batch of computations for models with width 200 m, mesh coarse. Blue is barrier, red is background sand, red lines indicate distance over which the gradient is computed

A.3 Results

Results are presented in terms of the effects on the gradient computed from the pipe tip (at -0.04 m inside the barrier) to 0.10 m upstream of this.
For the stage 2 calculations the results from the 100 m wide model with a finer and a coarser mesh are compared. The effect of width itself is addressed in the main report.

A.3.1 Effects on 2D gradients

A 2D gradient in the current memorandum is the gradient which is computed for models where the pipe is modelled along the entire width of the model. The flow situation can be understood to be effectively 2D in the barrier, the average along the barrier is computed.
For models with the same depth (40 m), leakage length (130 m), and contrast (4) the computed gradients in 2D are shown in the table below.

Table A.1. Computed average 2D gradients for models in stage 1 and stage 2

Model description	2D gradient for contrast 4	2D gradient for contrast 12
Stage 1	0.71	n.a.
Stage 2 mesh fine	0.73	0.37
Stage 2 mesh coarser	0.70	0.36

This indicates differences in the order of 4% can be expected for the 2D situation. However, the average 2D gradients are computed based on results along the entire width of the model. 3D factors are computed based on the gradients at a given distance from the pipe end. Due to local fluctuations in the head profile these can be more sensitive to mesh, as shown below.

A.4 Effects on 3D factor

A.4.1 Head and gradient profile along model width

The computed head and gradient along the width of the barrier is shown below for stage 2 models with a finer and a coarser mesh. In both models the pipe is extended 25 m along the barrier for the 3D effect, and models have the same depth (40 m), leakage length (130 m), model width 100 m, and contrast (4)
Significant scatter can be observed in the model with the coarser mesh.

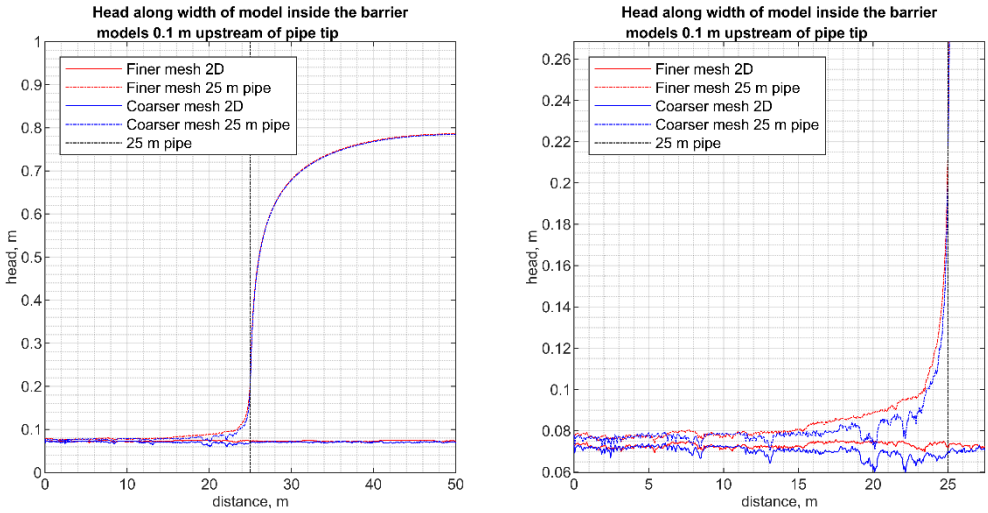

Figure A.4 Computed head profile along the model width 0.1 m upstream of the pipe tip in the barrier for models with finer and coarser mesh (refer text for details). Left half-width, right close up

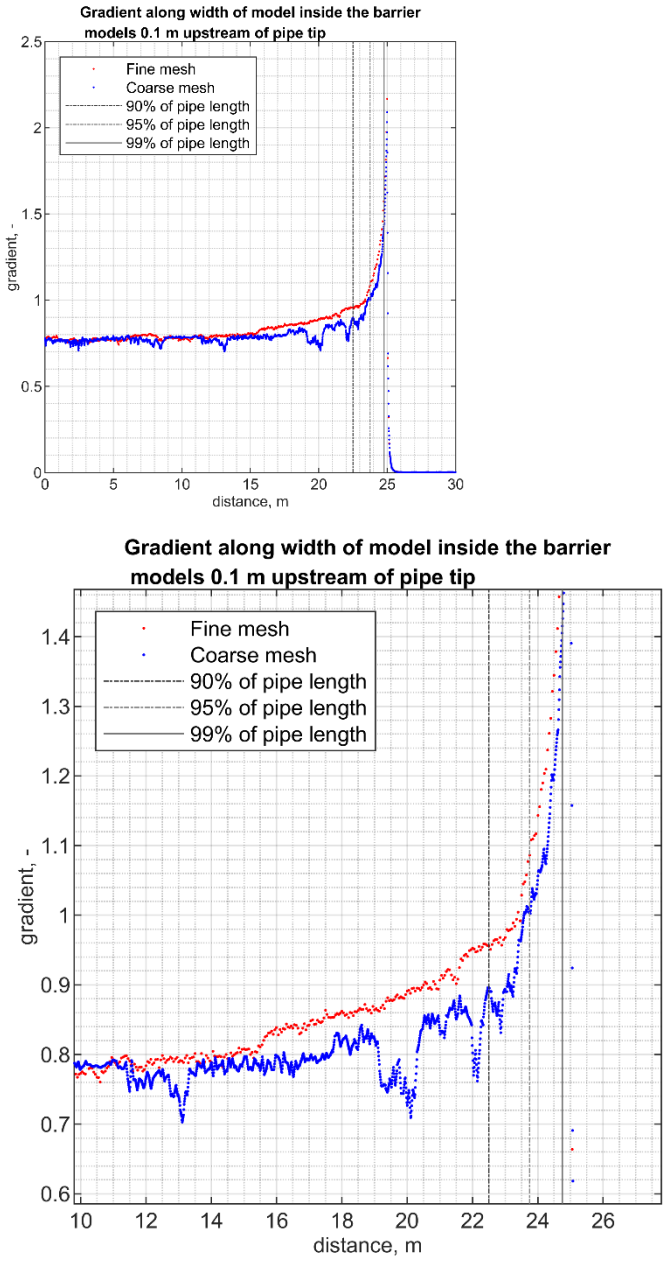

Figure A.5 Computed head profile along the model width 0.1 m upstream of the pipe tip in the barrier for models with finer and coarser mesh (refer text for details). Top half-width, bottom close up

Especially around 90% of the extent of the pipe in the gradient profile it is notable that the gradient fluctuates strongly.

A.4.2 Computed 3D factor at 99%, 95% and 90% of distance from centre axis

The 3D effect is expressed in terms of the gradient in the 3D situation (at 90%, 95% and 99% of the pipe extent, refer to main text for detail) divided by the 2D gradient. The 3D effect for models with the same depth (40 m), leakage length (130 m), and contrast (4) is shown in the table below.

Table A.2. Computed 3D effects for fine and coarse mesh in models of stage 2 with aquifer depth 40 m, aquifer width 100 m, barrier depth 2 m and contrast 4 and pipe extent 25 m

Model description	Finer mesh	Coarser mesh
99%	2.2	2.0
95%	1.5	1.4
90%	1.3	1.3

The fluctuations regarding the gradient that is computed with the coarser mesh affect the computed 3D effect. The value that is exactly at 90% (at 22.5 m pipe extent) is 0.90 giving a 3D effect of 1.3. Figure A5 shows that this is a local peak value. The minimum to the left of this (at 22.03 m pipe extent) is 0.77, and on the right is a minimum of 0.83 (at 22.87 m pipe extent) giving 3D effects of 1.1 and 1.2 respectively.

Table A.3. Computed 3D effects for fine and coarse mesh in models of stage 2 with aquifer depth 40 m, aquifer width 100 m, barrier depth 2 m and contrast 12 and pipe extent 25 m

Model description	Finer mesh	Coarser mesh
99%	2.9	2.7
95%	1.7	1.6
90%	1.4	1.4

The effect of the mesh is clearest for the gradients at 99% of the pipe extent. Possibly this is also due to the scatter observed in the computed head profile along the gradient in the model with a coarser mesh and a 25 m wide pipe. This scatter indicates that fluctuations of the 3D effect in the order of 10% might be expected based on mesh effects alone.
As the objective of this sensitivity study is to assess the sensitivity of the 3D effect to different parameters, the absolute value of the computed effect is of less importance. Also considering all other uncertainties, variations of 10% are considered insignificant. Therefore, the level of mesh refinement for the coarser mesh is considered sufficient for further application.

B Details calculations phase 3

B.1 Mesh details

This section presents mesh details for the models used. Unstructured meshes are used in order to achieve local refinements.
The figures below use colours to indicate the assigned size on the surfaces in colours. The mesh on the surface of the model is also shown.
Note that many options for mesh refinement resulted in either an inability of the mesh generator to construct a mesh, or resulted in meshes that were too large to compute in DgFlow. This limitation is considered significant for the feasibility of defining a 3D effect. It would have been preferable to refine the mesh in the entire volume of the barrier, however, with an element size of 0.06 m this was not possible (even with local refinements in the aquifer around the barrier and a coarse mesh in the rest of the model to limit the number of elements). It was possible with 0.08 m elements, however, this would not allow for a good resolution of the head profile inside the barrier as there are only two nodes upstream of the pipe tip.

B.2 Long model:

In the long model, the surfaces of mesh refinement are specified on the vertical surfaces. The base element size is 10 m.

B.2.1 BaseVar1

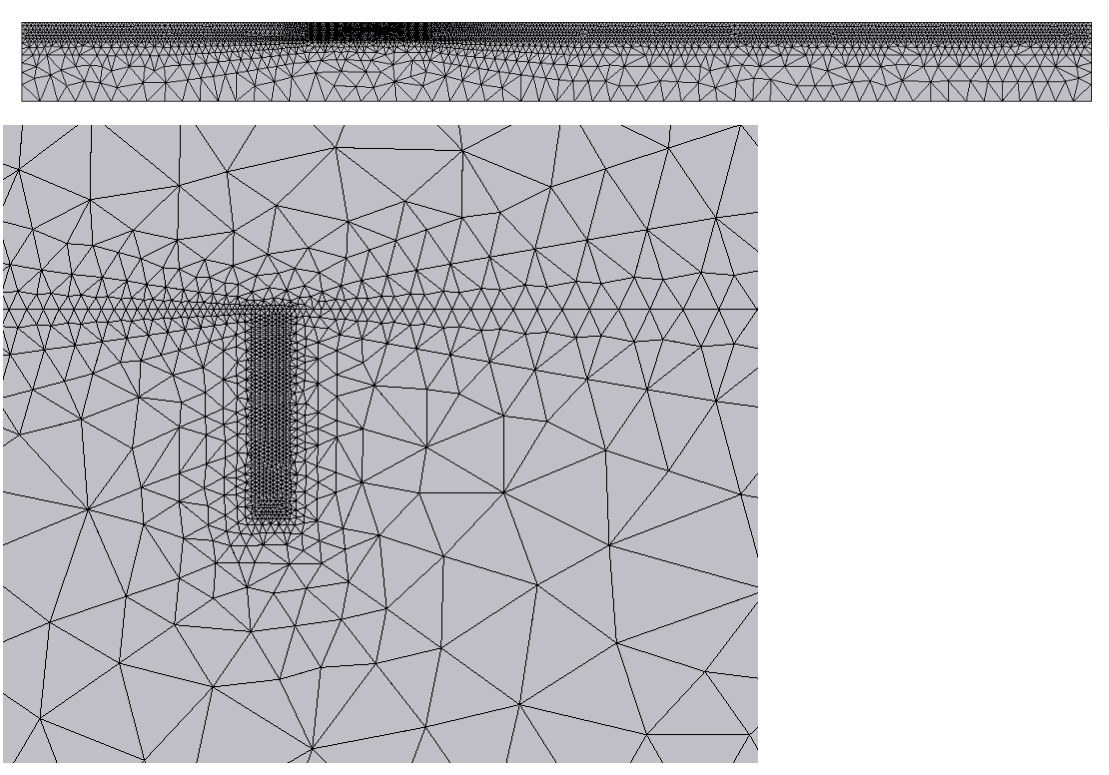

Figure B1 Mesh for the long models side view, top the entire model, bottom close up on the barrier

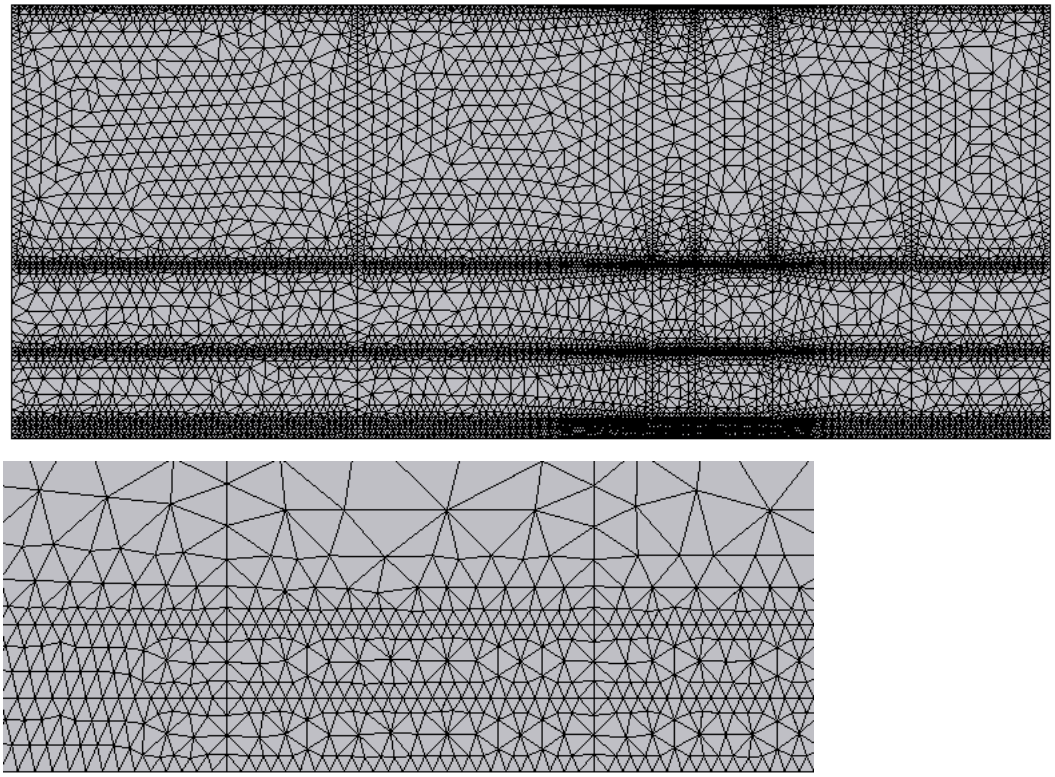

Figure B2 Mesh for the long models top view, top the entire model, bottom close up on the barrier

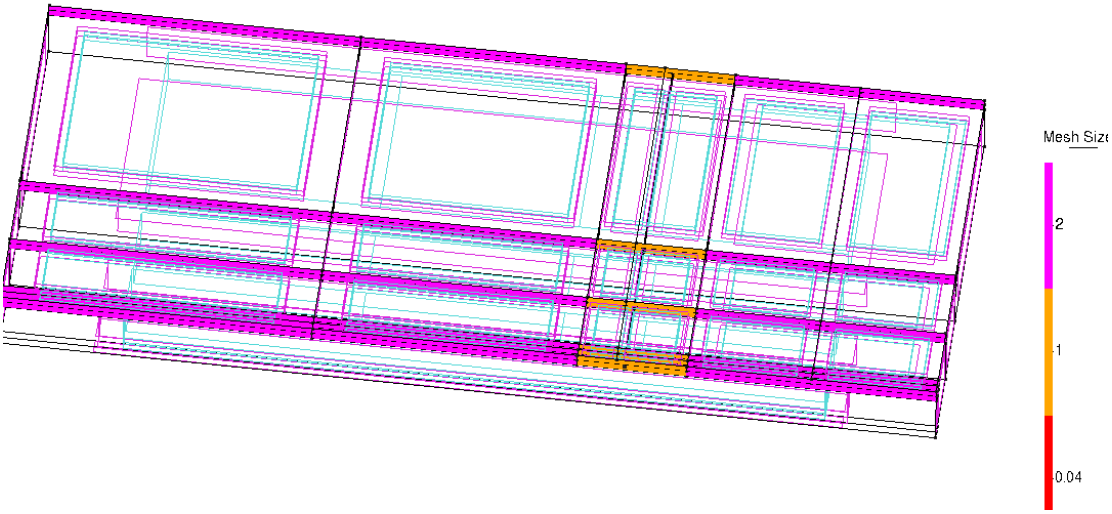

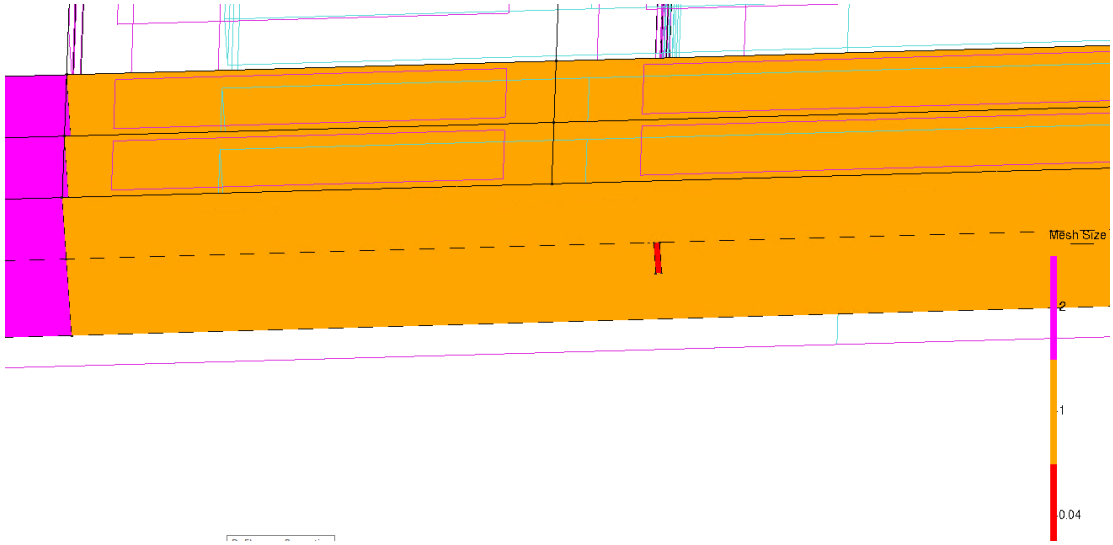

Figure B3 *Mesh refinement settings for the long models, top the entire model, bottom close up on the barrier. Mesh is refined on vertical sides in the model, blocks of 2 m upstream and downstream of the aquifer block containing the barrier. The aquifer block containing the barrier is refined to 1 m elements and the barrier itself to 0.04 m elements. Note that mesh sizes increase in between the surfaces which are refined*

B.3 Short models:

As the analysis of the large model showed that specifying local refinement on the vertical surfaces in the model results in significant mesh effects at these vertical surfaces, in the short models the refinements were specified on the horizontal surfaces. Due to limitations of the mesher there were various combinations which could not be meshed which might have given more homogeneous meshes.
The base element size is 8 m.

B.3.1 Short F2

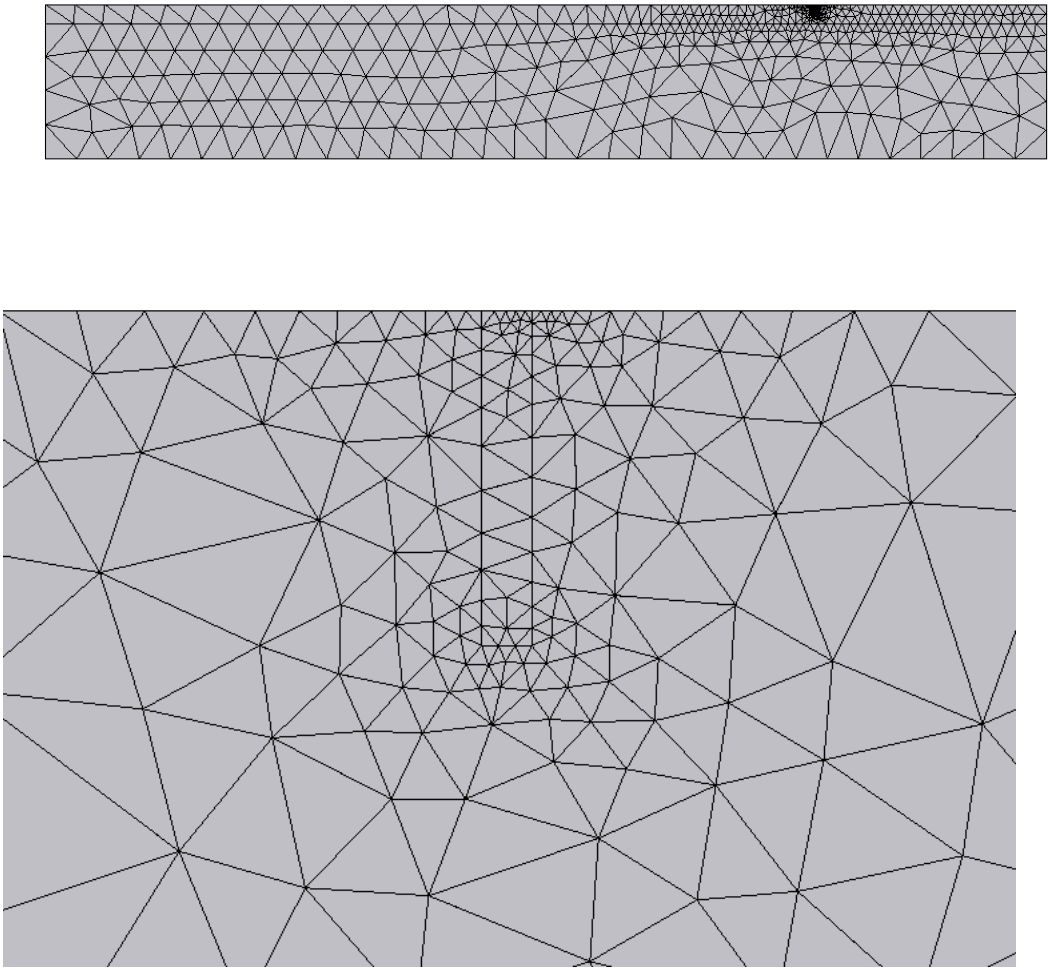

Figure B4 Mesh for the model Short f2 side view, top the entire model, bottom close up on the barrier

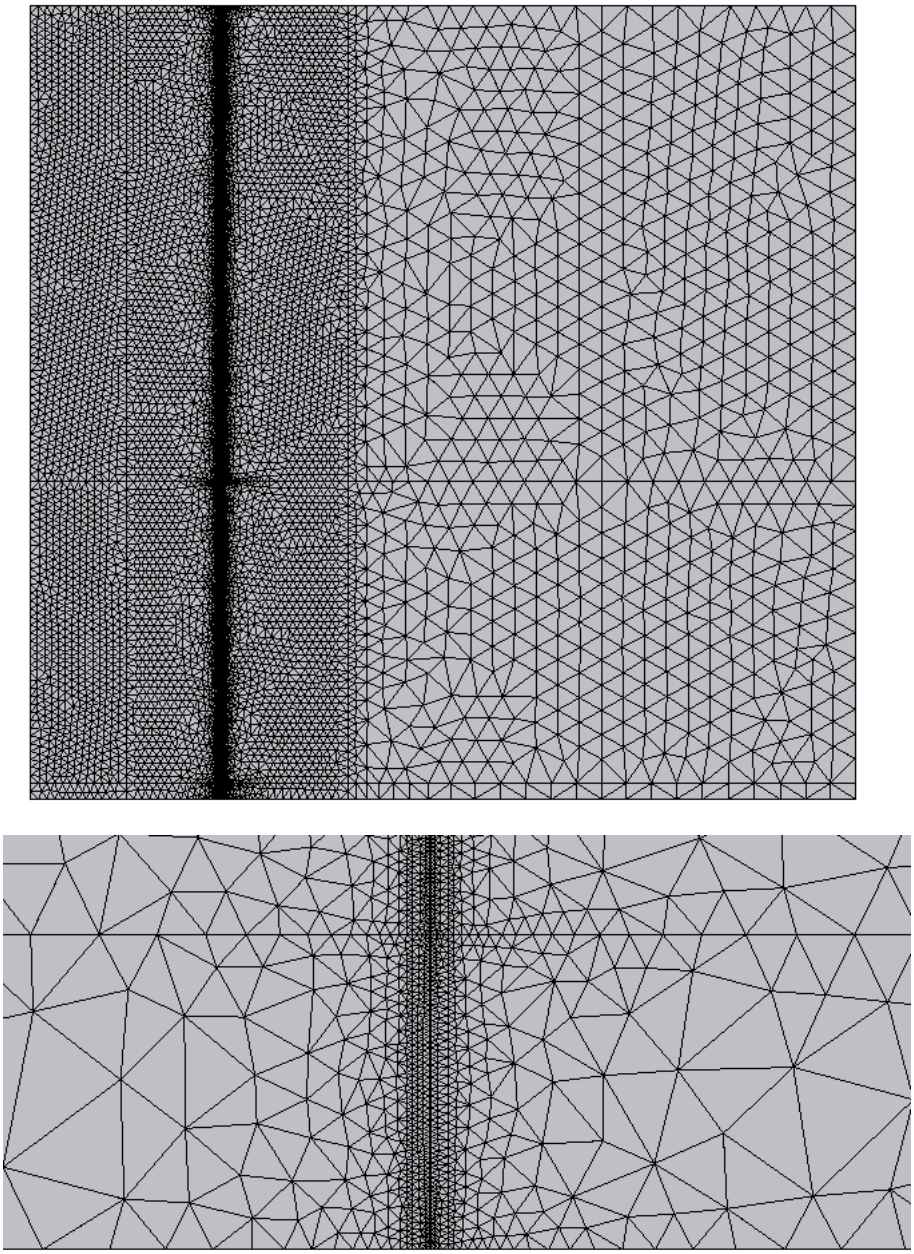

Figure B5 Mesh for the model Short f2 top view, top the entire model, bottom close up on the barrier

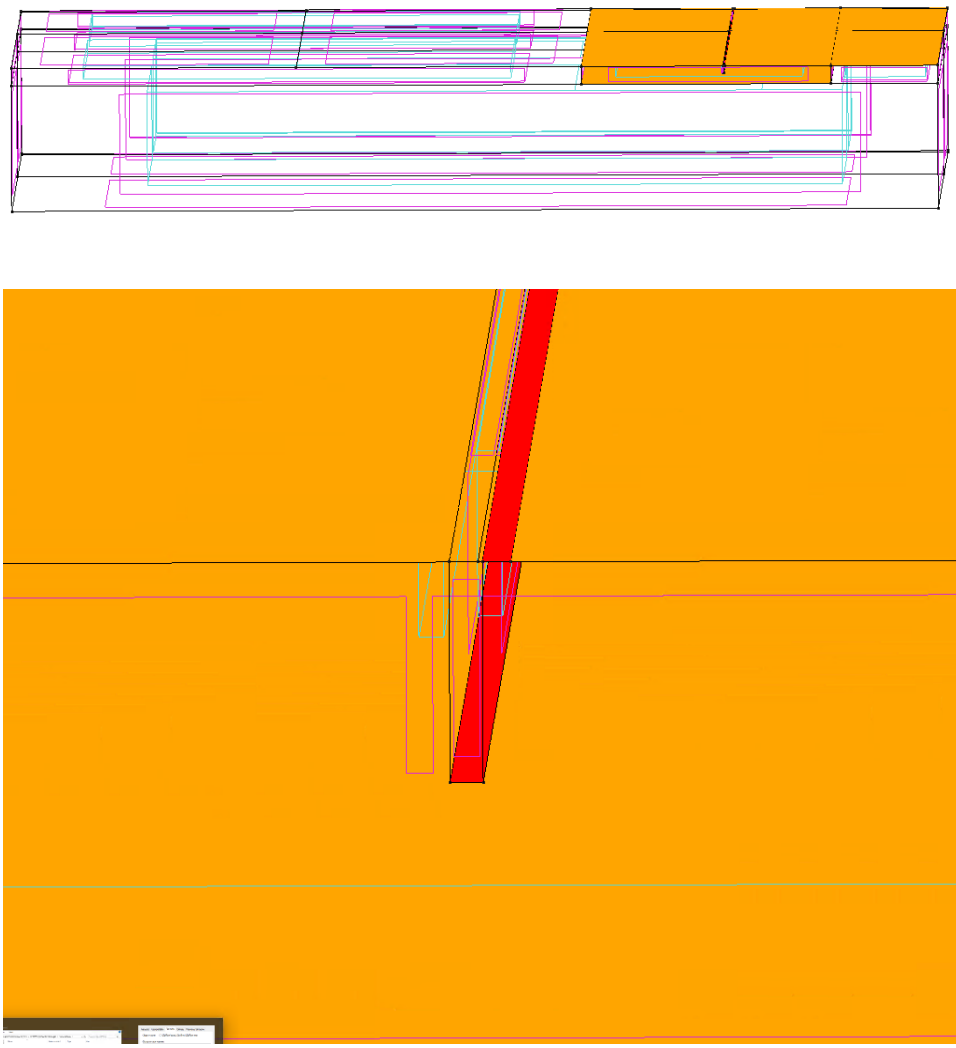

Figure B6 Mesh refinement settings for the model short f2, top the entire model, bottom close up on the barrier

B.3.2 Short F5

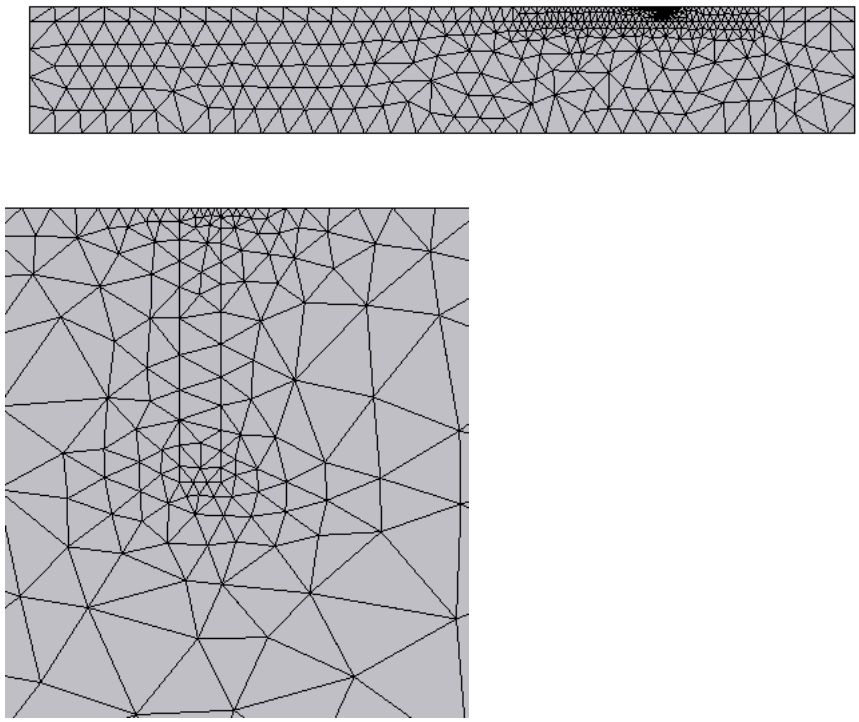

Figure B7 Mesh for the model Short f5 side view, top the entire model, bottom close up on the barrier

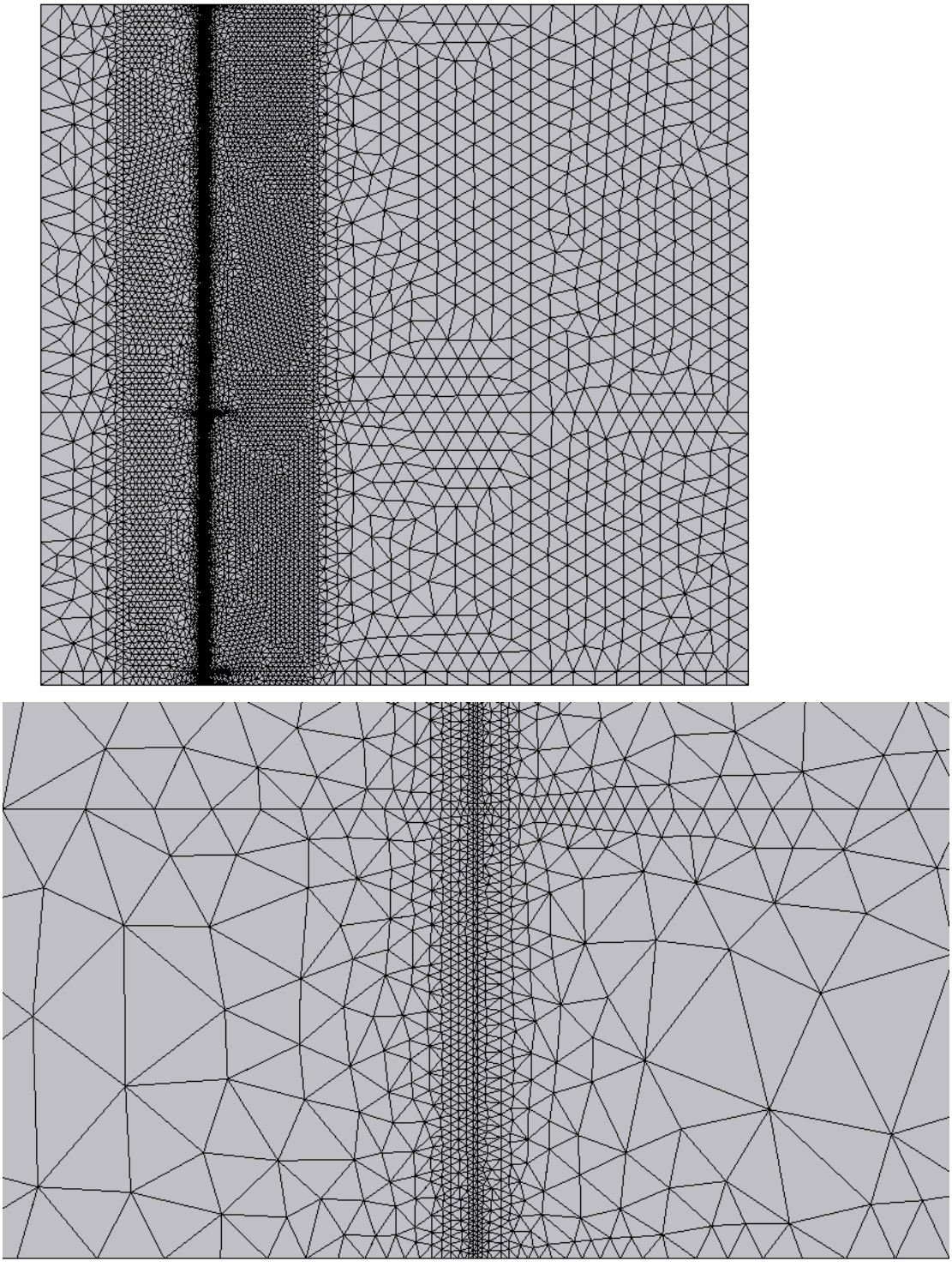

Figure B8 Mesh for the model Short f5 top view, top the entire model, bottom close up on the barrier

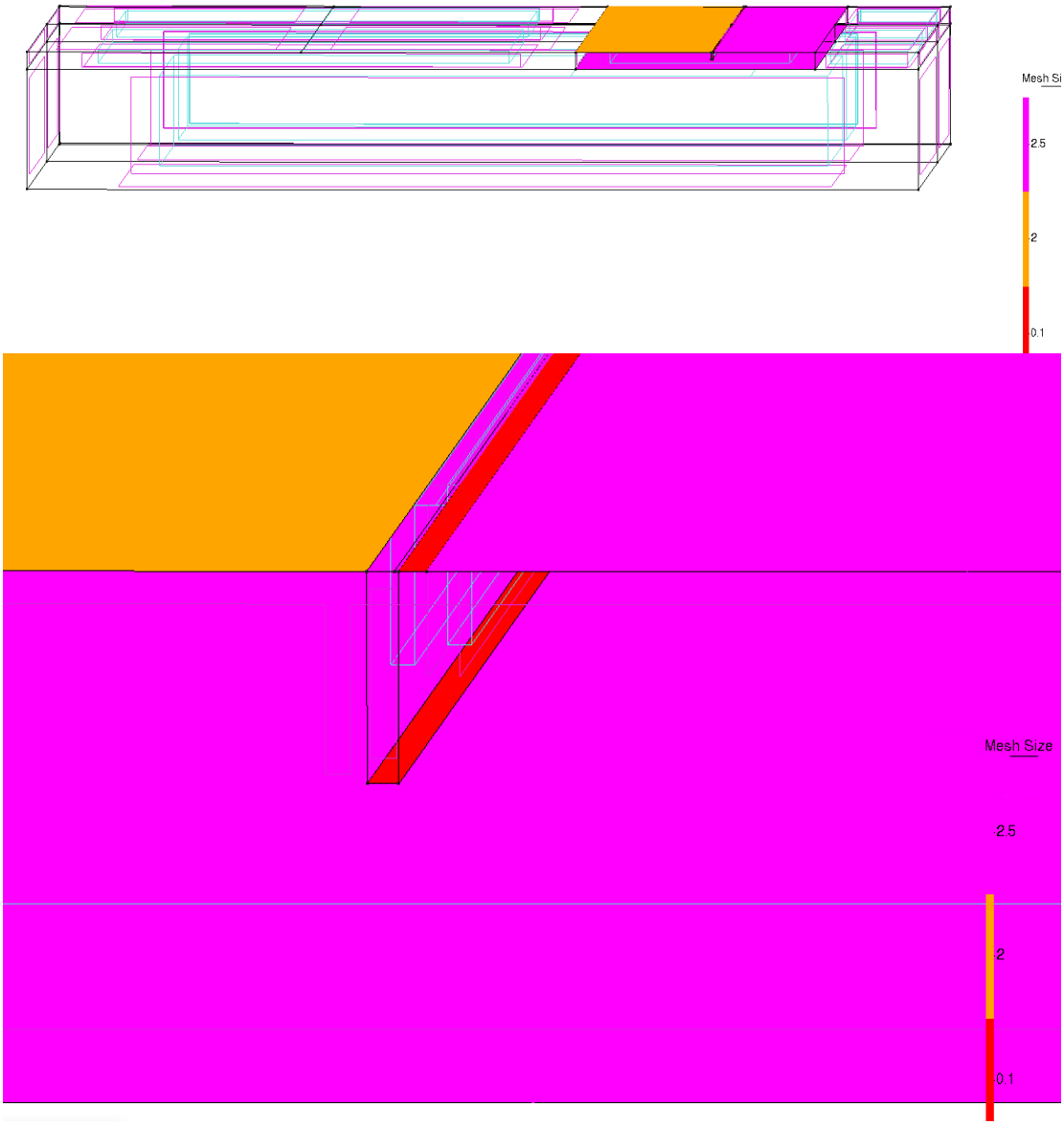

Figure B9 Mesh refinement settings for the model short f5, top the entire model, bottom close up on the barrier

B.4 Small Short models:

In the small short models the base element size is 8 m for Small Short and 4 m for Small Short f2.

B.4.1 Small Short

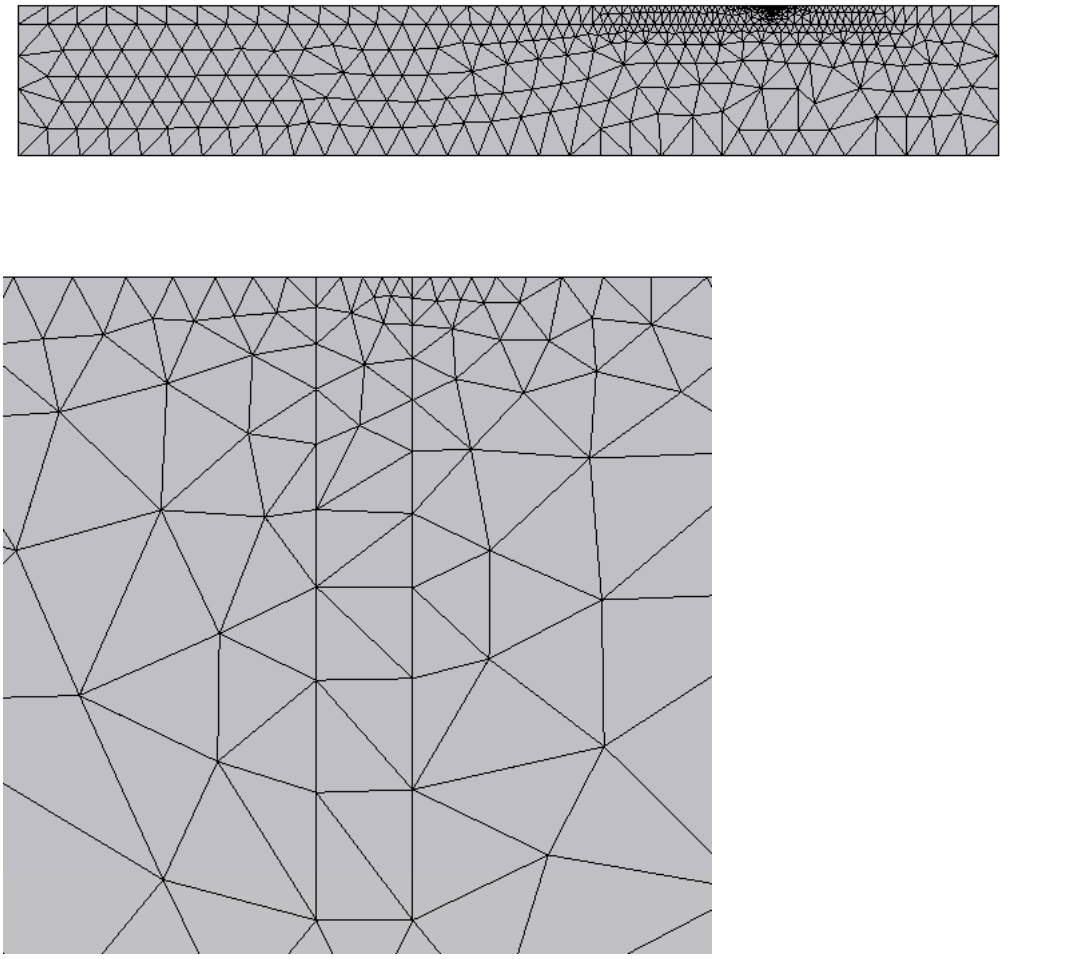

Figure B10 Mesh for the model Small Short side view, top the entire model, bottom close up on the barrier

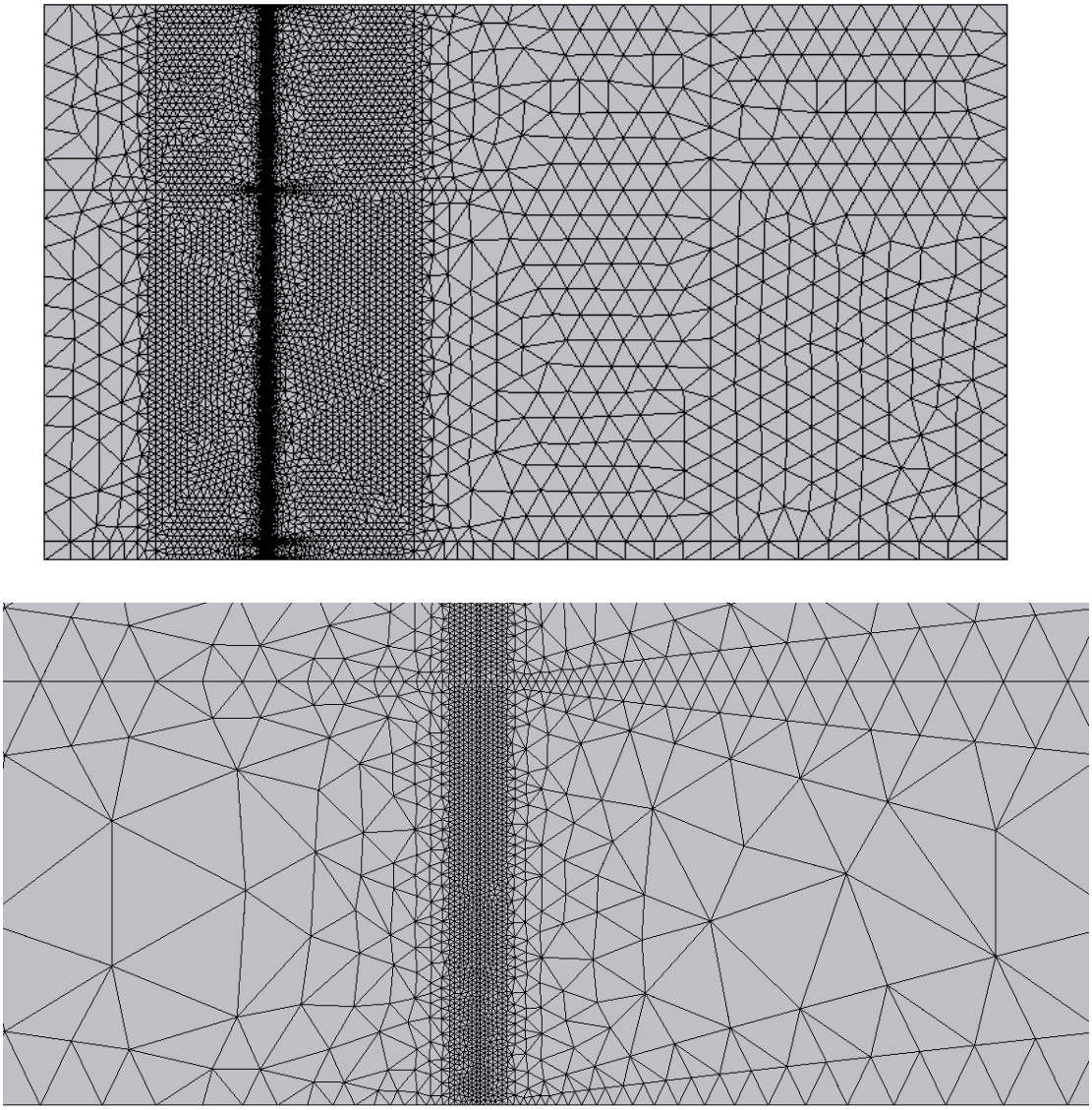

Figure B11 Mesh for the model Small Short top view, top the entire model, bottom close up on the barrier

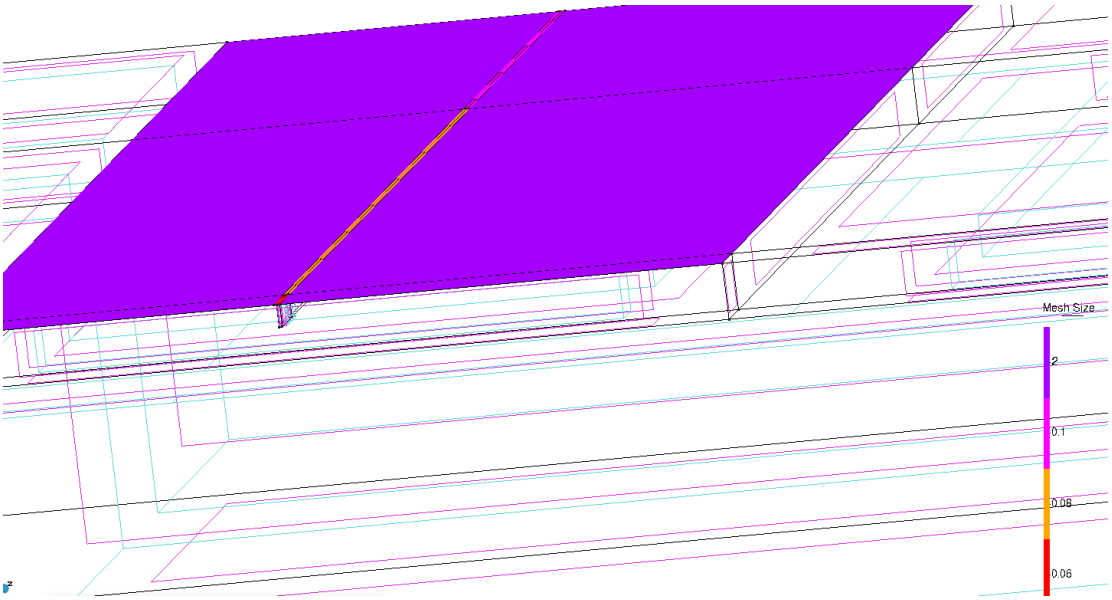

Figure B12 Mesh refinement settings for the model small short

B.4.2 Small Short f2

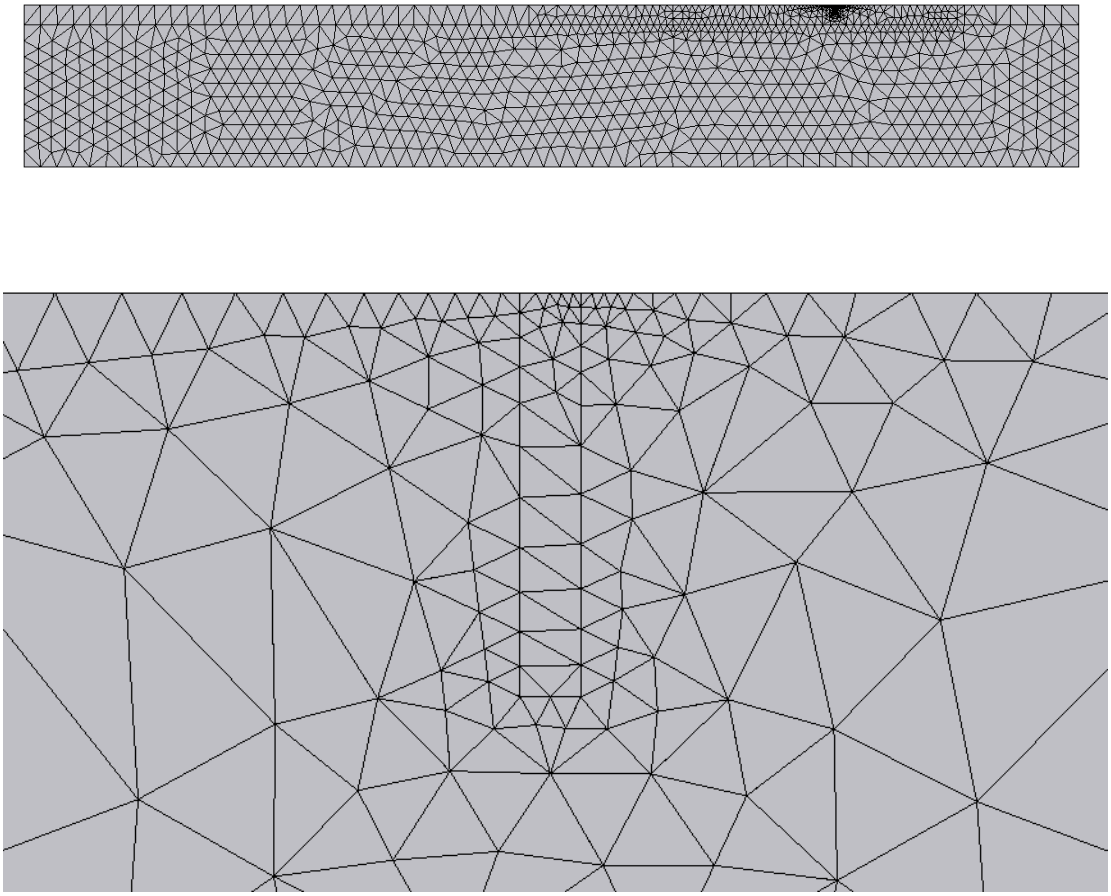

Figure B13 Mesh for the model Small Short f2 side view, top the entire model, bottom close up on the barrier

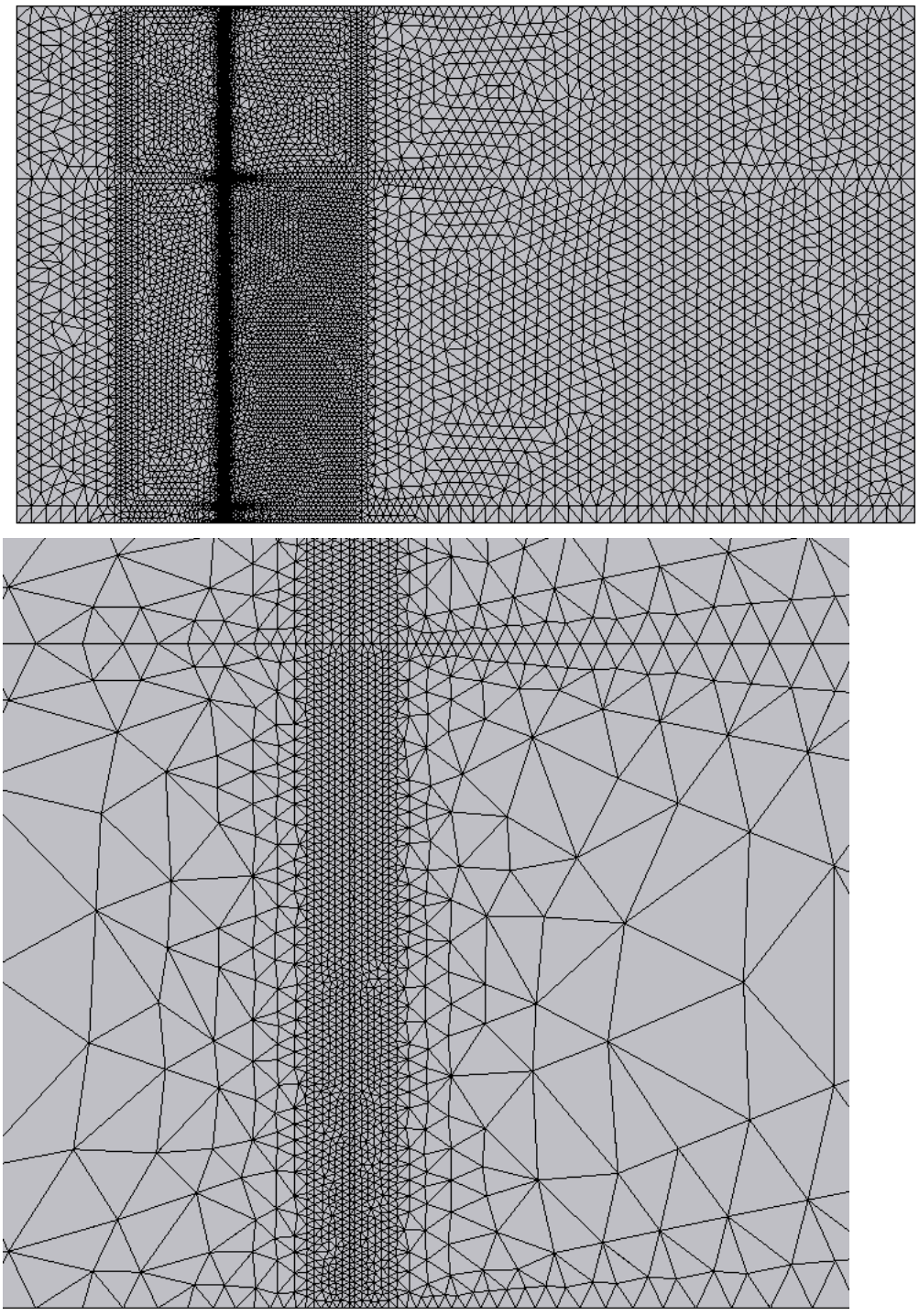

Figure B14 Mesh for the model Small Short f2 top view, top the entire model, bottom close up on the barrier

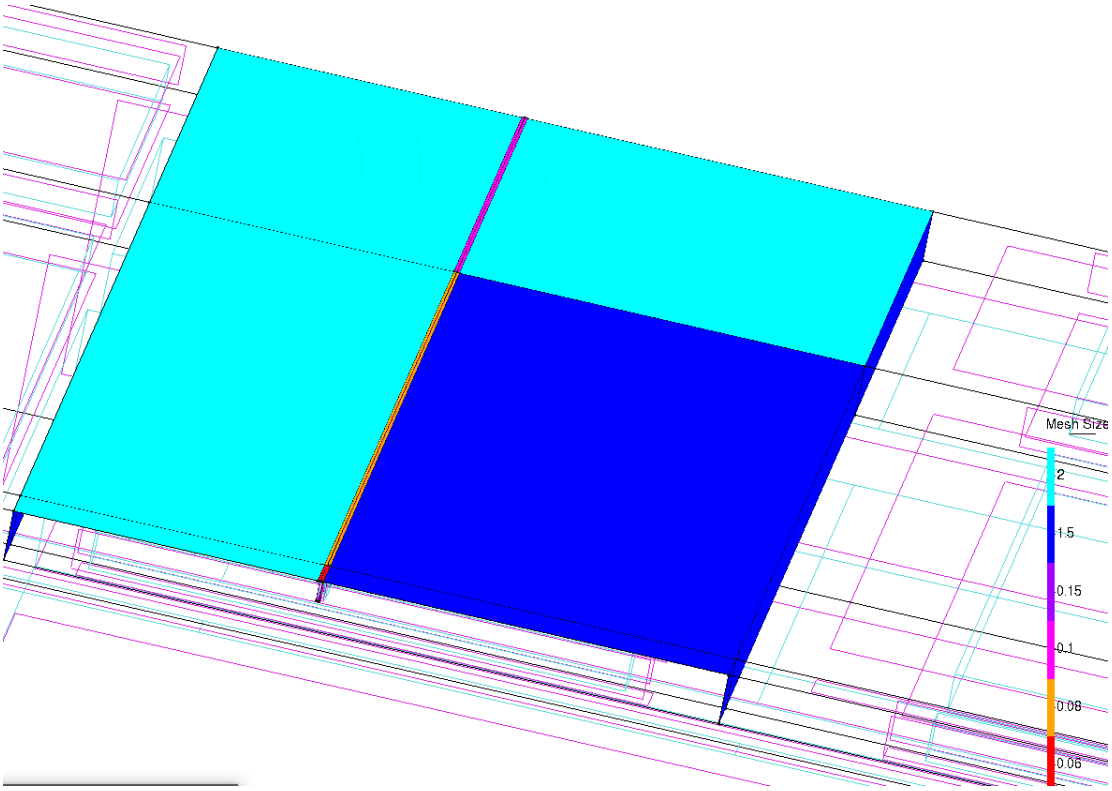

Figure B15 Mesh refinement settings for the model small short f2